

Sea Level Rise and Nuisance Flood Frequency Changes around the United States



City Dock in Annapolis, Maryland. Photo Credit: Amy McGovern.

Silver Spring, Maryland

June 2014



noaa National Oceanic and Atmospheric Administration

U.S. DEPARTMENT OF COMMERCE
National Ocean Service
Center for Operational Oceanographic Products and Services

**Center for Operational Oceanographic Products and Services
National Ocean Service
National Oceanic and Atmospheric Administration
U.S. Department of Commerce**

The National Ocean Service (NOS) Center for Operational Oceanographic Products and Services (CO-OPS) provides the National infrastructure, science, and technical expertise to collect and distribute observations and predictions of water levels and currents to ensure safe, efficient and environmentally sound maritime commerce. The Center provides the set of water level and tidal current products required to support NOS' Strategic Plan mission requirements, and to assist in providing operational oceanographic data/products required by NOAA's other Strategic Plan themes. For example, CO-OPS provides data and products required by the National Weather Service to meet its flood and tsunami warning responsibilities. The Center manages the National Water Level Observation Network (NWLON), a national network of Physical Oceanographic Real-Time Systems (PORTS[®]) in major U. S. harbors, and the National Current Observation Program consisting of current surveys in near shore and coastal areas utilizing bottom mounted platforms, subsurface buoys, horizontal sensors and quick response real time buoys. The Center establishes standards for the collection and processing of water level and current data; collects and documents user requirements which serve as the foundation for all resulting program activities; designs new and/or improved oceanographic observing systems; designs software to improve CO-OPS' data processing capabilities; maintains and operates oceanographic observing systems; performs operational data analysis/quality control; and produces/disseminates oceanographic products.

Sea Level Rise and Nuisance Flood Frequency Changes around the United States

**William Sweet
Joseph Park
John Marra
Chris Zervas
Stephen Gill**

June 2014



**U.S. DEPARTMENT OF COMMERCE
Penny Pritzker, Secretary**

**National Oceanic and Atmospheric Administration
Dr. Kathryn Sullivan, NOAA Administrator and Under Secretary of
Commerce for Oceans and Atmosphere**

**National Ocean Service
Dr. Holly Bamford, Assistant Administrator**

**Center for Operational Oceanographic Products and Services
Richard Edwing, Director**

NOTICE

Mention of a commercial company or product does not constitute an endorsement by NOAA. Use of information from this publication for publicity or advertising purposes concerning proprietary products or the tests of such products is not authorized.

TABLE OF CONTENTS

NOTICE.....	ii
TABLE OF CONTENTS	iii
LIST OF FIGURES	iv
LIST OF TABLES	v
EXECUTIVE SUMMARY	vi
INTRODUCTION.....	1
DATA AND METHODS	3
Cumulative Hours and Days with Nuisance Flooding	4
Current and 1950 Average Recurrence Interval of Daily Nuisance Flood Events	6
Monthly Distribution of Nuisance Floods and Related Physical Forcing Processes	7
FINDINGS.....	9
Historical SLR _{rel} and Changing Frequencies of Nuisance Flood Events	9
U.S. Northeast (NE) Coast.	10
U.S. Southeast (SE) Atlantic Coast.	12
U.S. Gulf Coast.	13
U.S. West Coast.....	14
Historical SLR _{rel} and Changing Nuisance Flood Event Probabilities	15
Patterns Associated with Year-to-Year Differences in Nuisance Flood Frequency.....	16
Seasonal Pattern of Nuisance Flood Events and Underlying Processes	18
CONCLUDING REMARKS	23
RECOMMENDATIONS.....	27
ACKNOWLEDGEMENTS	27
REFERENCES.....	29
APPENDIX 1.....	33
APPENDIX 2.....	35
ACRONYMS.....	58

LIST OF FIGURES

- Figure 1.** NOAA water level gauges used in this study and corresponding nuisance flood level. 3
- Figure 2.** (a) Average number of nuisance flood days between years 2007-2009 (meteorological years) that are correlated in (b) with the nuisance flood level elevation threshold by linear regression for the U.S. East Coast (NE and SE regions) gauges. 9
- Figure 3.** Hourly water level observations at the NOAA gauge at Sewells Point (Norfolk), Virginia for (a) 1950 and (b) 2012 and their (c) yearly water level distribution plotted with the nuisance flood level elevation threshold. All figures are plotted relative to 1980-2001 MSL datum and reveal in (a) and (b) a monthly spring-tide influence and a few discrete storm events. Readily apparent in (c) is the increase in MSL (change of distribution center relative to “0,” which is the 1983-2001 epoch MSL datum elevation) between 1950 and 2012. 10
- Figure 4.** (a) Northeast U.S. coastal topography at or below nuisance flood level elevations (image from “Flood Frequency” tab of NOAA Sea Level Viewer with NOAA gauges (green) used in this study). Shown in (b) are days per year (color bar not the same scale as “Days per Year” axis) with nuisance flooding at 23 gauges from Massachusetts to Virginia and (c) specifically at Atlantic City, New Jersey (gauge 10) plotted with annual average MSL. In (d) is a scatter plot of nuisance flood days at Atlantic City, New Jersey fitted with a quadratic curve starting in year 1950. 11
- Figure 5.** As in Figure 4, but for the Southeast U.S. coastline that includes 7 NOAA gauges (24-31) between North Carolina and the Atlantic coast of Florida. Nuisance flood events are shown for Charleston, South Carolina (gauge 28) in (c) and (d). 13
- Figure 6.** As in Figure 4, but for Gulf Coast that includes 8 NOAA gauges (32-39) between Florida and Texas. Nuisance flood events are shown for Naples, Florida (gauge 33) in (c) and (d). Note, Louisiana has not yet been mapped by the Sea Level Viewer and shown with cross-hashes. 14
- Figure 7.** As in Figure 4, but for U.S. Pacific coastline that includes 5 NOAA gauges (40-44) between California and Washington and gauge 45 at Honolulu, Hawaii (not shown in (a)). Nuisance flood events are shown for La Jolla, California (gauge 40) in (c) where the number of days per year with nuisance flooding is best fit by linear regression. 15
- Figure 8.** Return Periods of nuisance level flood events in (a) 1950 and (b) 2012 at NOAA gauges. 16
- Figure 9.** The Oceanic Niño Index (ONI) plotted with (a) monthly MSL (black line) from San Francisco, California that has been smoothed by a 5-month running filter and (b) annual counts of daily average nontidal residual (NTR; green bars) > 0.3 m at Sewells Point, Virginia. 18
- Figure 10.** Season with highest frequency of nuisance flood days over the 1980-2009 period as shown for each NOAA gauge in Appendix 2. 19
- Figure 11.** Maximum observed water levels per calendar day over the 1980-2009 period decomposed into a low-frequency MSL cycle, predicted tide (without the annual and semi-annual harmonic fits) and remaining nontidal residual (NTR) all smoothed by a 30-day running filter shown for (a) the Battery, New York, (b) Mayport, Florida, (c) San Francisco, California and (d) Port Isabel, Texas. All series are relative to their station MSL datum and plotted with the nuisance flood

level (yellow-magenta line) and MHHW datum elevation (black dot-dash). In the bottom plots, the number of nuisance flood hours and days (shared y-axis) are averaged by calendar month between 1980 and 2009..... 20

Figure 12. (a) Monthly mean volume transport of the Florida and Yucatan Currents over the 2000-2009 with their means in parenthesis that reveal a geostrophic-related inverse relationship to MSL cycle at Mayport, Florida and Port Isabel, Texas, respectively. In (b) are hourly astronomic tide predictions for San Francisco, California showing semi-annual spring tide strengthening during the winter and summer solstice time frames, which reach the nuisance flood level. 21

Figure 13. Calendar-day maxima over 1980-2009 (i.e., as shown in top plots of Figure 11a-d) are averaged to estimate (a) a ratio between the average of the NTR during (divided by) maximum water level and (b) the distance between the NOAA gauge’s nuisance flood level and the average tidal contribution during maximum water level. 22

Figure 14. Bubble plot of nuisance flood level (x-axis) versus quadratic constant (b_2 ; y-axis) from fit of annual number of nuisance flood days listed in Appendix 1 for East Coast (NE region in red and SE region in blue) gauges. Bubble size represents the goodness-of-fit (R^2) of each quadratic model fit. Only gauges with significant quadratic fits and hourly data starting prior to 1960 (Appendix 1) are included to minimize quadratic curve-fitting discrepancies due to gauge record length. 24

LIST OF TABLES

Table 1. NOAA water level gauges, location, start of analysis, MSL trend, and nuisance flood level (m)5

EXECUTIVE SUMMARY

The National Oceanic and Atmospheric Administration (NOAA) water level (tide) gauges have been measuring water levels around the U.S. for over a century, providing clear evidence of sea level rise relative to land (SLR_{rel}) around most of the continental United States and Hawaii. As SLR_{rel} increases mean sea level (MSL), there is naturally an increase in tidal datum elevations, which are typically used to delineate inundation thresholds. Direct consequences of rising sea level against fixed elevations such as *today's* built infrastructure also include increased inundation during extreme events both spatially and temporally. Not only are extreme flooding events reaching higher grounds and covering larger areas due to SLR_{rel} , the frequency and duration of these extreme flood events are increasing.

Another consequence of SLR_{rel} is the increase in *lesser extremes* such as occasional minor coastal flooding experienced during high tide. These events are becoming more noticeable and widespread along many U.S. coastal regions and are *today* becoming more of a *nuisance*. As sea levels continue to rise and with an anticipated acceleration in the rate of rise from ocean warming and land-ice melt, concern exists as to when more substantive impacts from tidal flooding of greater frequency and duration will regularly occur. Information quantifying these occurrences to inform mitigation and adaptation efforts and decision makers is not widely available.

In this report, we show that water level exceedances above the elevation threshold for “minor” coastal flooding (nuisance level) impacts established locally by the National Weather Service (NWS) have been increasing in time. More importantly, we document that event frequencies are accelerating at many U.S. East and Gulf Coast gauges, and many other locations will soon follow regardless of whether there is an acceleration of SLR_{rel} . Lastly, we show a regional pattern of increasingly greater event-rate acceleration as the height between MSL and a location’s nuisance flood threshold elevation decreases.

Impacts from recurrent coastal flooding include overwhelmed stormwater drainage capacity, frequent road closures, and general deterioration and corrosion of infrastructure not designed to withstand frequent inundation or salt-water exposure. From this, we conclude that there is a time horizon, largely dependent upon the local rate of SLR_{rel} , when critical elevation thresholds for various public/private/commercial serving systems will become increasingly compromised by tidal flooding. This concept of a non-linear impact trajectory needs to be recognized, as it is critical for coastal planning to prevent degradation to society-serving systems at risk from SLR_{rel} . The goal of this report is to heighten awareness of a growing problem of more frequent nuisance coastal flooding relative to a community’s living memory and to encourage resiliency efforts in response to impacts from SLR_{rel} .

INTRODUCTION

Thermal expansion of the world's oceans and melting of glaciers and ice sheets from climate warming has contributed to global sea level rise (SLR) of approximately 1.7 mm/yr over the last century (Church and White, 2011) and even higher rates (3.2 mm/yr; Merrifield et al., 2013) over the last several decades. Superimposed upon this trend are ocean-atmosphere circulation dynamics producing significant regional interannual mean sea level (MSL) variability. This variability can be expressed as low-frequency multi-month MSL anomalies, as well as higher-frequency *storminess* changes in storm surge event frequency along the coast (Sweet and Zervas, 2011; Thompson et al., 2013) from altered seasonal storm track tendencies (Hirsch et al., 2001). Regional variability is often coherent with climate forcings such as El Niño Southern Oscillation (ENSO) and the multi-decadal Pacific Decadal Oscillation (PDO) that, dependent upon their state, can also exacerbate (Merrifield et al., 2012) or suppress (Bromirski et al., 2011) long-term regional SLR rates. Vertical land motion also contributes to regional-to-local relative changes in long-term SLR_{rel} rates relative to land (Zervas et al., 2013). The net effect for most of the United States is a SLR_{rel} readily tracked by the U.S. National Oceanic and Atmospheric Administration (NOAA) National Water Level Observation Network (NWLON). NWLON is a nationwide monitoring program whose water level gauges have supported essential commerce-related activities for over a century, such as providing tide predictions and chart datums for safe navigation as well as boundary delineations for private property and federal and state economic zones. NWLON also provides potentially life-saving information in near real-time about extreme tropical and extratropical storm surges, tsunami warnings, and enhances coastal intelligence by establishing coastal-flood probabilities.

One consequence of SLR_{rel} (<http://tidesandcurrents.noaa.gov/sltrends>) is an increase in tidal datum elevations (CO-OPS, 2001), such as Mean Higher High Water (MHHW), that define perennial inundation levels. A more societal-important consequence of SLR_{rel} is the exacerbation of extreme flood event magnitudes and their frequencies from a perspective of fixed elevations (Hunter, 2010; Park et al., 2011; Tebaldi et al., 2012), such as those associated with private property and critical public-serving infrastructure and systems (e.g., transportation, energy generation and transmission, wastewater treatment, etc.). The increased probability occurs as a result of a lowered “freeboard” or gap between MSL and specific threshold flood elevations from SLR_{rel}. This results in smaller storm surge magnitudes increasingly impacting similar levels as time progresses. This reality was recently highlighted by Superstorm Sandy's impacts in October 2012 along the U.S. Mid-Atlantic (Sweet et al., 2013). However, neither changes in tidal datum elevations nor rare-event probabilities are readily apparent to the casual observer. The former is generally too gradual for noticeable impacts, or incurs successional changes over generational time scales (CO-OPS, 2001), whereas the latter is obscured by the infrequency of the extremely rare event (e.g., direct hurricane strike).

In this report, we describe a more tangible impact of SLR_{rel} as an increased frequency of minor (nuisance) tidal-related flooding, further refining the unbiased climate-change SLR indicator of Parker (1992). The increased frequency of nuisance tidal flooding along U.S. coastal regions is a growing problem with societal impacts (<http://www.csc.noaa.gov/tidalfloodingvis/>). We provide insight into patterns and trends associated with a nuisance-flood proxy derived from empirically calibrated levels at NWLON gauges, specifically the “minor” threshold elevation established by local Weather Forecasting Offices (WFO) of NOAA's National Weather Service (NWS).

Henceforth, we will refer to the NWS “minor” thresholds as a location’s *nuisance flood level*, which have been historically associated with minor coastal flooding impacts. We note that not every exceedance above the nuisance flood level implies that noticeable or widespread flooding has occurred or will occur; though, when concurrent with localized rainfall or a wind-forced storm surge, impacts can become quite severe and more similar to the higher NWS-defined levels (i.e., moderate and major) recently analyzed by Kriebel and Geiman (2013). Rather, the nuisance flood level provides a measure of localized propensity for community-specific minor impacts based upon documented observations. Nuisance flood level thresholds and the land elevations susceptible to event inundation are displayed in the “Flood Frequency” tab of the NOAA Sea Level Viewer (<http://csc.noaa.gov/slr/viewer/>) with supporting discussion in Marcy et al. (2011).

Three main questions are addressed in this report:

1. How has historical SLR_{rel} changed the:
 - frequency and duration of nuisance flood events?
 - probability of a nuisance flood event?
2. What climatic patterns are associated with year-to-year differences?
3. During what season do nuisance floods typically occur and why?

DATA AND METHODS

Hourly water levels, available from the Center for Operational Oceanographic Products and Services (CO-OPS) (<http://tidesandcurrents.noaa.gov/>), are utilized in this report to describe nuisance-related impacts. The hourly data and nuisance flood levels are relative to the latest National Tidal Datum Epoch (NTDE) which, in all but one instance (Galveston, Texas is a 1997-2001 epoch), references the 1983-2001 period. The water level observations were further decomposed into an astronomical tide (prediction) and a nontidal residual (NTR) component, with the latter forming in response to ocean and atmospheric forcing.

Though NOAA NWLON has 210 water level gauges in its network, with 52 gauges in the Great Lakes and 158 along the open coast, only about 75 of the open coast gauges have a minor coastal flooding elevation threshold (nuisance flood level) assigned to them by local NOAA NWS WFOs. Of these approximately 75 gauges, the majority are along the East and Gulf Coasts since these areas have the potential for larger storm surges than the West Coast, where wave impacts are more prevalent and whose effects are not generally captured (by design) by coastal water level gauges (Ruggiero, 2013). A total of 45 gauges are used in this report including Honolulu, Hawaii, whose nuisance flood level is defined and displayed (“high sea level forecasts” tab) by the Pacific Integrated Ocean Observing System (PacIOOS; <http://oos.soest.hawaii.edu/pacioos>) rather than the local NWS WFO. Inclusion criterion is based upon: 1) 30 years of verified hourly data and 2) sufficient exceedances above the nuisance flood level to produce discernable trends or patterns. Figure 1 shows the location and nuisance flood levels for the NOAA gauges used in the study. Table 1 provides the gauge name, position, range of data utilized, SLR_{rel} trend for study period, and NWS minor (nuisance) coastal flood threshold elevations.

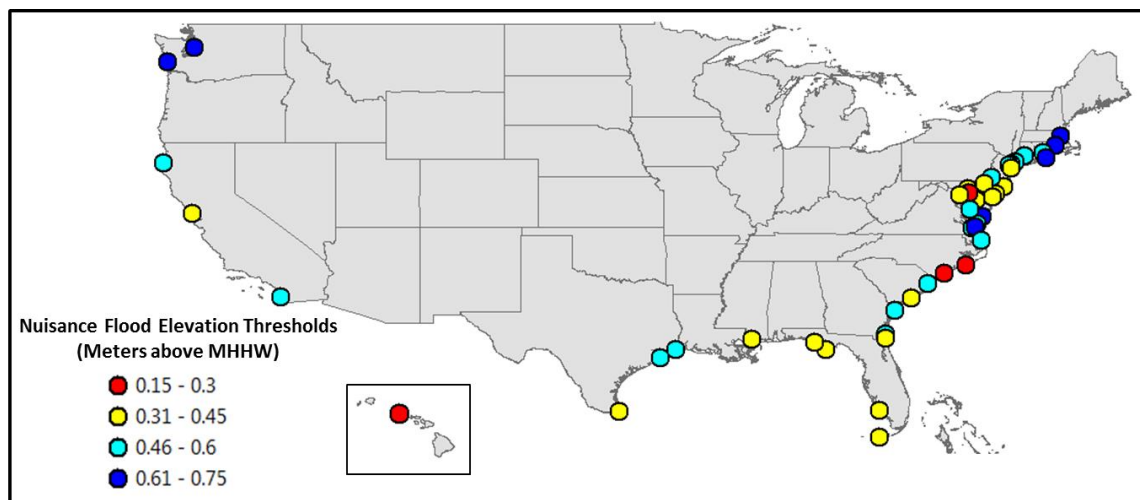


Figure 1. NOAA water level gauges used in this study and corresponding nuisance flood level.

Since water level record lengths vary by gauge (Table 1), an arbitrary start date of January 1, 1920 was chosen for the subsequent analysis. The 1920 start date truncates a few gauge records but ensures the majority of the other gauge record lengths are incorporated. The end date was 2013. Multiple analyses were performed and are described below. In “Findings” section, regionally representative gauge results will be highlighted to better illustrate the methods.

Cumulative Hours and Days with Nuisance Flooding

Hourly water level exceedances above the nuisance flood level are used to quantify both duration and frequency of historical impacts experienced locally. Two measures are shown in this report: 1) cumulative hours above the nuisance flood level elevation threshold during a year, and 2) number of days affected by nuisance level flooding (e.g., one day could represent one hour or an entire 24-hour period above the nuisance flood level) during a year. Henceforth, these two measures will be referred to as nuisance flood “hours” and “days,” whereas when the term “event” is used, both measures are collectively being referenced, though one “day” would more closely approximate one “event.” It should be noted that all exceedances above the nuisance flood level are accounted for, even the most extreme whose impacts would be considered *severe*, not *nuisance*. The daily definition as compared to the hourly summation reduces the relative contribution of severe storms exceeding the threshold for numerous hours. In semi-diurnal tidal regions (i.e., two high and two low tides a day) where two separate exceedances may occur in a day, the event is not counted twice. In both cases, results are shown only when 80% of a year’s hourly data are available. In this presentation, a year is defined as a meteorological year as to not split the winter season, which tends to be the dominant storm season for much of the Northern Hemisphere in terms of atmospheric activity (e.g., Hirsch et al., 2001) and related storm surges (Sweet et al., 2011; Thompson et al., 2013). We define the meteorological year from May to April, e.g., May 2012–April 2013 is reported as year 2012. NOAA provides an inundation analysis tool allowing further frequency and duration investigation in context to this report’s procedures and findings (<http://tidesandcurrents.noaa.gov/inundation>).

Table 1. NOAA water level gauges, location, start of *analysis*, MSL trend, and nuisance flood level (m)

	NOAA Tide Gauge	St. ID	Longitude	Latitude	Analysis Start (years)	MSL Trend (mm/yr)	Nuisance Flood Level (above MHHW)
1	Boston, MA	8443970	-71.052	42.355	1921	2.8	0.68
2	Providence, RI	8454000	-71.402	41.807	1938	2.26	0.66
3	New London, CT	8461490	-72.087	41.355	1938	2.57	0.60
4	Bridgeport, CT	8467150	-73.182	41.173	1970	2.87	0.48
5	Montauk, NY	8510560	-71.960	41.048	1947	3.2	0.60
6	Kings Point, NY	8516945	-73.765	40.810	1931	2.52	0.52
7	Battery, NY	8518750	-74.015	40.700	1920	3.15	0.50
8	Bergen Point, NY	8519483	-74.147	40.640	1981	4.93	0.52
9	Sandy Hook, NJ	8531680	-74.010	40.467	1922	4.08	0.45
10	Atlantic City, NJ	8534720	-74.418	39.355	1920	4.19	0.43
11	Cape May, NJ	8536110	-74.940	38.968	1965	4.61	0.38
12	Philadelphia, PA	8545240	-75.142	39.933	1920	3.09	0.49
13	Reedy Point, DE	8551910	-75.573	39.558	1979	3.67	0.42
14	Lewes, DE	8557380	-75.120	38.782	1920	3.46	0.41
15	Cambridge, MD	8571892	-76.068	38.573	1979	3.71	0.45
16	Baltimore, MD	8574680	-76.579	39.267	1920	3.25	0.41
17	Annapolis, MD	8575512	-76.482	38.983	1928	3.51	0.29
18	Washington D.C.	8594900	-77.022	38.873	1924	3.21	0.31
19	Wachapreague, VA	8631044	-75.687	37.607	1978	5.52	0.61
20	Kiptopeke, VA	8632200	-75.988	37.165	1976	3.57	0.48
21	Lewisetta, VA	8635750	-76.464	37.996	1970	5.59	0.46
22	Sewell Point, VA	8638610	-76.330	36.947	1927	4.58	0.53
23	Chesapeake Bay Bridge, VA	8638863	-76.113	36.967	1975	6.04	0.64
24	Duck, NC	8651370	-75.747	36.183	1978	4.58	0.55
25	Beaufort, NC	8656483	-76.670	34.720	1973	2.72	0.29
26	Wilmington, NC	8658120	-77.953	34.227	1935	2.02	0.25
27	Springmaid Pier, SC	8661070	-78.918	33.655	1977	3.62	0.58
28	Charleston, SC	8665530	-79.925	32.782	1921	3.11	0.38
29	Fort Pulaski, GA	8670870	-80.902	32.037	1935	3.01	0.46
30	Fernandina Beach, FL	8720030	-81.465	30.672	1920	2.21	0.59
31	Mayport, FL	8720218	-81.430	30.397	1928	2.43	0.44
32	Key West, FL	8724580	-81.808	24.553	1920	2.38	0.33
33	Naples, FL	8725110	-81.807	26.130	1965	2.34	0.35
34	Apalachicola, FL	8728690	-84.982	29.727	1976	1.77	0.42
35	Panama City, FL	8729108	-85.667	30.152	1973	1.57	0.35
36	Bay Waveland, MS	8747437	-89.325	30.325	1978	3.96	0.45
37	Sabine Pass, TX	8770570	-93.870	29.730	1981	5.49	0.58
38	Galveston, TX	8771510	-94.788	29.285	1957	6.61	0.60
39	Port Isabel, TX	8779770	-97.215	26.060	1944	3.79	0.34
40	La Jolla, CA	9410230	-117.257	32.867	1924	2.01	0.51
41	San Francisco, CA	9414290	-122.466	37.806	1920	2.00	0.35
42	Humboldt Bay, CA	9418767	-124.217	40.767	1977	3.93	0.56
43	Toke Point, WA	9440910	-123.967	46.707	1972	0.42	0.63
44	Seattle, WA	9447130	-122.339	47.603	1920	2.24	0.65
45	Honolulu, HI	1612340	-157.867	21.307	1920	1.24	0.22

To provide a physical basis for the trends in nuisance flood days, annual MSL values and their long-term trends are also shown. A yearly MSL value, which is an average of hourly water levels

over a year, is not reported if the gauge's hourly water level record is less than 80% for any particular year (as to synchronize with the yearly nuisance event statistics, Table 1). The annual MSL values are relative to the gauge's current MSL datum such that the values range from negative to positive with the "zero" near the current epoch's midpoint. Plotting relative to another tidal datum or epoch would have no effect on the magnitude of the SLR_{rel} trend apparent in each gauge's MSL values. The long-term SLR_{rel} trends for each gauge are listed in Table 1 and closely match those computed by Zervas (2009) and updated through 2012 at <http://tidesandcurrents.noaa.gov/sltrends>.

Current and 1950 Average Recurrence Interval of Daily Nuisance Flood Events

To quantify *extreme* events, extreme value statistics are employed to characterize the upper tail of a water level distribution. A common derived measure is the average recurrence interval, often termed return period, which is the inverse of the probability of exceeding a particular elevation threshold. A simple and effective method to quantify probabilities is the Annual Maximum Method (AMM), which fits a series of annual maximum water level with a Generalized Extreme Value (GEV) distribution. Zervas (2013) uses a GEV fit of annual maximum to quantify extreme characteristics at NOAA NWLON gauges (<http://tidesandcurrents.noaa.gov/est>). The main weakness of the AMM/GEV is that only one event per year is used, which ignores other significant events that occur during the same year and often leads to less robust results for gauges with shorter record lengths and higher frequency (<1 year) estimates of lesser extreme events.

In this report we use a Peak Over Threshold (POT)/Point Process approach, which utilizes multiple events per year to estimate the return periods for each gauge's nuisance flood level (Coles, 2001). We use the 97th percentile (%) of daily maximum water levels as the high threshold (not the nuisance level threshold) to study statistical exceedance properties. Consecutive events are filtered by a three-day window to ensure independence resulting in approximately eight events per year on average. Similar criteria were used by Mendez et al. (2006) for wave data and for water level extremes throughout the Pacific region (<http://www.pacificstormsclimatology.org>) as discussed in Kruk et al. (2013). It is assumed that the distribution of the number of exceedances per year follows a Poisson distribution and that the threshold excesses (y) are modeled using a Generalized Pareto Distribution (GPD) given by

$$(1) \quad \begin{aligned} H(y, \sigma, \xi) &= 1 - (1 + \xi y / \sigma)^{-1/\xi} & \xi \neq 0 \\ H(y, \sigma, \xi) &= 1 - \exp(-y/\sigma) & \xi = 0 \end{aligned}$$

where $\sigma > 0$ is the GPD scale parameter and ξ is the shape parameter. The combination of the Poisson and GPD models are related to GEV parameters by $\sigma = \sigma^* + \xi(u - \mu)$ with μ the GEV location parameter, u the high threshold and σ^* the GEV scale parameter and the event rate, $\lambda = [(1 + \xi(u - \mu) / \sigma^*)^{-1/\xi}]$. The return level, y_N , is given by Mendez et al. (2006) as

$$(2) \quad \begin{aligned} y_N &= \mu - \sigma^* / \xi [1 - (-\log(1-q))]^{-\xi} & \xi \neq 0 \\ y_N &= \mu - \sigma^* \log(-\log(1-q)) & \xi = 0 \end{aligned}$$

where $1/q$ is the return period (years) with $0 < q < 1$. The GEV location parameter represents the median, the scale parameter (both GEV and GPD) represents the spread, and the shape parameter represents the skew of the distribution. Parameters are estimated by the maximum likelihood method, and the 95% confidence intervals are estimated via the delta method (Rice, 1994).

For the extreme value analysis, the water level data series are detrended by their local MSL trend (Table 1). Detrending normalizes the data relative to the current NTDE in order to compare events in time. To estimate current (2012) probabilities, the return level interval curves, which are valid for the mid-point (e.g., 1992) of the current epoch (e.g., 1983-2001), are raised to 2012 MSL elevations (MSL trend multiplied by 20 years). For 1950 probabilities, a gauge's return level interval curves are lowered to 1950 MSL (i.e., a height equal to its MSL trend \times 42 years). Bottom left plots in Appendix 2 show the GPD Poisson model results for 2012 and 1950 and their elevation differences described here. Similar time-adjustment procedures and further method description is given by Sweet et al. (2013). The method is a quasi-nonstationary method that accounts for long-term SLR_{rel} effects, but no other time-varying considerations (e.g., Menendez and Woodworth, 2010).

Monthly Distribution of Nuisance Floods and Related Physical Forcing Processes

The monthly mean distributions of the nuisance flood hours and days are shown for a recent 30-year period (1980-2009). No attempt is made to discern whether or not seasonal-scale variability has been changing in time. In order to identify processes contributing to high water conditions, we decomposed the maximum daily water level into three components:

- A low-frequency seasonal MSL cycle component, which is similar to the amplitudes and phases of the annual (Sa) and semi-annual (Ssa) harmonic constituents and the 12-month MSL cycle derived by Zervas (2009)
- The predicted tide without the Sa and Ssa harmonic constituents included using T_tide analysis routines (Pawlowicz et al., 2002)
- The remaining NTR after the above components are removed

The maximum water level and its components are identified over the same 30-year period (e.g., 1980-2009) and for each calendar day of the year (e.g., Jan 1, 2...Dec 31). For the maximum water level and its predicted tide and NTR components, a 30-day running mean filter (smoothed) has also been applied in order to highlight patterns rather than individual event influences (e.g., Figure 3-8 in Marra et al., 2012). Subsequently, component summation is not precisely additive due to the smoothing process. But, shown with respect to the nuisance flood level, the components provide a sense of process significance during high-water formation typical for nuisance flooding events.

FINDINGS

Historical SLR_{rel} and Changing Frequencies of Nuisance Flood Events

A large spatial variability in the frequency of nuisance level flooding exists across the U.S. Figure 2a shows the average number of nuisance flood days for a recent three-year period of 2007-2009 (meteorological years: May 2007–April 2010), which corresponds to statistics shown on the NOAA Sea Level Viewer for a similar time period. It should be stressed that the elevation thresholds for minor nuisance flooding are location-specific elevations and derived empirically by NOAA National Weather Service (NWS) Weather Forecasting Offices (WFOs) for NOAA coastal water level gauges from local knowledge of impacts over time. Nuisance flood levels represent susceptibility to flooding inherent to the natural topography and hydrological conditions, as well as reflect any mitigation efforts of the human-altered environment (e.g., flood-defense and storm-water measures). Areas with higher values of nuisance flood days (>20 days) are located along the Mid-Atlantic and in the Chesapeake Bay, the coasts of North and South Carolina, and southern Texas. Not surprisingly, a strong negative correlation ($p < 0.01$) exists between a gauge's number of nuisance flood days (2007-2009 mean) and its flood level elevation threshold, as shown in Figure 2b for the Northeast and Southeast regions ($R^2 = 0.73$). The variance accounted for by the linear regression model is smaller ($R^2 = 0.50$) when all gauges are included, which is a result of smaller tidal ranges (along the Gulf Coast) and lessened storm surge potential (along the West Coast) compared to the U.S. East Coast, which lessen a location's annual occurrences of exceeding its nuisance flood level.



Figure 2. (a) Average number of nuisance flood days between years 2007-2009 (meteorological years) that are correlated in (b) with the nuisance flood level elevation threshold by linear regression for the U.S. East Coast (NE and SE regions) gauges.

The values shown in Figure 2 are not consistent in time. Rather, nuisance flooding has been increasing at NOAA gauges across the U.S. over the last century from increases in local MSL. Long-term changes in nuisance flood frequency occur because local SLR_{rel} raises MSL and the entire distribution of both high- and low-water events affecting higher and higher elevations in time, as illustrated at Sewells Point, Virginia (Figure 3). Trends derived from linear regression on the annual number of nuisance flood days are statistically significant at the 90% level at 41 of

the 45 gauges analyzed (Appendix 1). At the majority of the gauges analyzed (28 of 45 gauges), the rate of change of nuisance flood days has been accelerating (significant at the 90% level) over the last half-century, whereas SLR_{rel} rates have not necessarily been accelerating. Several stations not showing significant acceleration have shorter record lengths (start in 1970s) and thus may be unable to distinguish an accelerating rate of change largely initiating in the 1970s-1980s and observed at the other nearby gauges (e.g., Duck, North Carolina). The response becomes nonlinear as the water level distribution increasingly exceeds the nuisance flooding level elevation resulting in an accelerating increase of the annual number of event per year (increases in MSL result in an increasingly larger “area under the curve” that surpasses the threshold in Figure 3). In this regard, the acceleration observed (e.g., in Figures 4a, 5a, 6a) occurs in response to SLR_{rel} and not from an increasing *storminess* trend, which has been relatively unchanged within the Mid-Atlantic region over the 20th century (Zhang et al., 2000). Results of linear and quadratic regression on the number of days with nuisance flooding from 1950-2012 (or when the data record starts) are listed in Appendix 1.

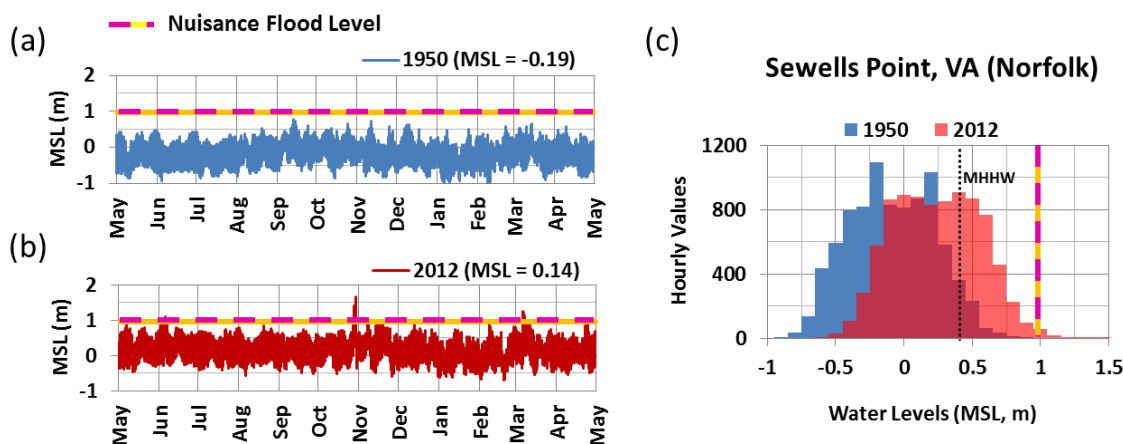


Figure 3. Hourly water level observations at the NOAA gauge at Sewells Point (Norfolk), Virginia for (a) 1950 and (b) 2012 and their (c) yearly water level distribution plotted with the nuisance flood level elevation threshold. All figures are plotted relative to 1980-2001 MSL datum and reveal in (a) and (b) a monthly spring-tide influence and a few discrete storm events. Readily apparent in (c) is the increase in MSL (change of distribution center relative to “0,” which is the 1983-2001 epoch MSL datum elevation) between 1950 and 2012.

There are regional rate-of-change patterns around the U.S. The following sections provide regional views of historical nuisance flood patterns, the low-lying areas within the region potentially susceptible to nuisance level flooding, and representative gauges for closer result inspection. Gauge-specific results are listed in Appendix 2.

U.S. Northeast (NE) Coast. There has been a significant increase of nuisance flooding occurrences along the U.S. NE Atlantic Coast (Figure 4b) largely in response to high regional SLR_{rel} rates (approximately 3-5 mm/yr) from vertical land subsidence (Boon et al., 2010; Zervas et al., 2013) most notable in the Mid-Atlantic region and lower Chesapeake Bay. In the last several decades, there has been a rate increase of nuisance flood days (Ezer, 2014) with 19 of the 23 NOAA gauges experiencing an accelerating response (Appendix 1). This nuisance flood frequency rate increase may reflect multi-decadal rate increases in regional SLR trends (Ezer and

Corlett, 2012; Boon 2012) associated with Gulf Stream system dynamics (Sallenger et al., 2012; Knop, 2013), though it is unclear if this regional SLR is from a direct transport slowdown or interaction with Mid-Atlantic Bight Slope Current (Ezer et al., 2013; Rossby et al., 2014). The New England gauges are an exception, with a lower event frequency, likely due to higher nuisance flood level threshold elevations (Figure 1), supportive of recent analysis by Kriebel and Geiman (2013). Figure 4a indicates (in red) the topography at or below nuisance flood level elevations.

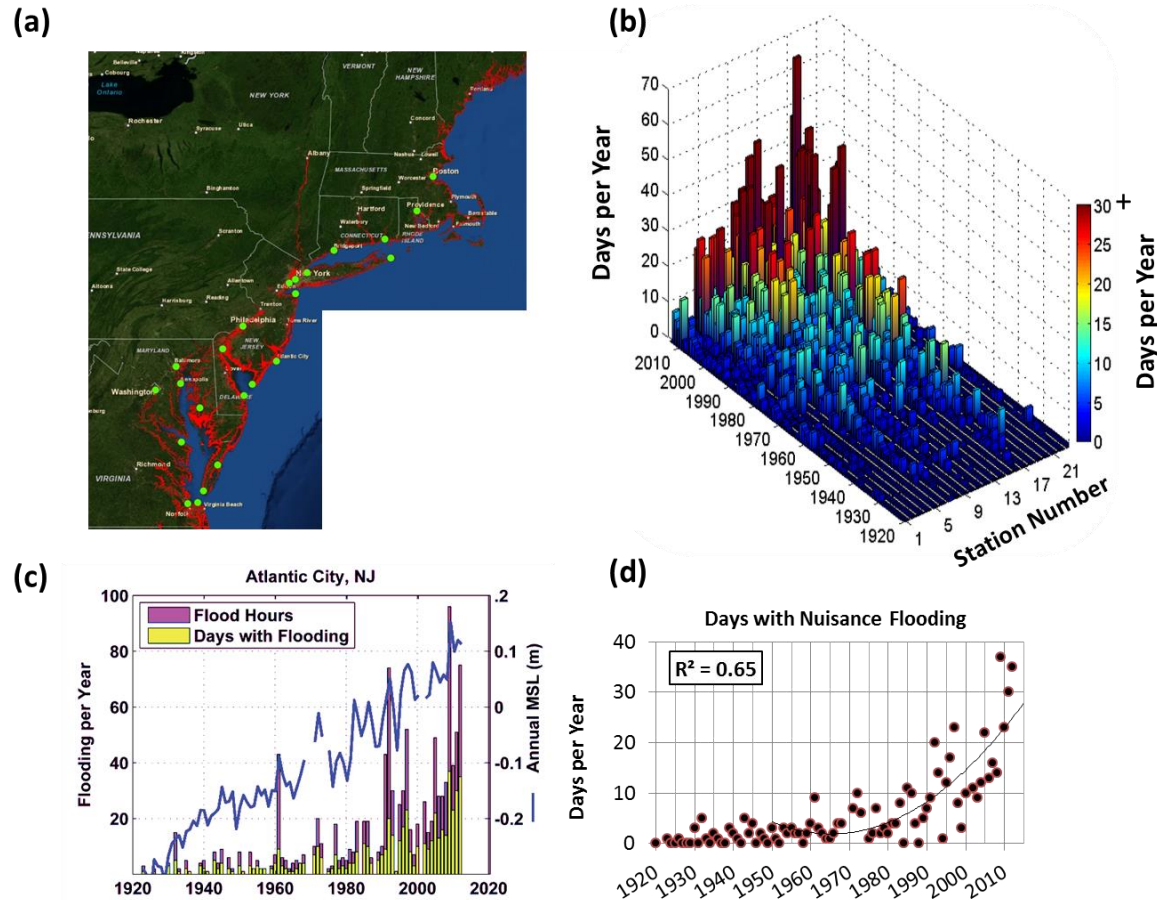


Figure 4. (a) Northeast U.S. coastal topography at or below nuisance flood level elevations (image from “Flood Frequency” tab of NOAA Sea Level Viewer with NOAA gauges (green) used in this study). Shown in (b) are days per year (color bar not the same scale as “Days per Year” axis) with nuisance flooding at 23 gauges from Massachusetts to Virginia and (c) specifically at Atlantic City, New Jersey (gauge 10) plotted with annual average MSL. In (d) is a scatter plot of nuisance flood days at Atlantic City, New Jersey fitted with a quadratic curve starting in year 1950.

Data from the NOAA gauge (number 10) at Atlantic City, New Jersey is provided as a regionally representative gauge. In Figure 4c, nuisance flood hours and days at Atlantic City, NJ are shown plotted with the annual average MSL. A high SLR_{rel} trend exists at this location (4.19 mm/yr, Table 1) with noticeable interannual MSL and nuisance-event variability (discussed below in “...year-to-year differences...” section). Nuisance flood days per year, which are shown as a

scatter plot in Figure 4d, can be seen to accelerate since the 1980s when fitted ($R^2=0.65$) with a quadratic curve for the 1950-2012 period.

U.S. Southeast (SE) Atlantic Coast. Large regions of the U.S. Southeast Atlantic Coast are susceptible to nuisance level flooding (Figure 5a), occurrences of which have been readily increasing since the 1980s (Figure 5b). In fact, five of the eight NOAA gauges are now on an accelerating nuisance flood frequency trajectory (Appendix 1). Local rates of SLR_{rel} , which largely reflect differences in vertical land subsidence rates, are variable (approximately 2-3 mm/yr; Zervas et al., 2013) with locally higher rates at Springmaid Pier, South Carolina (possibly related to a datum shift and/or questionable monthly MSL records) and Duck, North Carolina (possibly related to its short data record length). The large increases in nuisance flood events found in Charleston, South Carolina and Fort Pulaski, Georgia reflect higher SLR_{rel} rates, whereas at Beaufort and Wilmington, North Carolina, lower nuisance flood level thresholds themselves are a factor. In this region, sea levels are affected by the Gulf Stream system (e.g., Florida Current), whose seasonal variability influences the MSL cycle and short-term perturbations contribute to nuisance flood event formation (Sweet et al., 2009). However, there is no known evidence of SLR_{rel} trends increasing in this region over the last several decades. Data from the NOAA gauge at Charleston, South Carolina (Figure 5c), however, clearly shows the acceleration in nuisance flood days since the 1980s (Figure 5d).

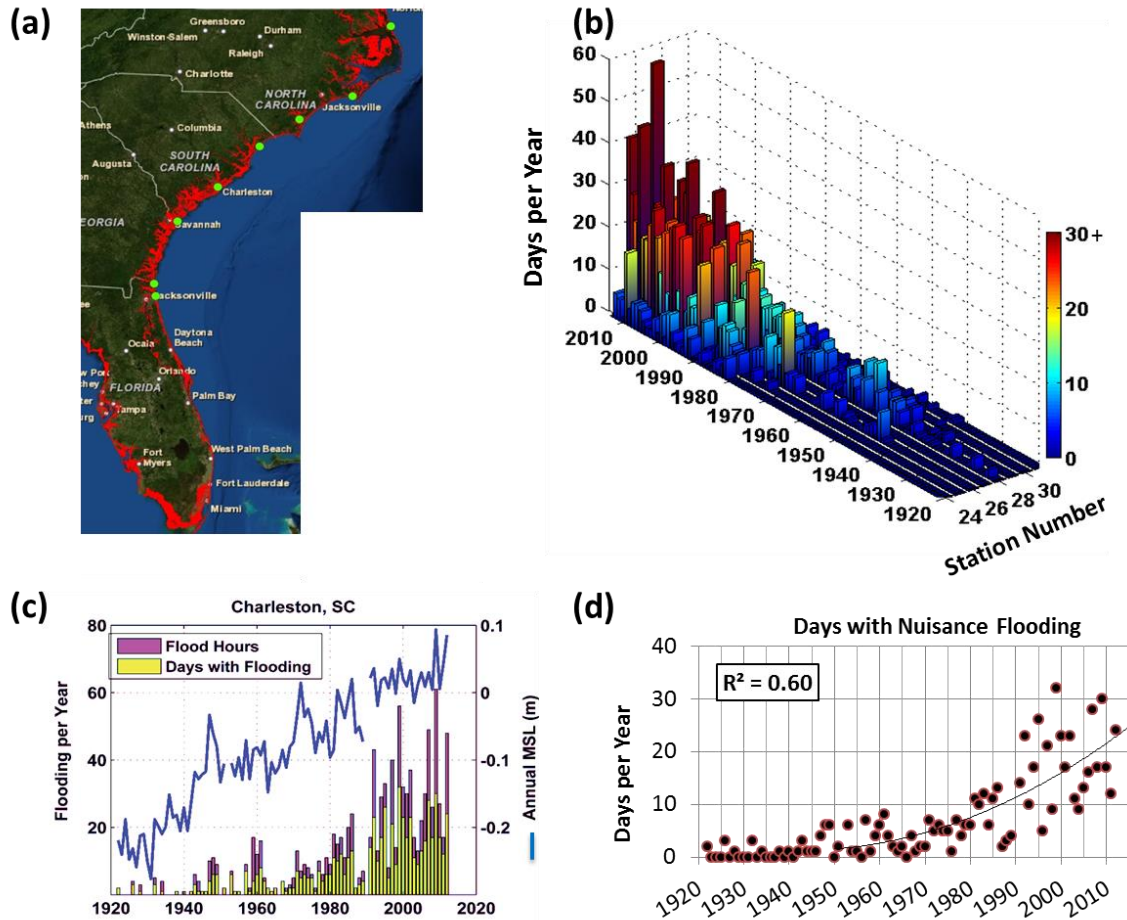


Figure 5. As in Figure 4, but for the Southeast U.S. coastline that includes 8 NOAA gauges (24-31) between North Carolina and the Atlantic coast of Florida. Nuisance flood events are shown for Charleston, South Carolina (gauge 28) in (c) and (d).

U.S. Gulf Coast. Along Texas and Louisiana, SLR_{rel} rates are often very high (approximately 5-10 mm/yr) due to land subsidence, which is highest regionally along the Mississippi River Delta and in areas affected by human-induced factors such as subsurface freshwater and oil withdrawal (Holzer and Galloway, 2005). The number of days with nuisance level flooding has also been increasing (Figure 6b), with four of the eight NOAA gauges undergoing response acceleration (Appendix 1), affecting highly developed as well as less-developed regions (Figure 5a). The gauges with highest SLR_{rel} (Galveston and Sabine Pass, Texas) do not, however, correspond to the gauges with the current highest number of nuisance events (Figure 2), since their nuisance flood level elevations are higher (Figure 1). It is possible that the higher levels reflect current flood defense mitigation measures. The NOAA gauge at Naples, Florida shows recent multi-decadal increases in nuisance flood hours and days (Figure 6c) similar to the Atlantic regions, though with large interannual variability (Figure 6d).

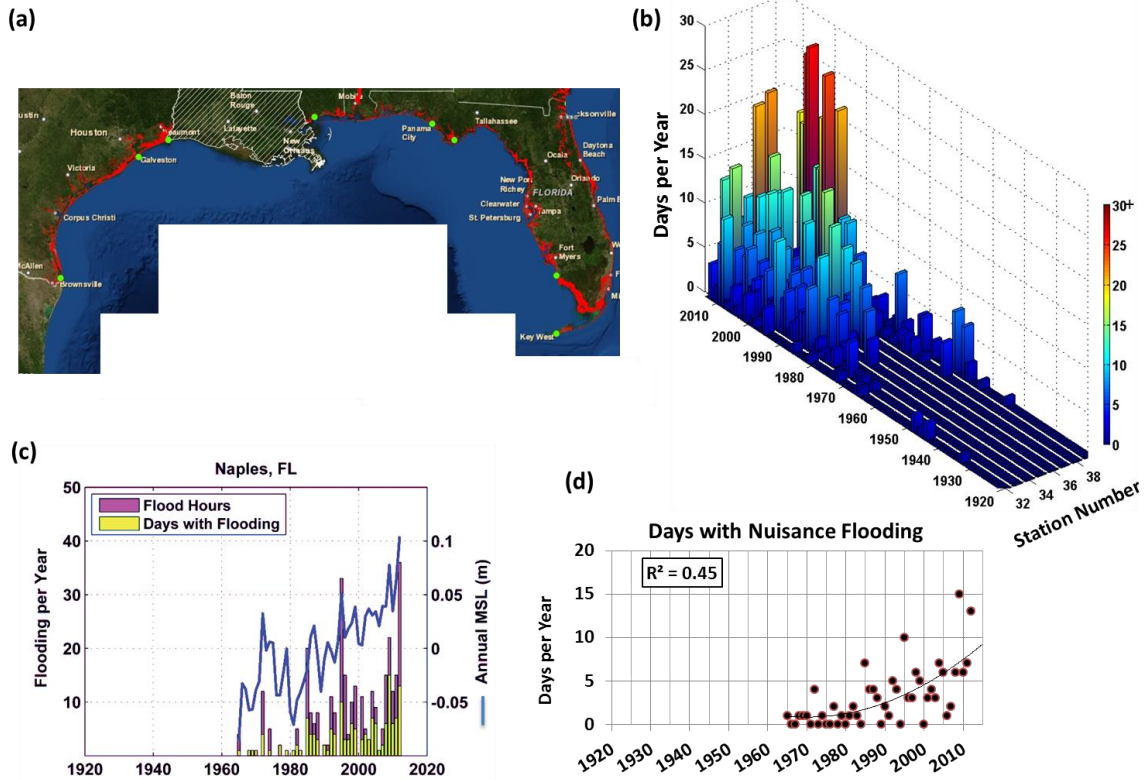


Figure 6. As in Figure 4, but for Gulf Coast that includes 8 NOAA gauges (32-39) between Florida and Texas. Nuisance flood events are shown for Naples, Florida (gauge 33) in (c) and (d). Note, Louisiana has not yet been mapped by the NOAA Sea Level Viewer and is shown with cross-hashes.

U.S. West Coast. Along the U.S. West Coast, long-term SLR_{rel} rates are generally less than along the Gulf and East Coasts (Table 1). Here, vertical land subsidence is not a significant contributor and there has also been a small apparent decrease in SLR rates over the last several decades (NRC, 2012). This slowdown is attributed to a wind-forced response associated with the negative phase of the PDO (Bromirski et al., 2011), also involved in recent SLR rate increases within the tropical western Pacific basin (Merrifield et al., 2012). Another important factor is that ENSO drives large year-to-year MSL variability, such as the MSL rise during the last strong El Niño event in 1997 (discussed below in “...year-to-year differences...” section). As such, the trend in nuisance flood days has been more gradual since the 1980s as compared to other regions (Figure 7b). The West Coast is unlike the Gulf and East Coasts with its narrow continental shelf that prohibits large wind-driven storm surge setups and has steeper inland topography, which limits the amount of land exposed to potential coastal flooding (Figure 7a). However, this region does have a significant wave climate and is susceptible to wave impacts (Ruggiero, 2013), whose effects are generally not measured by gauges and not necessarily associated with *tidal nuisance flooding*. The high values in Figure 7b occur at NOAA gauge 45 in Honolulu, Hawaii, which is in the middle of the North Pacific Ocean, and reflect its lower nuisance flood elevation threshold (Table 1). In Figure 7c, nuisance flood hours and days at La Jolla, California are shown. The MSL plot (blue line in Figure 7c) reveals the timing and extent of the apparent SLR slow-down starting in the 1980s. Large year-to-year variability can be observed in both MSL and nuisance

event frequency and reflects ENSO-forcing. The scatter plot shown in Figure 7d reveals a linear increase over time, but is quite noisy (lower R^2 values) due to the interannual variability.

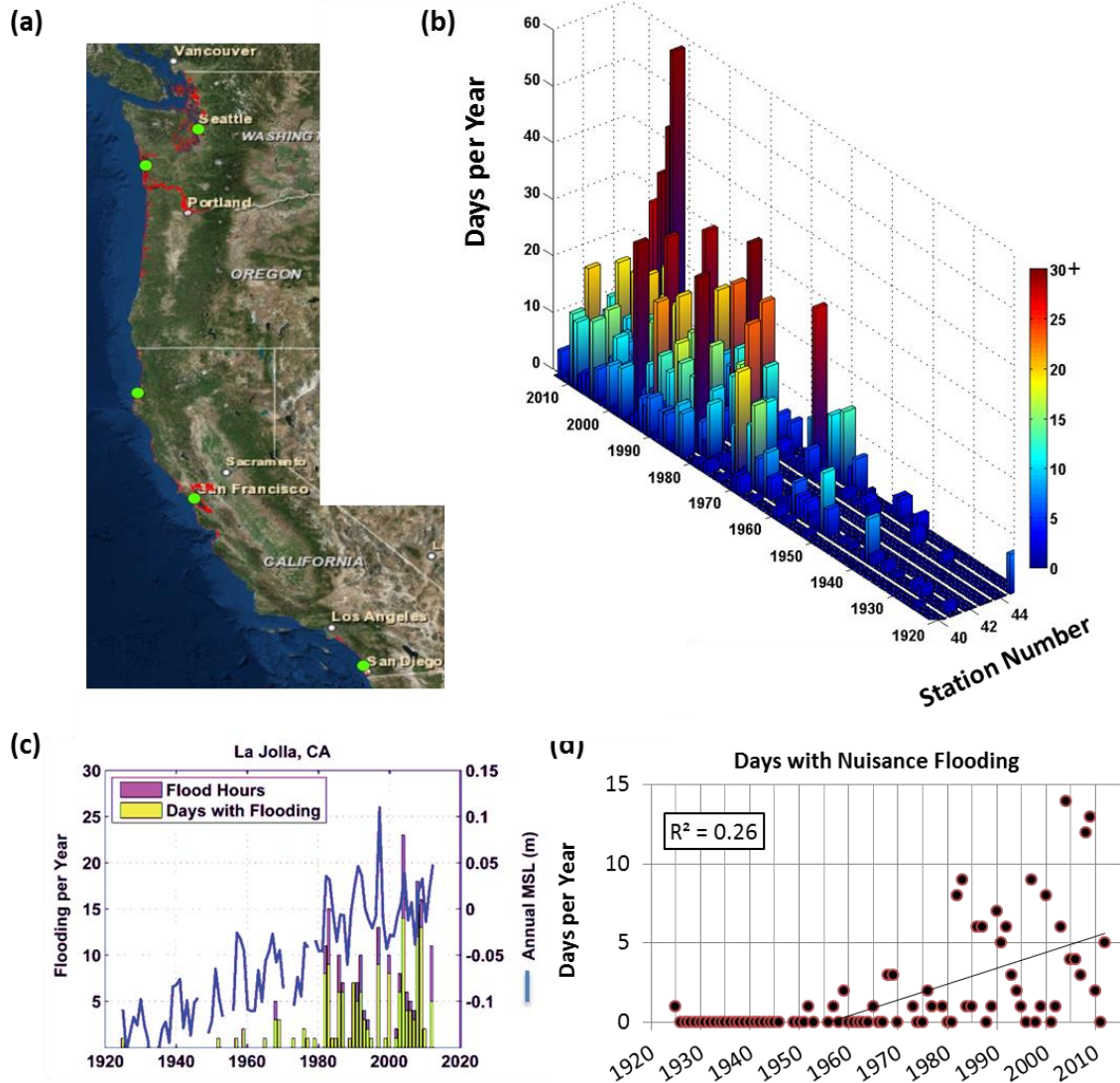


Figure 7. As in Figure 4, but for U.S. Pacific coastline that includes 5 NOAA gauges (40-44) between California and Washington and gauge 45 at Honolulu, Hawaii (not shown in (a)). Nuisance flood events are shown for La Jolla, California (gauge 40) in (c) where the number of days per year with nuisance flooding is best fit by linear regression.

Historical SLR_{rel} and Changing Nuisance Flood Event Probabilities

Here we examine how nuisance level events have changed over time in terms of their probability of recurrence (bottom left plots in Appendix 2), since this type of estimate is useful for risk-exposure planning (Marbaix and Nicholls, 2007). In the mid-20th century (e.g., the year 1950) when MSL was lower, a more extreme event would have been required to drive water levels to the nuisance flood level elevation. In 1950, events causing nuisance flooding generally had

return periods between approximately 1-5 years (black dash and yellow-magenta dash line intersections in Appendix 2 plots; Figure 8b). Since then, SLR_{rel} has increased the reach of high tides (i.e. MHHW tidal datum elevation) and lesser-magnitude storms can more readily cause observable impacts. By 2012 (Figure 8a), the probabilities of a nuisance flood event have increased throughout much of the U.S., with return periods typically <0.25 year (3 months) at most NOAA gauges.

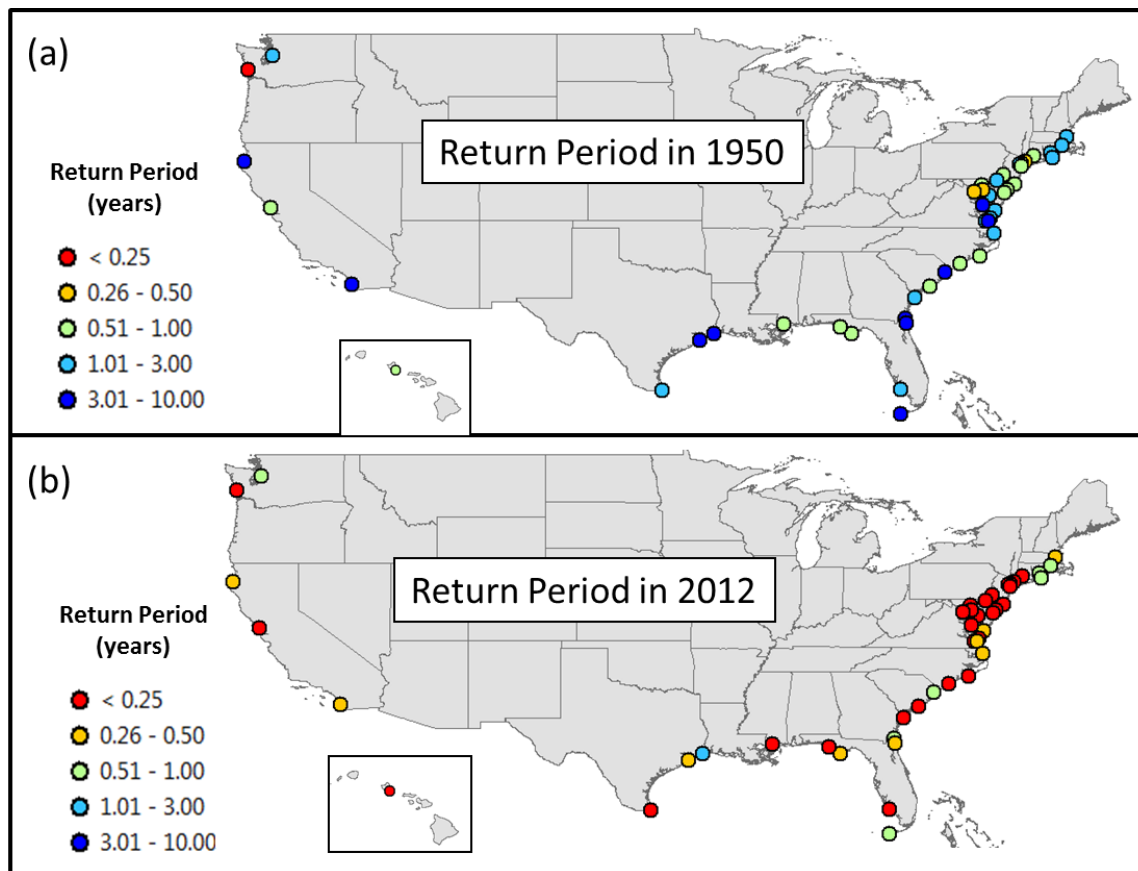


Figure 8. Return Periods of nuisance level flood events in (a) 1950 and (b) 2012 at NOAA gauges.

Patterns Associated with Year-to-Year Differences in Nuisance Flood Frequency

Superimposed upon the long-term changes in nuisance flood frequencies are noticeable year-to-year variability present across the regions. Year-to-year variability occurs in response to prolonged regional-scale MSL changes and/or differences in typical storm-track patterns (i.e., *storminess*). Diagnosing physical drivers of each gauge’s response is beyond the scope of this report. However, there are some broad and recognizable patterns in both MSL and nuisance flood event frequency (Figures 4-7; Appendix 2) related to ENSO. We use the Oceanic Niño Index (ONI) since it is operationally tracked and updated by NOAA (http://www.cpc.ncep.noaa.gov/products/analysis_monitoring/ensostuff/ensoyears).

Along the U.S. West Coast, NOAA gauges’ MSL vary coherently (Chelton and Davis 1982) with high (low) MSL and number of days with nuisance flooding corresponding to ENSO warm

El Niño (cool La Niña) like conditions (e.g., Figure 7b). Recent pronounced El Niño events occurred during the years (meteorological) of 1972, 1982, 1986/87, 1991, 1997, 2004 and 2009 (Figure 9a). El Niño is characterized by a deepened thermocline along the eastern Pacific boundary off of the U.S. West Coast from poleward-propagating Kelvin waves and wind-forced shelf processes resulting in an elevated sea level anomaly for months at a time (Enfield and Allen, 1980; Chelton and Davis, 1982; Miller et al., 1997). During a pronounced El Niño, nuisance flooding often occurs during periods of elevated perigean-spring (aka “King”) tides. Conditions during notable La Niña, such as 1984, 1988, 1998-2000, 2007 and 2010/11 are characterized by lower MSL and less nuisance flooding. Figure 9a illustrates the U.S. West Coast MSL-ENSO relationship with data from the NOAA gauge in San Francisco, CA. It can be seen that MSL, which has been detrended by its long-term SLR_{rel} rate and smoothed by a 5-month running mean filter, changes according to ENSO phase by 10-20 cm in magnitude. Close inspection of Figure 7c (and other West Coast gauges in Appendix 2) shows a similar pattern of elevated (lower) MSL and number of days with nuisance level flooding during warm or El Niño (cool or La Niña) conditions. The ENSO relationship is slightly obscured by the effect of the SLR_{rel} trend itself, which gradually elevates MSL, thereby increasing the likelihood of more days above the nuisance flood level in time.

Although ENSO does not have a direct oceanic impact along the U.S. Northeast Coast as it does along the West Coast, a global *teleconnection* (e.g., atmospheric-to-oceanic) impact is felt. ENSO has been shown to affect year-to-year differences in frequency of winter extratropical storms (Hirsch et al., 2001; Eichler and Higgins, 2006). Storms tend to have an increased (decreased) likelihood to track northeastward along the U.S. East Coast during the warm (cool) ENSO phase, more heavily impacting the coastal regions north of Cape Hatteras, NC (Eichler and Higgins, 2006; Thompson et al., 2013). Sweet and Zervas (2011) showed that during cool months (October–April) of stronger El Niños since 1960, there was a much higher incidence of days with average NTR (approximate storm surge) values >0.3 m (approximately 1 foot) and higher MSL along the Mid-Atlantic Coast than during neutral or cool La Niña-like conditions. This occurred in response to changes in regional sea level pressure fields over Eastern Canada and the Gulf of Mexico, which steered a more zonal jet stream and extratropical storm track along the East Coast and strengthened the northerly component of the prevailing wind fields off the U.S. Northeast Coast. An annual (meteorological) count of daily mean NTR values >0.3 m is shown at Sewells Point, Virginia (Figure 9b) to illustrate the relationship found by Sweet and Zervas (2011). Similar NTR results exist at other Mid-Atlantic locations, and this pattern increases the likelihood for nuisance level flood events independent of spring high-tide synergy. At Atlantic City, New Jersey (Figure 4c) and elsewhere along the mid-Atlantic Coast (Appendix 2), years of stronger El Niños (listed above) are associated with elevated MSL and progressively higher incidences (i.e., also affected by SLR_{rel} trend) of nuisance flood events.

Along the Southeast Atlantic Coast, the annual MSL and nuisance level event response to ENSO are less defined, and they are largely unrecognizable along the Gulf of Mexico Coast. However, during the last strong El Niño in 2009, many gauges showed a similar response (i.e., elevated MSL and/or nuisance flood events) though not necessarily from the same underlying processes. In these regions as well as the Northeast Coast, MSL and nuisance flood frequencies have remained elevated since the 2009 El Niño. Within the Northwest Atlantic Ocean (region offshore U.S. Northeast Coast), significant sea surface warming has occurred since 2000 and has been exceptionally warm since 2012. This ocean warming is associated with the mostly concurrent

negative phase of the North Atlantic Oscillation (NAO) (Xue et al., 2013) coupled with an observed northward shift in the jet stream and reduced evaporative cooling (Chen et al., 2014) whose net effect has deepened the thermocline and raised sea surface heights. The East Coast warming may also be linked to the multi-decadal rate increases in regional mean SLR trends (Ezer and Corlett, 2012; Boon 2012) and Gulf Stream system dynamics (Sallenger et al., 2012; Knop, 2013).

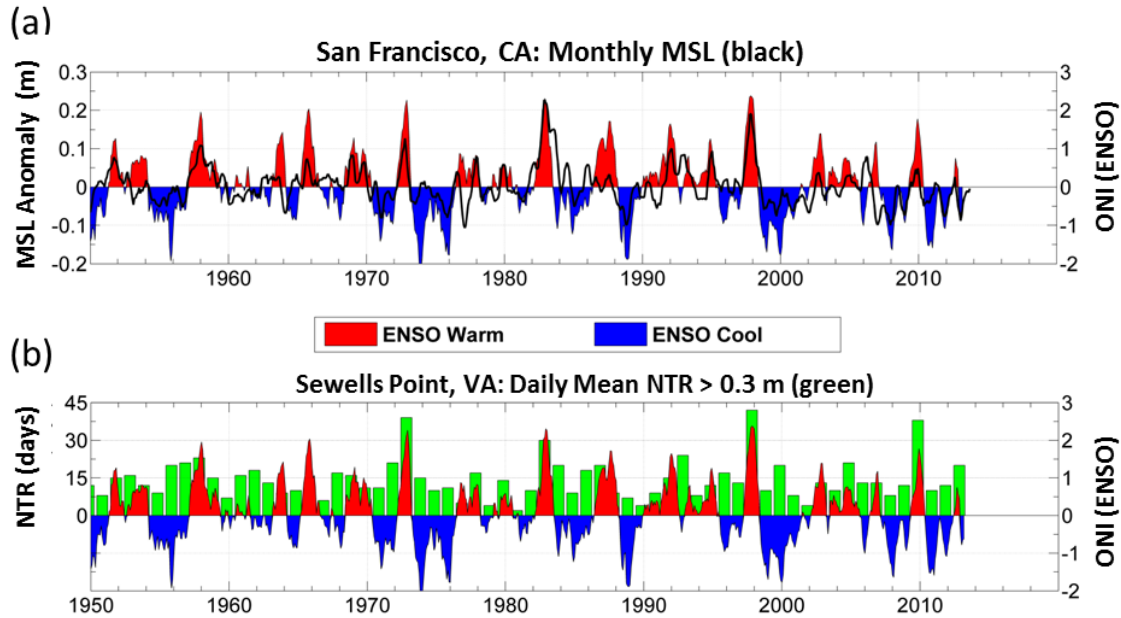


Figure 9. The Oceanic Niño Index (ONI) plotted with (a) monthly MSL (black line) from San Francisco, California that has been detrended and smoothed by a 5-month running filter and (b) annual counts of daily average nontidal residual (NTR; green bars) > 0.3 m at Sewells Point, Virginia.

Seasonal Pattern of Nuisance Flood Events and Underlying Processes

In the preceding sections, we show nuisance flood event frequencies increasing in time from SLR_{rel} with large year-to-year variability from MSL and/or storminess changes often related to ENSO. Here, we provide mean climatology patterns for 1980-2009 that describe typical timing of nuisance events during a year. We make no attempt to assess if intra-annual changes are occurring in terms of seasonal MSL changes within the Gulf of Mexico (Wahl et al., 2014). Figure 10 shows the season with the most occurrences of nuisance flood days. Regional differences include a winter-time maximum along the Northeast and Pacific Coasts and a fall-time maximum along the Mid-Atlantic, Southern, and Gulf Coasts. Regionally representative gauges are examined in Figure 11 to assess how the phasing (timing) of low and high-frequency NTR and tidal processes contribute to high-water formation and lead to nuisance flooding. Figures for all gauges are shown in Appendix 2.



Figure 10. Season with highest frequency of nuisance flood days over the 1980-2009 period as shown for each NOAA gauge in Appendix 2.

The season with highest nuisance event frequency reflects upon one or more regionally significant processes. Along the Northeast Atlantic Coast, the winter-time maximum occurs in response to nor'easterly wind storm event (nor'easters) forcing, which is highest between late fall and early spring (Hirsch et al., 2001). As such, NTR frequency and magnitude are enhanced, as is the frequency of nuisance flood events along much of the mid-Atlantic. This pattern is highlighted at the Battery, New York, where a >30 cm changing NTR cycle (green line, Figure 11a) outweighs the approximately 15-cm MSL cycle (blue dash), which is out of phase to the NTR cycle and forms in response to seasonal heating (e.g., coldest in winter, warmest by late summer). The tide component shows little seasonal variability in its tide range (blue line is fairly flat). Two NOAA gauges (Washington D.C. and Philadelphia, Pennsylvania), whose levels are influenced by riverine discharge, reveal spring-time maxima (Figure 10, green dots) associated with increased river flows.

Along the Southeast Atlantic Coast, nor'easters as well as the infrequent hurricane strike can elevate sea level; however, typically their NTR signal is less frequent or short-lived, and the net contribution (e.g., after 30-day filter smoothing) is less pronounced than in the Northeast. The transition to a fall-time maximum southward along the East Coast (Figure 10) occurs largely in response to changing strength and phasing of the MSL cycle. The MSL cycle has a prominent peak in mid-fall, which is ≥ 0.25 m higher than in mid-winter (blue dash, Figure 11b). The fall-time maximum in the MSL cycle enables modest storm surges to more readily produce nuisance level events. Similar to the Northeast, the spring tide range has little seasonal variability.

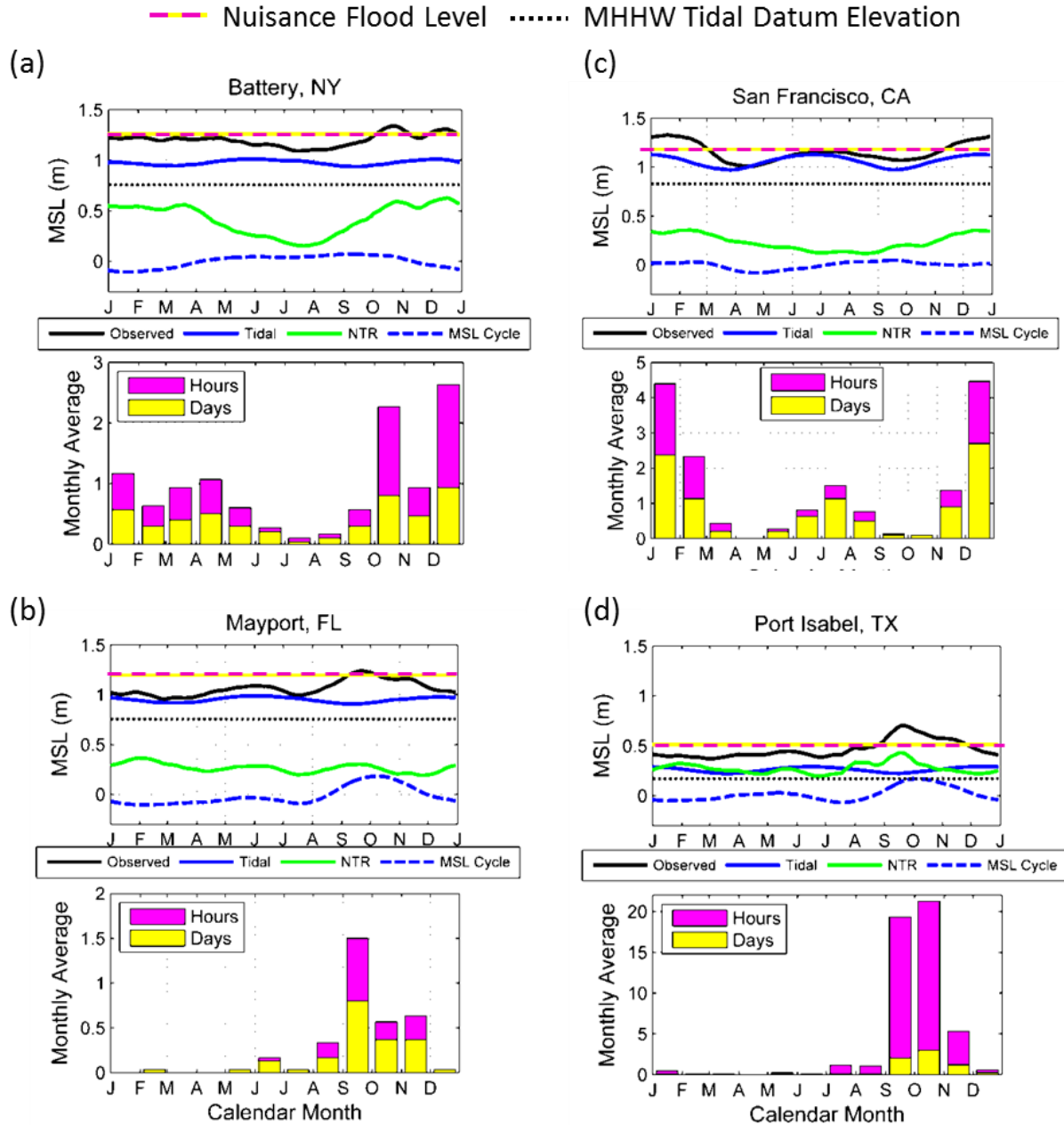


Figure 11. Maximum observed water levels per calendar day over the 1980-2009 period decomposed into a low-frequency MSL cycle, predicted tide (without the annual and semi-annual harmonic fits) and remaining nontidal residual (NTR) all smoothed by a 30-day running filter shown for (a) the Battery, New York, (b) Mayport, Florida, (c) San Francisco, California and (d) Port Isabel, Texas. All series are relative to their station MSL datum and plotted with the nuisance flood level (yellow-magenta line) and MHHW datum elevation (black dot-dash). In the bottom plots, the number of nuisance flood hours and days (shared y-axis) are averaged by calendar month between 1980 and 2009.

Along the Gulf Coast, the NTR is a more significant high water contributor, similar in magnitude to the rather small tide range. Similar to the Southeast Atlantic Coast, the NTR reveals little seasonal variability, except for the infrequent fall-time NTR spike associated with tropical storms (see Appendix 2 for gauges with much higher nuisance hours than impacted days). Also,

the MSL cycle is quite pronounced and similar in magnitude to the NTR. Collectively, the MSL cycle and NTR patterns create the observed water level maxima (black line) in the fall, exacerbating hurricane impacts and the frequency of nuisance flood events. Similar to the Southeast and Mid-Atlantic Coasts, where seasonal changes of the Gulf Stream System drive concurrent geostrophic-related MSL changes along the Mid-Atlantic (Sweet et al., 2009; Ezer et al., 2013), the annual cycles of MSL in the Gulf and Loop Current System also co-vary. Figure 12a shows an inverse relationship between seasonal cycles of MSL at Mayport, Florida and Port Isabel, Texas (some apparent lag) and volume transport (in Sverdrup, Sv = 10^6 m³/sec) of the Florida and Yucatan Currents (data: www.aoml.noaa.gov/phod/altimetry/cvar), which feed the Gulf Stream and Loop Current, respectively. MSL and volume transport are computed using data from 2000-2009 and are shown relative to their mean value over this period.

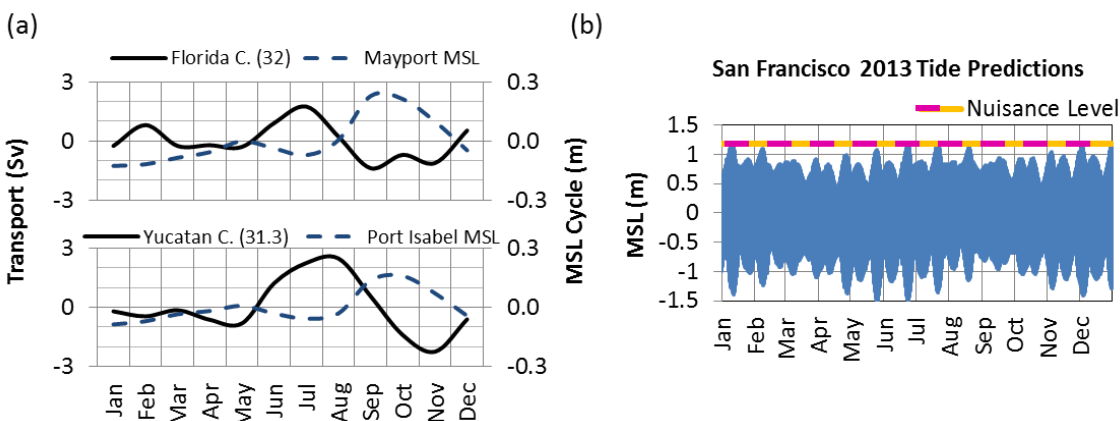


Figure 12. (a) Monthly mean volume transport of the Florida and Yucatan Currents over the 2000-2009 with their means in parenthesis that reveal a geostrophic-related inverse relationship to MSL cycle at Mayport, Florida and Port Isabel, Texas, respectively. In (b) are hourly astronomic tide predictions for San Francisco, California showing semi-annual spring tide strengthening during the winter and summer solstice time frames, which reach the nuisance flood level.

Along the West Coast, the spring-tide range is a more substantial component than along the East or Gulf Coasts. The tide cycle has a larger (15 cm at San Francisco in Figure 11c) semi-annual strengthening near the times of perigean spring tides during the winter and summer solstices (Figure 12b), which is typical for much of the Northern Pacific Ocean (Merrifield et al., 2007). Regionally, the MSL annual cycle has a spring-time low from wind-driven upwelling. The NTR component is elevated during the fall-spring stormy season, and more so along the Pacific Northwest Coast (Allan and Komar, 2006), where winter storms track east from the Aleutian Low atmospheric center of action. But, compared to the other regions, the NTR is generally of less significance than the tide contribution due to the narrow continental shelf along the West Coast that inhibits the wind-driven component of storm-surge buildup. Large wave events typically cause most impacts along the West Coast and Pacific Islands (Ruggiero, 2013; Hoeke et al., 2013). In response, nuisance flood events are more frequent at times of highest “king tides” along the West Coast and Pacific, and more so in the winter, due to the addition of the higher NTR contribution.

A ratio comparing the mean of the NTR contribution (green line) and the maximum water level observation (black line in top plot of Figure 11) is helpful in assessing the significance of

individual components of high-water and nuisance flooding. A low ratio, as described by Marra et al. (2012) and Merrifield et al. (2013), helps identify regions where the tide range is a much larger contributor than the NTR magnitude (Figure 13a). These regions include the West Coast (and Honolulu) where the NTR component is small (narrow continental shelf), as well as sections of the Southeast and Northeast Atlantic Coast, where the tide range is large. Mid-Atlantic gauges have larger NTR components and mid-range valued ratios (e.g., due to nor'easter storm surges along a wide continental shelf). The Chesapeake Bay and the Gulf of Mexico Coasts have large ratios, higher relative importance of the NTR compared to the tidal range.

The ratio in Figure 13a can also be used to help predict when a nuisance flood might form; regions where the ratio is small, higher tides tend to be the event driver, whose timing is readily predicted by NOAA (e.g., http://tidesandcurrents.noaa.gov/tide_predictions). In other regions, higher NTR contributions generally occur concurrently. A “NTR of concern” (Figure 13b) provides an estimate for the 1980-2009 period of the height of the nuisance flood level (yellow-magenta line) above the mean tide height (blue line) during maximum water level (smoothed, black line), as shown in Figure 11 and in Appendix 2. A smaller value in Figure 13b is of more concern because less *freeboard* exists.

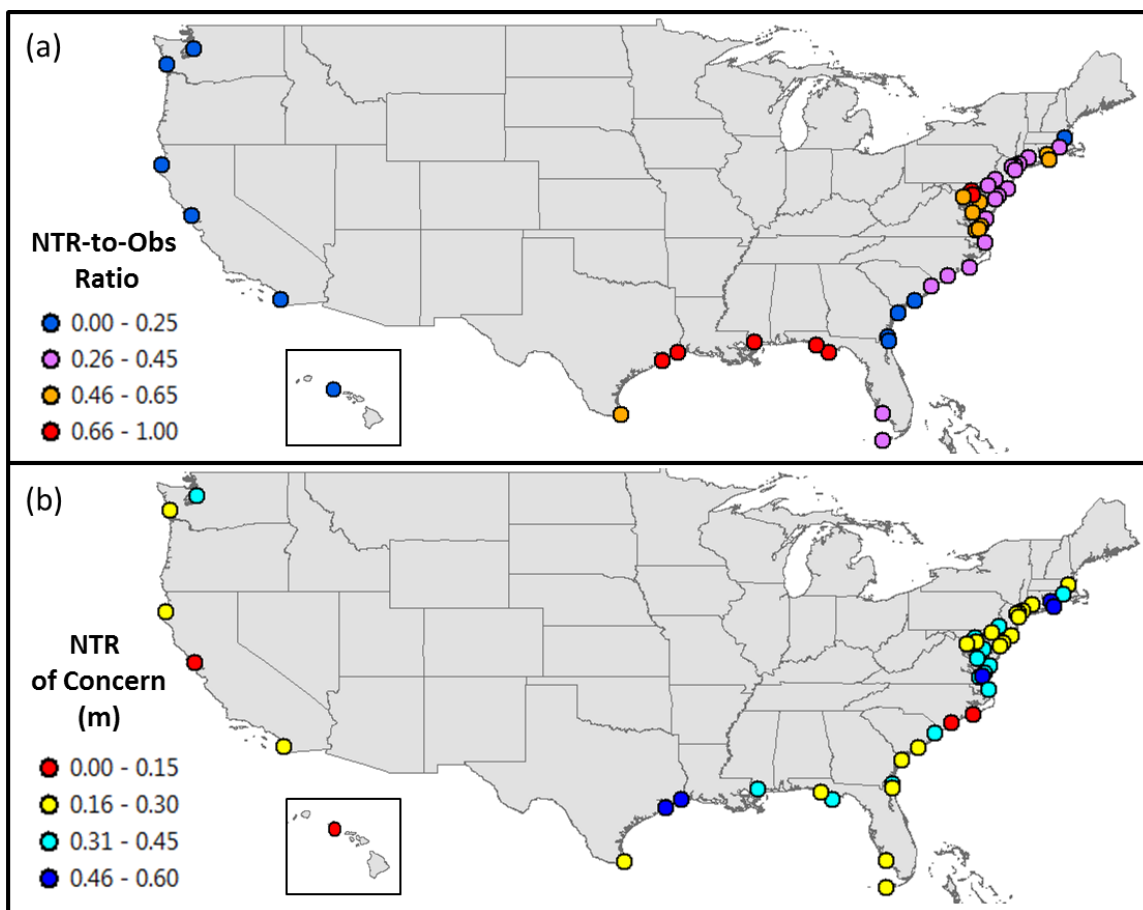


Figure 13. Calendar-day maxima over 1980-2009 (i.e., as shown in top plots of Figure 11a-d) are averaged to estimate (a) a ratio between the average of the NTR during (divided by) maximum water level and (b) the distance between the NOAA gauge’s nuisance flood level and the average tidal contribution during maximum water level.

CONCLUDING REMARKS

NOAA water level gauges have been measuring water levels around the U.S. for over a century. Their observations clearly show that much of the U.S. is experiencing long-term SLR_{rel} (<http://tidesandcurrents.noaa.gov/sltrends>), which has been steadily increasing the effects of extreme events through time and exacerbating their frequency relative to fixed elevations. What is becoming more noticeable and widespread are the high-tide flood events that many coastal regions are now perennially experiencing. These impacts *today* are generally minor, localized and a *nuisance* to the communities in which they occur. These events are typically recognized as repetitive flooding of coastal roadways and private and commercial properties during certain times of the year. When concurrent with localized rainfall or a wind-forced storm surge, impacts are worse, overwhelm storm water drainage systems and further stress other vulnerable public works (<http://csc.noaa.gov/tidalfloodingvis>). The extent and frequency of nuisance tidal flooding is of growing concern due to on-going SLR_{rel} and likely future rate acceleration from ocean heating and land-ice melt (Church et al., 2013; Parris et al., 2012).

In this report we show that the duration and frequency of nuisance-tidal flooding is intensifying around the U.S. We use the NOAA NWS WFO “minor” threshold elevation for coastal flooding impacts as our *nuisance flood level*, which have been empirically calibrated to specific water level gauge elevations based upon local historical impact monitoring. Moderate and major impact thresholds are also assigned by NOAA NWS WFOs (<http://water.weather.gov/ahps>). There are approximately 75 NOAA gauges around the U.S. with empirically defined flood level thresholds, and of those, we analyze 45 gauge records (including one gauge in Honolulu whose level is defined locally by PacIOOS researchers). The coastal regions potentially exposed to flooding at these elevations are shown under the “Flood Frequency” tab of the NOAA Sea Level Viewer (<http://csc.noaa.gov/slr/viewer/>).

We derive two measures—cumulative duration (hours) and number of days exceeding the nuisance flood level threshold per year—to provide estimates of *today’s* impact rate and how this rate has grown in time. We note several regionally consistent relationships (below).

Relationships of societal importance

1. *The lower the threshold, the higher the yearly frequency of nuisance flooding events.* The annual number of days currently (2007-2009 average) impacted by nuisance level flooding is highly (negative) correlated to the height of the flood threshold elevation (Figure 2b).
2. *The frequency of nuisance flooding events is increasing and accelerating in many locations.* The annual number of days impacted by nuisance flooding is increasing at an accelerated rate along much of the U.S. East and Gulf Coasts.
3. *The rate of (above) acceleration is higher as the gap lessens between the local flood threshold elevation and MHHW.* Acceleration (quadratic) constants characterizing how nuisance flood days change over time (Appendix 1) versus the nuisance flood levels reveals a strong negative correlation ($p < 0.01$) for East Coast gauges (Figure 14).

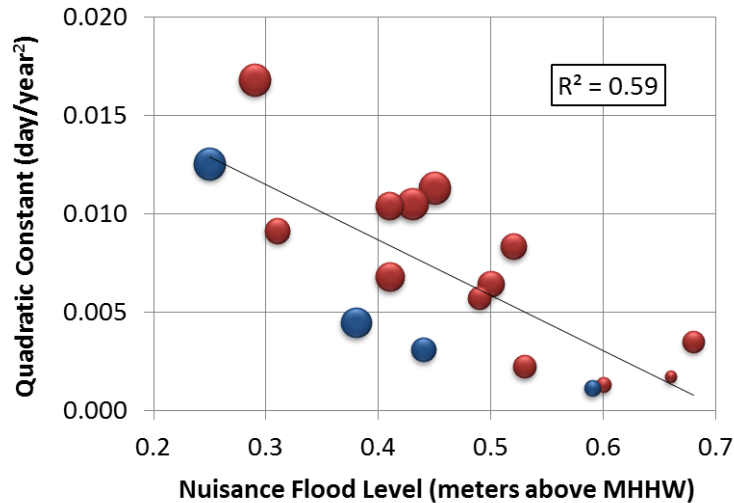


Figure 14. Bubble plot of nuisance flood level (x -axis) versus quadratic constant (b_2 ; y -axis) from fit of annual number of nuisance flood days listed in Appendix 1 for East Coast (NE region in red and SE region in blue) gauges. Bubble size represents the goodness-of-fit (R^2) of each quadratic model fit. Only gauges with significant quadratic fits and hourly data starting prior to 1960 (Appendix 1) are included to minimize quadratic curve-fitting discrepancies due to gauge record length.

Relationship (3) occurs as SLR_{rel} increases the rate of annual-event exceedances above the elevation thresholds characterized by exponential growth in the water level distribution (e.g., elevations between the nuisance flood level and MHHW in Figure 3). Relationship (2) depends upon the extent of annual variability in local MSL respective to a gauge's SLR_{rel} trend. The West Coast is different than the Gulf and East Coasts due to direct forcing of ENSO, which creates prolonged changes in MSL with large year-to-year variability. Strong El Niños like the 1982 and 1997 events (meteorological years) drive 0.2-0.3 m MSL anomalies for months (e.g., Figure 9, though MSL has been smoothed) and a spike in days with nuisance level flooding (e.g., Figure 7c). Moreover, since the last strong 1997 El Niño, MSL along the West Coast has remained relatively stationary due in part to PDO-related factors (Bromirski et al., 2011) and changes in nuisance flood event frequency, which is best characterized as a linear increase with higher signal variance (lower R^2). Along the U.S. East Coast, strong El Niños increase storm-surge frequency (Sweet and Zervas, 2011; Thompson et al., 2013), but MSL is less affected, typically though the preponderance of storm surges. But, East Coast MSLs have been steadily increasing over the last several decades (e.g., Figure 3c), and the event rate of nuisance flood events is accelerating and well characterized by a quadratic relationship (Appendix 1, Figure 14). Year-to-year differences in storm surge frequency are presumed of lesser importance, since this process has a more stationary behavior than MSL, which is rising (e.g., Zhang et al., 2000). Interannual storm surge variability might be a factor in some regions like the Gulf Coast where the tide range is small and nuisance flood level elevations can be relatively high. All of these considerations may help explain why not all approximately 75 NOAA gauges with NWS-defined nuisance flood levels show discernable time-dependent trends.

In terms of event probabilities, nuisance flood events have clearly changed over time, for instance since the 1950s, when many coastal regions were developing. In 1950, such events would have the probability of recurring every couple of years (Figure 8), whereas today, they

occur so frequently due to decades of SLR_{rel} that they are no longer classified as an *extreme* event. To better plan for these recurring impacts, we have quantified the season that typically has the highest occurrences of nuisance flooding during the year (Figure 10) and highlighted the related physical forcing processes (Figure 11). In regions like the West Coast, where storm surge magnitudes are bathymetrically constrained by the narrow continental shelf, nuisance flooding is more tidally controlled (Figure 13a) and readily predictable using NOAA Tide Predictions (http://tidesandcurrents.noaa.gov/tide_predictions). In regions like the Gulf Coast and Chesapeake Bay, nuisance flooding typically happens at higher tide levels, but a substantial NTR contribution is also needed, either from a local storm or a longer-term regional event contributing to a *quiet* sea level (NTR) anomaly (e.g., Sweet et al., 2009). We have quantified a typical NTR contribution required during periods of higher tidal range (spring tides) to cause local nuisance level flooding (Figure 13b).

Together, the *relationships of societal importance* might be further refined to more broadly assess potential impacts from tidal-related coastal flooding over a range of elevations. Such a refinement might permit flood frequency and duration estimates at particular thresholds for locations lacking a nearby water level gauge but having a local tide datum as provided by the NOAA Vertical Datum Transformation Tool (vdatum.noaa.gov). These relationships are not intended to explicitly determine where and for how long minor flooding will occur, since local baseline hydrologic conditions vary with the weather and by topo-bathymetric and land-cover response characteristics. The relationships do establish a degree of susceptibility for large regions of the U.S. Coast to coastal flooding at various elevations above *today's* high tide.

In closing, it is important to stress that SLR_{rel} exacerbates impacts over a range of elevation thresholds relative to *today's fixed reference frame* (e.g., Figure 3c). At very high thresholds, such as those of the 100-year event experienced during rare hurricane strikes (not observable in Figure 3c), SLR_{rel} has and will continue to nonlinearly compress recurrence probabilities in the future because smaller (with higher probability) storm surges will be able to impact similar elevations. The same is true for impacts from lesser extremes or nuisance-like tides, which we describe here in terms of average annual frequency and duration. We find that with lower threshold elevations, nuisance-level events are more commonplace and their event frequencies change in time at increasingly higher rates (Figure 14) simply from linear SLR_{rel} . Any acceleration in SLR_{rel} will only further intensify inundation impacts over time, and will further reduce the time between flood events. It is therefore apparent that a time horizon exists, largely dependent upon the local rate of SLR_{rel} , when critical elevation thresholds for various public/private/commercial serving systems will become increasingly compromised by tidal flooding in the future. We stress that in many areas, *the frequency of nuisance flooding is already on an accelerating trajectory, and many other locations will soon follow even with a continuation of linear SLR_{rel} rates*. This fact needs to be recognized, as it is critical for coastal planning entities to prevent critical-system degradation from SLR impacts and to promote resiliency efforts in general.

RECOMMENDATIONS

Continued research of trends and patterns associated with nuisance coastal flooding should help identify regionally important processes (e.g., tide variations, ENSO influences, ocean current circulation, etc.) involved in event occurrence to facilitate near-term predictions and seasonal outlooks of their potential impacts. Systematic score-keeping of locally important (e.g., sector-specific) threshold exceedances at NOAA gauges by communities would permit monitoring for important frequency changes in tidal-related flooding. Coupled with new, innovative, crowd-source-like technologies (e.g., various “King Tide websites”), this effort would help spatially delineate vulnerabilities, allowing for better local (street-level) calibration/validation of model-based decision tools. In short, tracking sensible indicators of SLR_{rel} like nuisance tidal flooding and recognizing their impacts will heighten awareness, bridge today’s perceptions with a community’s living memory, and facilitate planning and resiliency efforts.

ACKNOWLEDGEMENTS

We would like to thank Doug Marcy, Matt Pendleton, and Billy Brooks of NOAA’s Coastal Services Center (CSC) for reviewing this report, providing the high resolution graphics in Figures 4a, 5a, 6a, 7a, and advancing the idea of investigating recurrent tidal flooding using NWS thresholds in the geographic/spatial (mapping) display of the NOAA Sea Level Viewer. We would also like to thank Jeff Williams of the U.S. Geological Survey (USGS), Patrick O’Brien of the U.S. Army Corps of Engineers, and Jayantha Obeysekera of the South Florida Water Management District for their review of this manuscript and constructive comments.

REFERENCES

- Allan, J.C. and Komar, P.D., 2006: Climate controls on US West Coast erosion processes. *J. of Coastal Res.*, 22(3), 511–529. West Palm Beach (Florida), ISSN 0749-0208.
- Boon, J.D.; Brubaker, J.M., and Forrest, D.R., 2010: Chesapeake Bay Land Subsidence and Sea Level Change: An Evaluation of Past and Present Trends and Future Outlook. Special Report No. 425 in *Applied Marine Science and Ocean Engineering*. Gloucester Point, Virginia: Virginia Institute of Marine Science, 42p, Appendices A, B.
- Boon, J. D., 2012: Evidence of sea level acceleration at U.S. and Canadian tide stations, Atlantic Coast, North America, *J. Coastal Res.*, 28, 1437–1445, doi:10.2112/JCOASTRES-D-12-00102.1.
- Bromirski, P.D., A.J. Miller, R.E. Flick, and G. Auad, 2011: Dynamical suppression of sea level rise along the Pacific coast of North America: Indications for imminent acceleration, *J. Geophys. Res.*, 116, C07005, doi: 10.1029/2010JC006759.
- Chelton, D. B., and R. E. Davis, 1982: Monthly mean sea level variability along the west coast of North America, *J. Phys. Oceanogr.*, 12(8), 757–784, doi:10.1175/1520-0485(1982)012.
- Chen, K., G. G. Gawarkiewicz, S. J. Lentz, and J. M. Bane, 2014: Diagnosing the warming of the Northeastern U.S. Coastal Ocean in 2012: A linkage between the atmospheric jet stream variability and ocean response, *J. Geophys. Res. Oceans*, 119, 218–227, doi: 10.1002/2013JC009393.
- Church, J., and N. White, 2011: Sea-level rise from the late 19th to the early 21st century, *Surv. Geophys.*, 32(4), 585–602, doi: 10.1007/s10712-011-9119-1.
- Church, J.A., P.U. Clark, A. Cazenave, J.M. Gregory, S. Jevrejeva, A. Levermann, M.A. Merrifield, G.A. Milne, R.S. Nerem, P.D. Nunn, A.J. Payne, W.T. Pfeffer, D. Stammer and A.S. Unnikrishnan, 2013: Sea Level Change. In: *Climate Change 2013: The Physical Science Basis. Contribution of Working Group I to the Fifth Assessment Report of the Intergovernmental Panel on Climate Change* [Stocker, T.F., D. Qin, G.-K. Plattner, M. Tignor, S.K. Allen, J. Boschung, A. Nauels, Y. Xia, V. Bex and P.M. Midgley (eds.)]. Cambridge University Press, Cambridge, United Kingdom and New York, NY, USA.
- Coles, S.G., 2001. An introduction to statistical modeling of extreme values. London, Springer. 208pp.
- CO-OPS, 2001: Tidal datums and their applications, Special Publication NO. CO-OPS1, NOAA, National Ocean Service Center for Operational Oceanographic Products and Services, 111p, appendix.
- Eichler, T., and W. Higgins, 2006: Climatology and ENSO-related variability of North American extratropical cyclone activity. *J. Climate*, 19, 2076–2093.
- Enfield, D. B., and J. S. Allen, 1980: On the structure and dynamics of monthly mean sea level anomalies along the Pacific coast of North and South America. *J. Phys. Oceanogr.*, 10, 557-578.

- Ezer, T., and W. B. Corlett, 2012: Is sea level rise accelerating in the Chesapeake Bay? A demonstration of a novel new approach for analyzing sea level data, *Geophys. Res. Lett.*, 39, L19605, doi: 10.1029/2012GL053435.
- Ezer, T., L. P. Atkinson, W. B. Corlett, and J. L. Blanco, 2013: Gulf Stream's induced sea level rise and variability along the U.S. mid-Atlantic coast, *J. Geophys. Res. Atmos.*, 118, 685–697, doi:10.1002/jgrc.20091
- Ezer, T., 2014: Why are sea level rise and flooding accelerating along the U.S. East Coast? TechSurge Workshop of the Marine Technology Society (MTS), Norfolk, VA, <http://mtshamptonroads.org/mtshr>.
- Hirsch, M. E., A. T. DeGaetano, and S. J. Colucci, 2001: An East Coast winter storm climatology. *J. Climate*, 14, 882–899.
- Hoeke, R.K., K.L. McInnes, J. Kruger, R. McNaught, J. Hunter, and S. Smithers, 2013: Widespread inundation of Pacific islands by distant-source wind-waves. *Global Env. Change*, 108: 128-138.
- Holzer, T.L., and Galloway, D.L., 2005: Impacts of land subsidence caused by withdrawal of underground fluids in the United States, in Ehlen, J., Haneberg, W.C., and Larson, R.A., eds., *Humans as Geologic Agents: Boulder, Colorado, Geological Society of America Reviews in Engineering Geology*, v. XVI, p. 87–99, doi: 10.1130/2005.4016(08).
- Hunter, J., 2010: Estimating sea-level extremes under conditions of uncertain sea-level rise. *Climatic Change*, 99, 331–350, doi: 10.1007/s10584-009-9671-6.
- Kopp, R.E., 2013: Does the mid-Atlantic United States sea level acceleration hot spot reflect ocean dynamic variability? *Geophys. Res. Lett.*, 40, 3981–3985, doi:10.1002/grl.50781.
- Kruk, M.C., J. J. Marra, P. Ruggiero, D. Atkinson, M. Merrifield, D. Levinson, M. Lander, 2013: Pacific Storms Climatology Products (PSCP): Understanding Extreme Events. *Bull. Amer. Meteor. Soc.*, 94, 13–18. doi: <http://dx.doi.org/10.1175/BAMS-D-11-00075.1>
- Kriebel D. and J. Geiman. 2013: A Coastal Flood Stage to Define Existing and Future Sea-Level Hazards. *J. of Coastal Res.* In-Press.
- Marbaix, P. and Nicholls, R. J. 2007: Accurately determining the risks of rising sea level. *Eos*, Transactions of the American Geophysical Union, 88: 441 – 442.
- Marcy, D. and coauthors, 2011: Flooding Impacts.” In *Proceedings of the 2011 Solutions to Coastal Disasters Conference, Anchorage, Alaska, June 26 to June 29, 2011*, edited by Louise A. Wallendorf, Chris Jones, Lesley Ewing, and Bob Battalio, 474–90. Reston, VA: American Society of Civil Engineers.
- Marra, J. J., Merrifield, M. A., & Sweet, W. V., 2012: Sea Level and Coastal Inundation on Pacific Islands. In V. W. Keener, J. J. Marra, M. L. Finucane, D. Spooner, & M. H. Smith (Eds.), *Climate Change and Pacific Islands: Indicators and Impacts*. Report for the 2012 Pacific Islands Regional Climate Assessment (PIRCA). Washington, DC: Island Press.

- Mendez, F. J., M. Menendez, A. Luceño, and I. J. Losada, 2006: Estimation of the long-term variability of extreme significant wave height using a time-dependent Peak Over Threshold (POT) model, *J. Geophys. Res.*, 111, C07024, doi:10.1029/2005JC003344.
- Menéndez, M., and P. L. Woodworth, 2010: Changes in extreme high water levels based on a quasi-global tide-gauge data set, *J. Geophys. Res.*, 115, C10011, doi:10.1029/2009JC005997.
- Merrifield, M. A., Y. L. Firing, and J. J. Marra, 2007: Annual Climatologies of Extreme Water Levels, paper presented at Extreme Events: Proceedings 15th ‘Aha Huliko’a Hawaiian Winter Workshop, University of Hawaii at Manoa, Honolulu, HI.
- Merrifield, M. A., P. R. Thompson, and M. Lander, 2012: Multidecadal sea level anomalies and trends in the western tropical Pacific, *Geophys. Res. Lett.*, 39, L13602, doi:10.1029/2012GL052032.
- Merrifield, M.A., P. Thompson, R. S. Nerem, D. P. Chambers, G. T. Mitchum, M. Menéndez, E. Leuliette, J. J. Marra, W. Sweet, and S. Holgate, 2013: [Global Oceans] Sea level variability and change [in “State of the Climate in 2012”]. *Bull. Amer. Meteor. Soc.*, 94 (8), S68-S72.
- Merrifield, M. A., A. S. Genz, C. P. Kontoes, and J. J. Marra, 2013: Annual maximum water levels from tide gauges: Contributing factors and geographic patterns, *J. Geophys. Res. Oceans*, 118, 2535–2546, doi:10.1002/jgrc.20173.
- Miller, A. J., W. B. White, and D. R. Cayan, 1997: North Pacific thermocline variations on ENSO timescales, *J. Phys. Oceanogr.*, 27(9), 2023–2039, doi: 10.1175/1520-0485(1997)027.
- National Research Council, 2012: Sea-Level Rise for the Coasts of California, Oregon, and Washington: Past, Present, and Future. Washington, DC: The National Academies Press.
- Park J., Obeysekera J., Irizarry M., Trimble P., 2011: Storm Surge Projections and Implications for Water Management in South Florida, *Climatic Change*, Special Issue: SLR in Florida: An Emerging Ecological and Social Crisis, Volume 107, Numbers 1-2, 109-128,
- Parker, B.B. 1992: Sea level as an indicator of climate and global change. *Mar. Tech. Soc. J.* 25(4): 13–24.
- Parris, A., P. Bromirski, V. Burkett, D. Cayan, M. Culver, J. Hall, R. Horton, K. Knuuti, R. Moss, J. Obeysekera, A. Sallenger, and J. Weiss, 2012: Global Sea Level Rise Scenarios for the US National Climate Assessment. NOAA Tech Memo OAR CPO-1. 37 pp.
- Pawlowicz, R., B. Beardsley, and S. Lentz, 2002: Classical tidal harmonic analysis including error estimates in MATLAB using T_TIDE, *Computers and Geosciences* 28, 929-937.
- Rice, J., 1994: Mathematical Statistics and Data Analysis. 2d ed. Duxbury, 651 pp.

- Rosby, T., C. N. Flagg, K. Donohue, A. Sanchez-Franks, and J. Lillibridge, 2014: On the long-term stability of Gulf Stream transport based on 20 years of direct measurements, *Geophys. Res. Lett.*, 41, 114–120, doi: 10.1002/2013GL058636.
- Ruggiero, P., 2013: Is the intensifying wave climate of the U.S. Pacific northwest increasing flooding and erosion risk faster than sea-level rise? *J. of Waterway, Port, Coastal & Ocean Engineering*, 139, 88–97.
- Sallenger, A. H., K. S. Doran, and P. A. Howd, 2012: Hotspot of accelerated sea-level rise on the Atlantic coast of North America, *Nat. Clim. Change*, 2, 884–888, doi:10.1038/nclimate1597.
- Sweet, W., Zervas, C., and Gill, S., 2009: Elevated East Coast Sea Levels Anomaly: June–July 2009. NOAA Technical Report NOS CO-OPS 051, 28p.
- Sweet, W. V., and C. Zervas, 2011: Cool-season sea level anomalies and storm surges along the U.S. East Coast: Climatology and comparison with the 2009/10 El Niño. *Mon. Wea. Rev.*, 139, 2290–2299.
- Sweet, W.V., C. Zervas, S. Gill, J. Park, 2013: Hurricane Sandy Inundation Probabilities of Today and Tomorrow [in “Explaining Extreme Events of 2012 from a Climate Perspective”]. *Bull. Amer. Meteor. Soc.*, 94 (9), S17–S20.
- Tebaldi, C., B. H. Strauss, and C. E. Zervas, 2012: Modeling sea level rise impacts on storm surges along US coasts. *Environ. Res. Lett.*, 7, 014032, doi:10.1088/1748-9326/7/1/014032.
- Thompson, P. R., G. T. Mitchum, C. Vonesch, J. Li, 2013: Variability of Winter Storminess in the Eastern United States during the Twentieth Century from Tide Gauges. *J. Climate*, 26, 9713–9726. doi: <http://dx.doi.org/10.1175/JCLI-D-12-00561.1>.
- Wahl, T., F. M. Calafat, and M. E. Luther, 2014: Rapid changes in the seasonal sea level cycle along the US Gulf coast from the late 20th century, *Geophys. Res. Lett.*, 41, 491–498, doi: 10.1002/2013GL058777.
- Xue and coauthors, 2013: Sea surface temperature [in "State of the Climate in 2012"]. *Bull. Amer. Meteor. Soc.* 94(8), S111-146.
- Zervas, C., 2009: Sea Level Variations of the United States 1854–2006. NOAA Technical Report NOS CO-OPS 053, 75p, Appendices A–E.
- Zervas, C., 2013: Extreme Water Levels of the United States 1893-2010. NOAA Technical Report NOS CO-OPS 67 56p, Appendices I-VIII.
- Zervas, C., S. Gill, and W. V. Sweet, 2013: Estimating vertical land motion from long-term tide gauge records. NOAA Tech. Rep. NOS CO-OPS 65, 22 pp.
- Zhang, K., B. C. Douglas, and S. P. Leatherman, 2000: Twentieth century storm activity along the U.S. East coast. *J. Climate*, 13, 1748–1760.

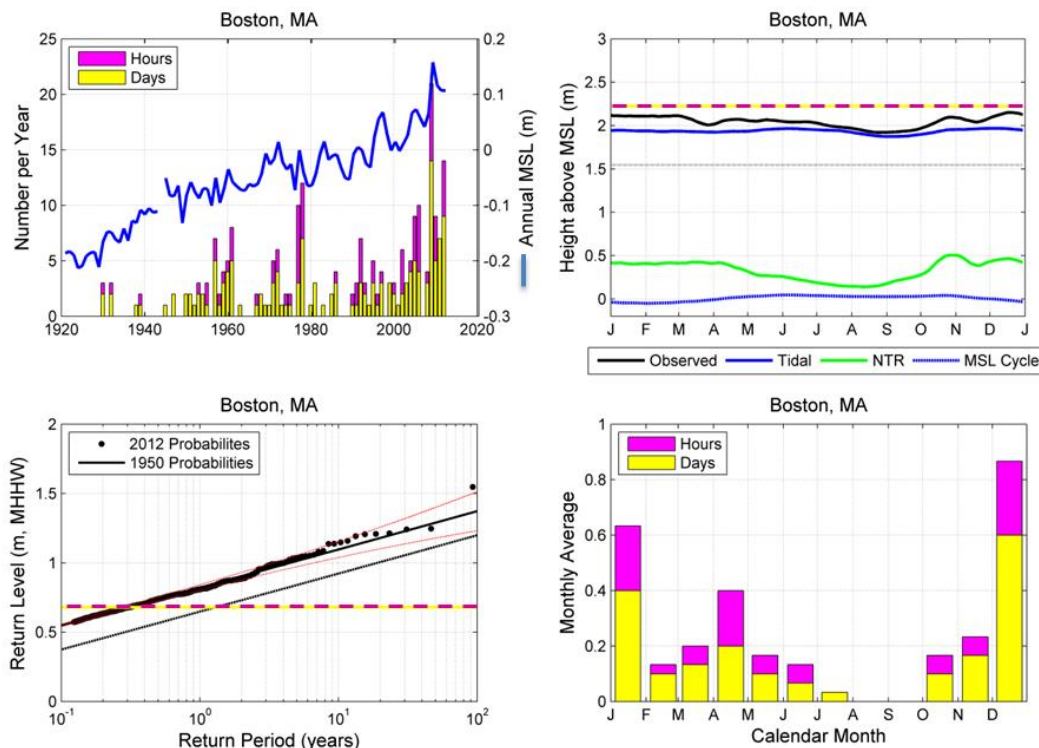
APPENDIX 1

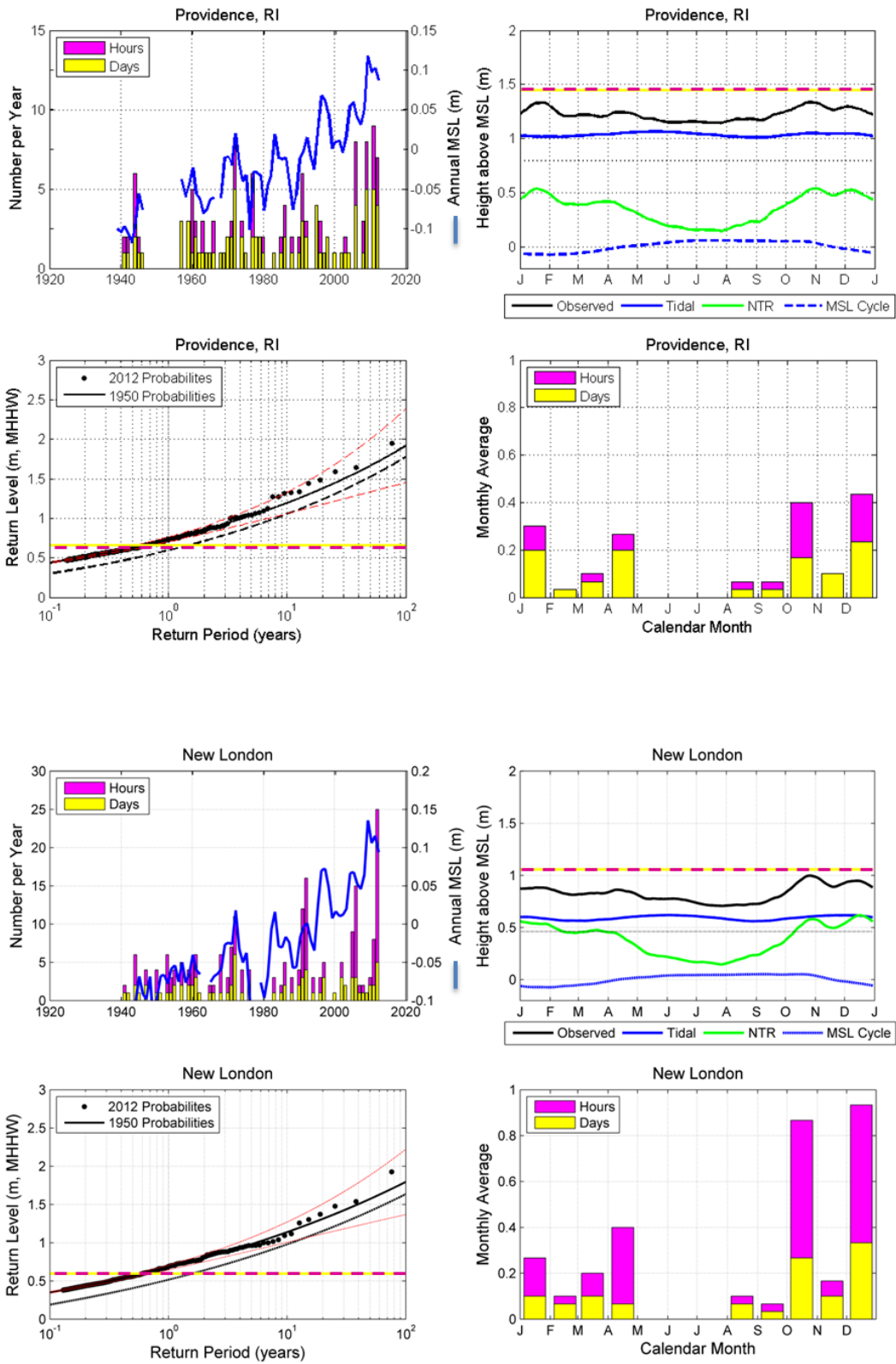
*Gauge name, analysis start date, model coefficients from linear and quadratic fits of days per year impacted by nuisance flooding and goodness of fit (R^2). Both models use data starting in 1950 (e.g., $t_{(1950)} = 1$) or when data becomes available and ends in year (meteorological) 2012. Trend (b_1) and acceleration coefficients (b_2) are **bold** when significant at the 90% level.*

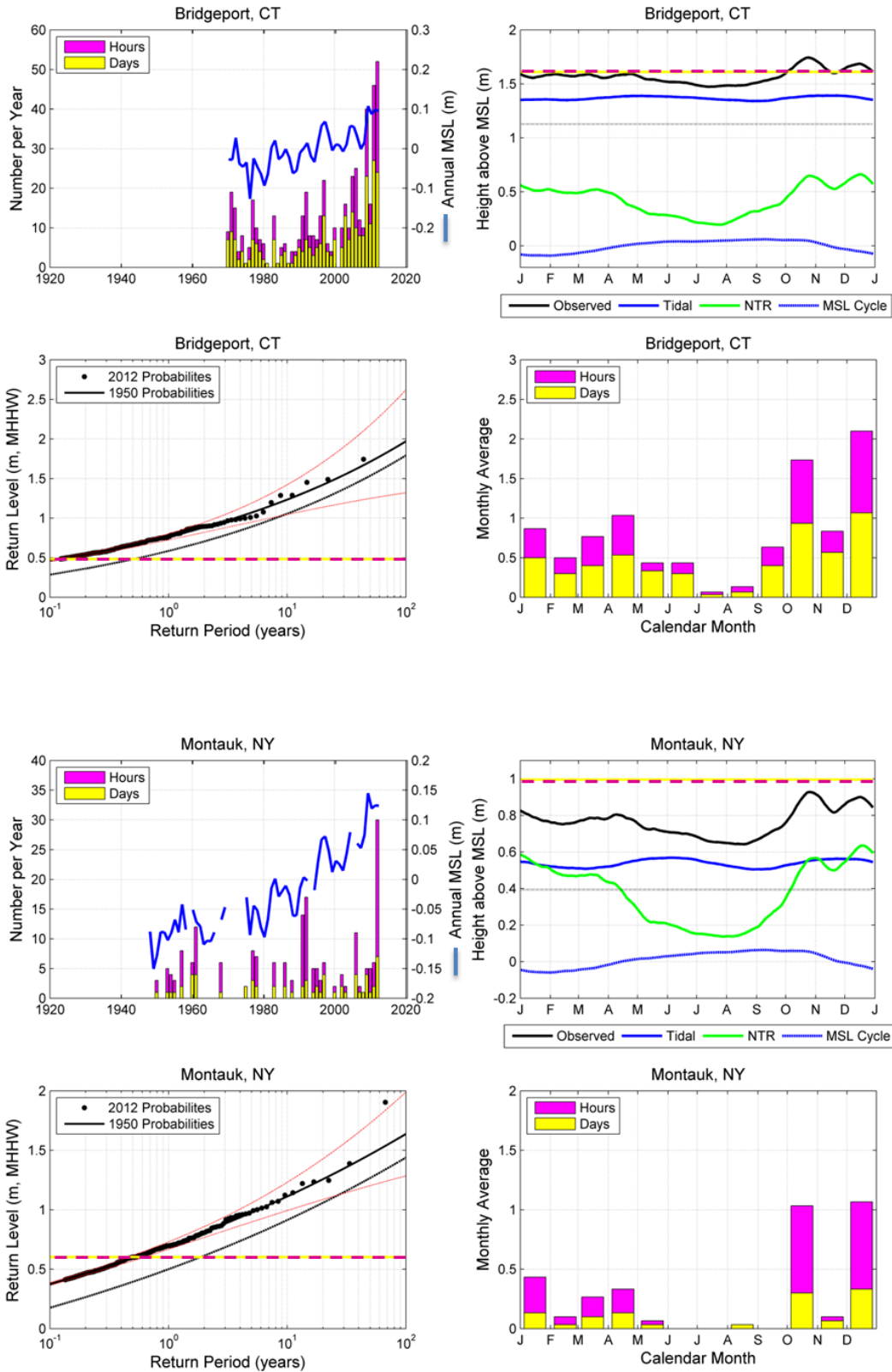
	Linear Model $y=b_1*t + b$			Quadratic: $y=b_2*t^2 + b_1*t + b$					
	Station Name	Start (year)	b_1	b	R^2	b_2	b_1	b	R^2
1	Boston, MA	1921	0.047	0.7	0.12	0.0035	-0.18	3.2	0.30
2	Providence, RI	1938	0.007	1.1	0.01	0.0017	-0.11	2.9	0.09
3	New London, CT	1938	0.012	0.9	0.03	0.0009	-0.04	1.4	0.07
4	Bridgeport, CT	1970	0.281	-5.2	0.33	0.0240	-1.74	33.5	0.63
5	Montauk, NY	1947	0.023	0.4	0.08	0.0013	-0.06	1.3	0.15
6	Kings Point, NY	1931	0.158	1.9	0.26	0.0083	-0.37	7.5	0.44
7	Battery, NY	1920	0.146	0.2	0.29	0.0064	-0.27	4.7	0.44
8	Bergen Point, NY	1981	0.301	-8.9	0.38	0.0230	-1.92	42.8	0.51
9	Sandy Hook, NJ	1922	0.334	-2.6	0.52	0.0113	-0.39	5.2	0.67
h	Atlantic City, NJ	1920	0.327	-2.4	0.51	0.0105	-0.34	4.6	0.65
11	Cape May, NJ	1965	0.652	-14.1	0.54	0.0320	-1.96	33.5	0.74
12	Philadelphia, PA	1920	0.145	0.0	0.23	0.0057	-0.22	4.1	0.33
13	Reedy Point, DE	1979	0.338	-10.8	0.35	0.0207	-1.62	33.9	0.43
14	Lewes, DE	1920	0.251	0.4	0.35	0.0104	-0.43	8.4	0.50
15	Cambridge, MD	1979	0.253	-8.5	0.46	0.0185	-1.46	29.6	0.65
16	Baltimore, MD	1920	0.165	-0.6	0.38	0.0068	-0.27	4.1	0.55
17	Annapolis, MD	1928	0.567	-3.8	0.53	0.0168	-0.51	7.7	0.66
18	Washington D.C.	1924	0.384	1.3	0.37	0.0091	-0.20	7.5	0.42
19	Wachapreague, VA	1978	0.090	-1.9	0.11	0.0009	0.01	-0.1	0.12
20	Kiptopeke, VA	1976	0.208	-5.2	0.28	0.0036	-0.12	1.8	0.29
21	Lewisetta, VA	1970	0.257	-8.0	0.45	0.0111	-0.72	12.0	0.56
22	Sewell Point, VA	1927	0.097	-0.1	0.30	0.0022	-0.05	1.4	0.34
23	Ches. Bay Bridge, VA	1975	0.105	-2.7	0.21	0.0008	0.03	-1.3	0.22
24	Duck, NC	1978	0.159	-3.9	0.25	0.0016	0.01	-0.7	0.25
25	Beaufort, NC	1973	0.894	-26.2	0.69	0.0206	-0.95	12.4	0.73
26	Wilmington, NC	1935	0.542	-6.6	0.57	0.0125	-0.26	2.2	0.66
27	Springmaid Pier, SC	1977	0.060	-1.0	0.08	0.0049	-0.39	8.6	0.13
28	Charleston, SC	1921	0.347	-1.8	0.57	0.0045	0.06	1.4	0.60
29	Fort Pulaski, GA	1935	0.194	0.4	0.37	0.0018	0.08	1.7	0.38
30	Fernandina Beach, FL	1920	0.026	0.1	0.11	0.0011	-0.05	0.9	0.17
31	Mayport, FL	1928	0.068	-0.9	0.24	0.0031	-0.13	1.2	0.38
32	Key West, FL	1920	0.043	-0.7	0.20	0.0020	-0.09	0.8	0.31
33	Naples, FL	1965	0.153	-3.0	0.40	0.0042	-0.18	2.7	0.45
34	Apalachicola, FL	1976	0.096	-1.4	0.12	0.0007	0.03	0.1	0.12
35	Panama City, FL	1973	0.155	-2.4	0.14	0.0118	-0.91	20.0	0.24
36	Bay Waveland, MS	1978	0.259	-4.5	0.27	0.0093	-0.60	14.1	0.30
37	Sabine Pass, TX	1981	0.026	-0.4	0.02	-0.0042	0.44	-10.4	0.05
38	Galveston, TX	1957	0.029	0.0	0.14	0.0010	-0.04	1.0	0.17
39	Port Isabel, TX	1944	0.218	-2.6	0.34	0.0069	-0.22	2.1	0.42
40	La Jolla, CA	1924	0.100	-0.7	0.26	0.0006	0.06	-0.2	0.27
41	San Francisco, CA	1920	0.130	3.0	0.12	-0.0026	0.30	1.2	0.13
42	Humboldt Bay, CA	1977	0.146	-3.2	0.17	-0.0045	0.57	-12.4	0.18
43	Toke Point, WA	1972	0.088	7.0	0.03	-0.0062	0.63	-3.9	0.04
44	Seattle, WA	1920	0.026	0.6	0.05	0.0007	-0.02	1.1	0.06
45	Honolulu, HI	1920	0.278	-0.3	0.19	0.0000	0.28	-0.3	0.19

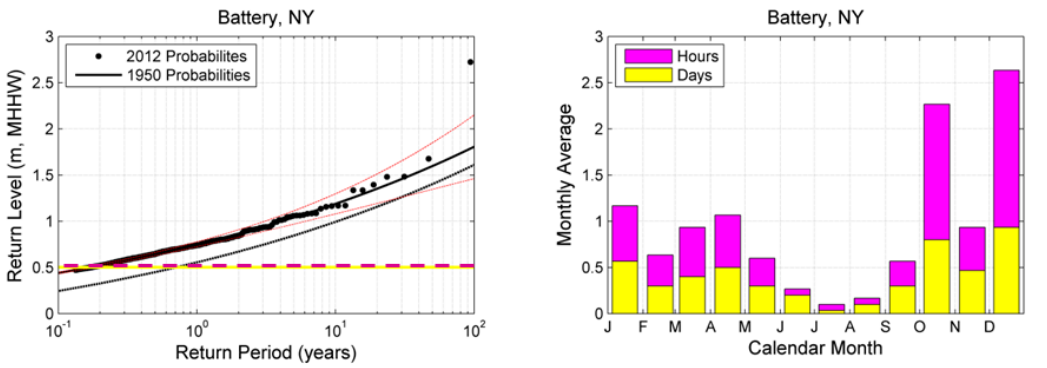
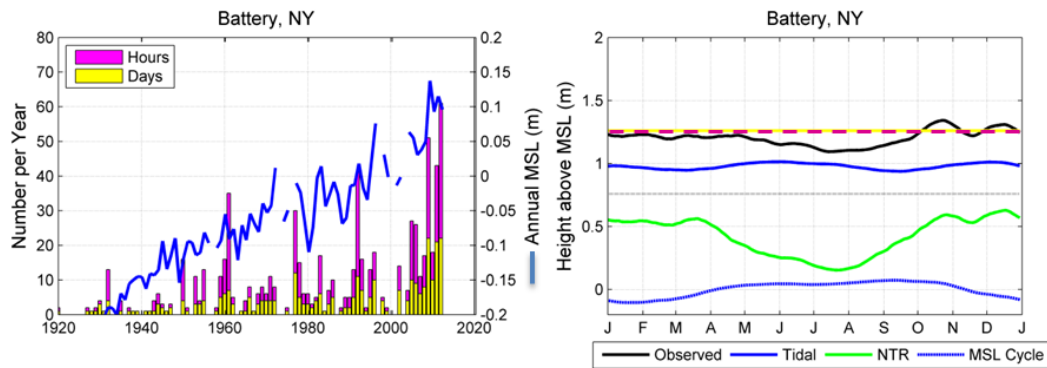
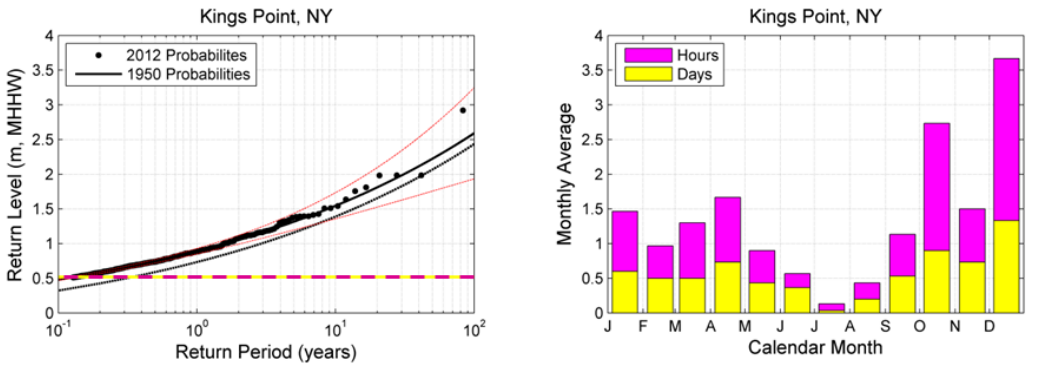
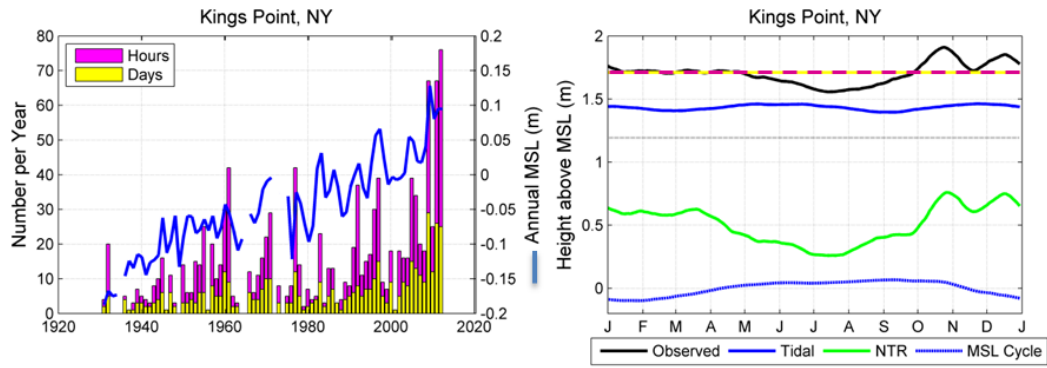
APPENDIX 2

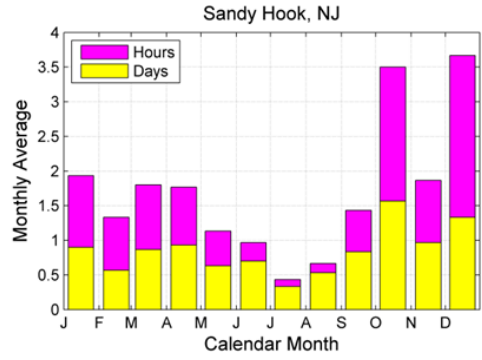
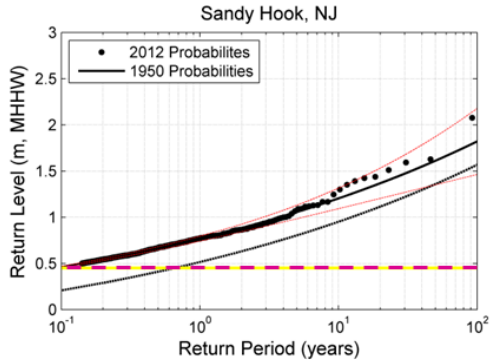
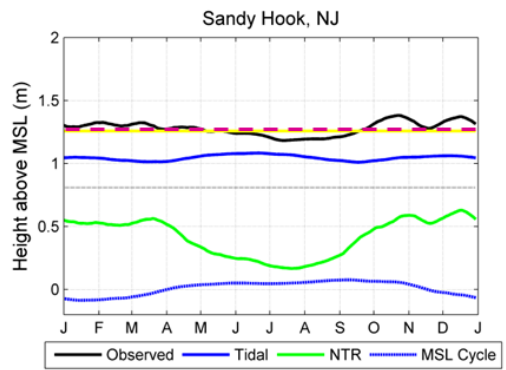
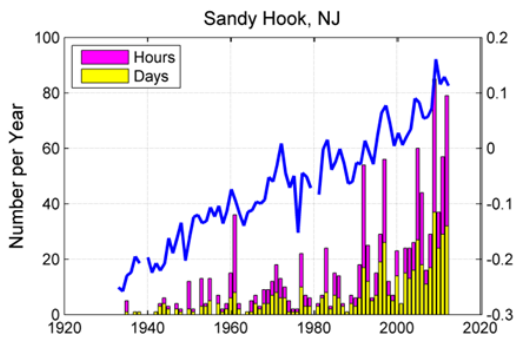
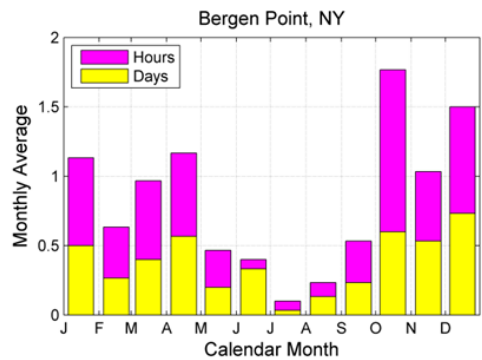
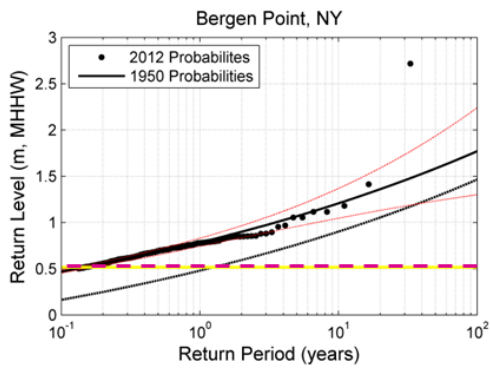
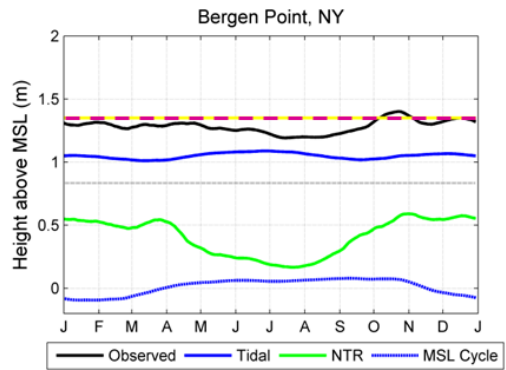
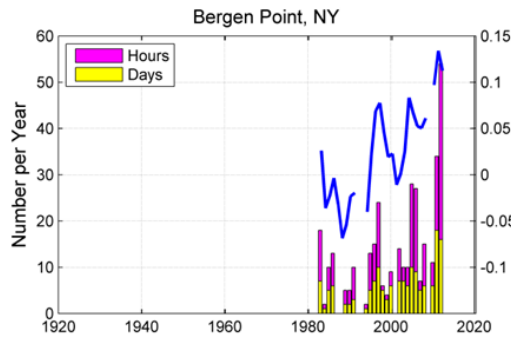
- (top left) show nuisance flood events (cumulative hours and impacted days) per meteorological year with annual MSL through 2012 (i.e., May 2012 – April 2013). Note: if the number of hours and days are numerically equivalent, only the top values (days in yellow) appear.
- (bottom left) show return level interval curves from a Peak Over Threshold (POT) / Point Process approach fit to a Generalized Pareto Distribution (GPD). The 2012 modeled values (black line), their 95% confidence intervals (red dash) and POT picks (dots) are shown relative to the nuisance flood level (yellow-magenta line). 1950 values (black dash) are the 2012 values lowered by a distance equal to the local relative sea level rise (SLR_{rel}) trend (mm/yr) shown in Table 1 for a 62-year period.
- (top right) show maximum water levels (black) per calendar day over the 1980-2009 period decomposed into a low-frequency MSL cycle (blue dot), predicted tide (blue; no S_a and S_{sa} harmonic fits) and nontidal residual (NTR; green). All series are smoothed by a 30-day running filter and plotted relative to each gauge's MSL tidal datum shown with the nuisance flood level (yellow-magenta) and MHHW tidal datum (black dot).
- (bottom right) show average nuisance flood events (shared y-axis) by calendar month over 1980-2009. Note: if the number of hours and days are numerically equivalent, only the top values (days in yellow) appear.

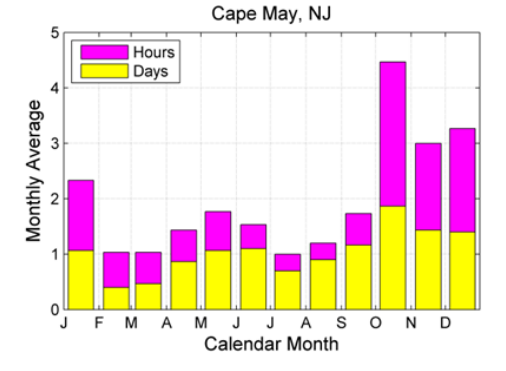
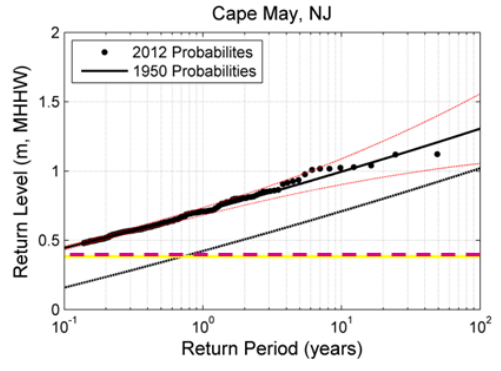
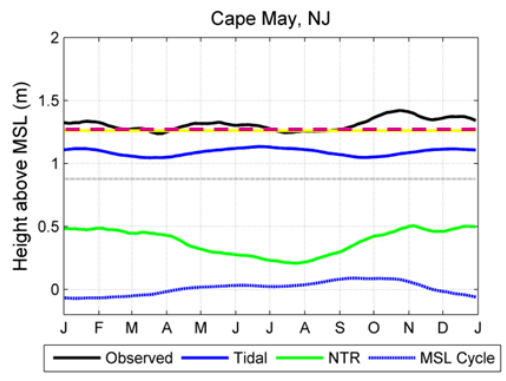
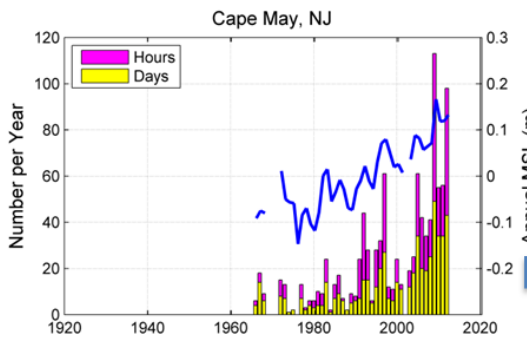
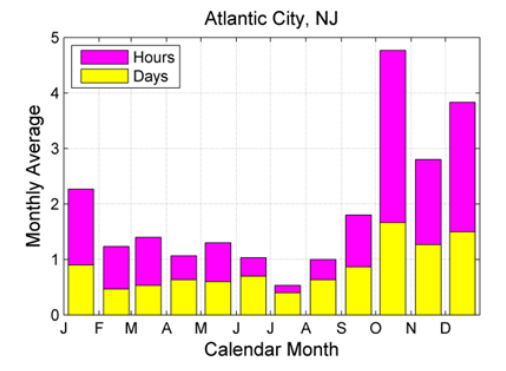
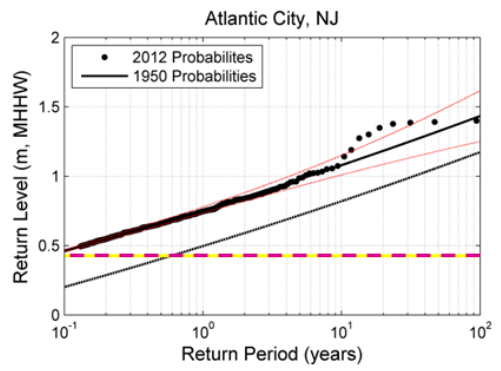
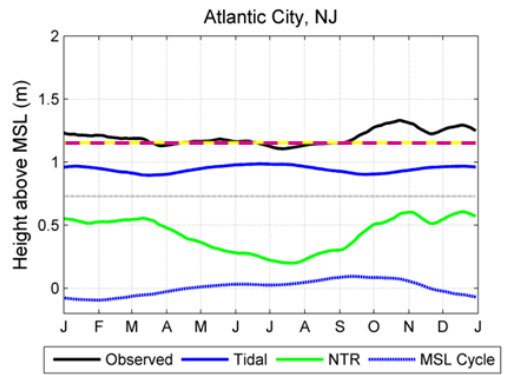
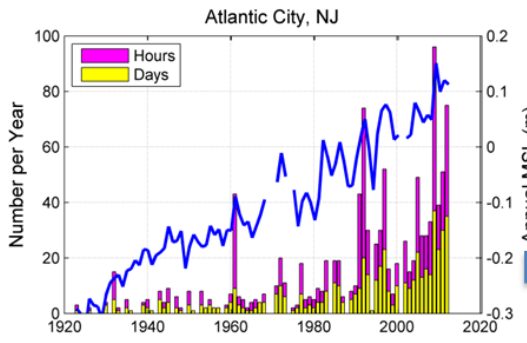


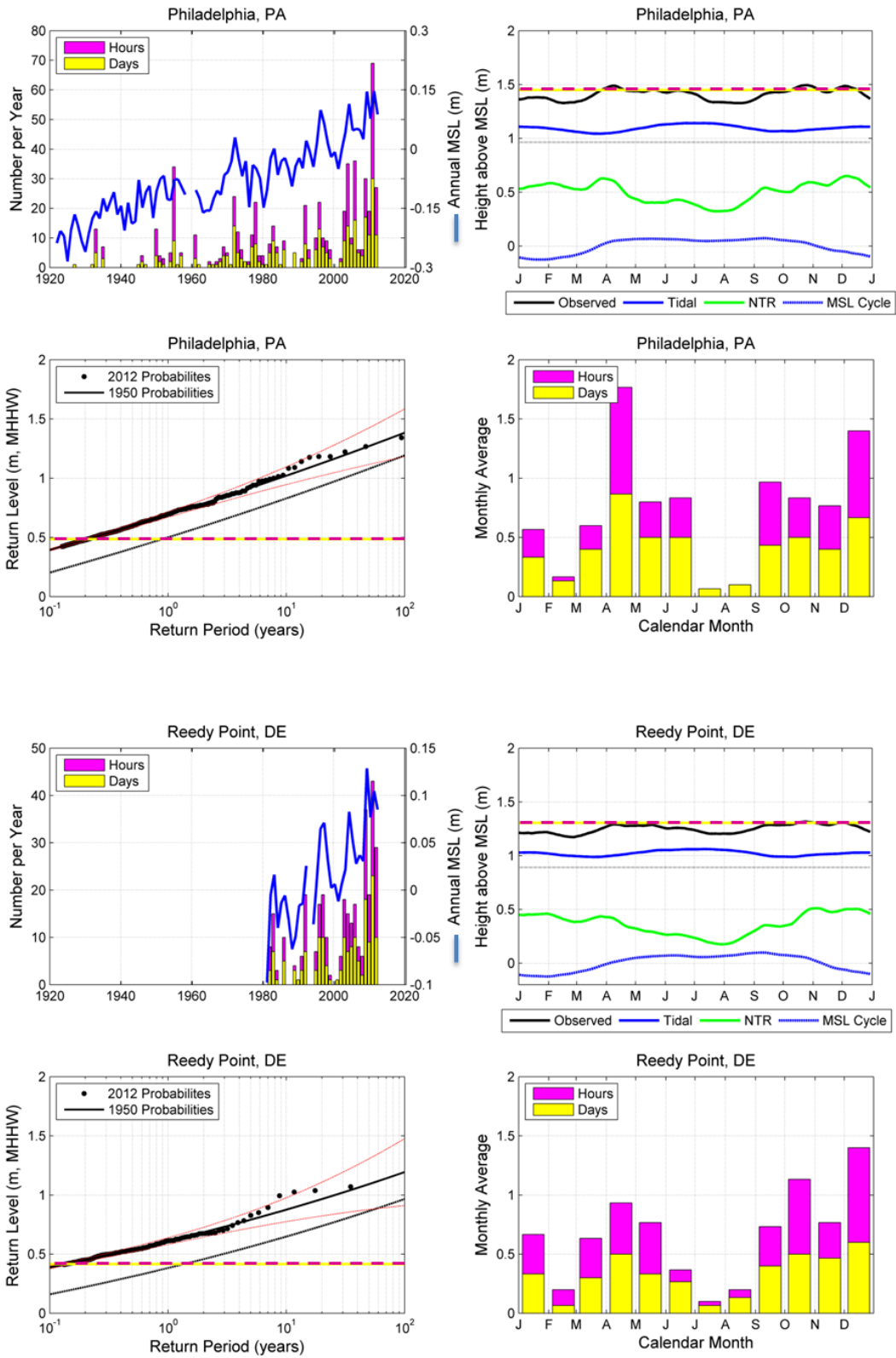


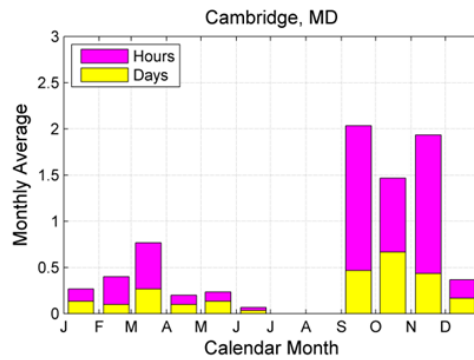
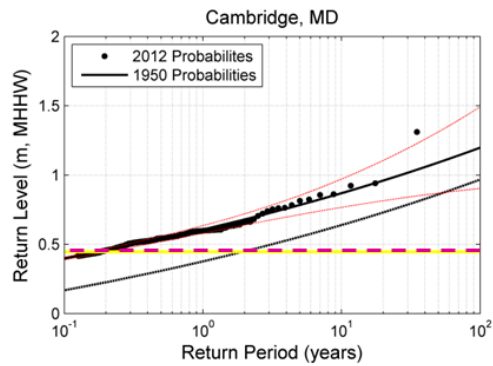
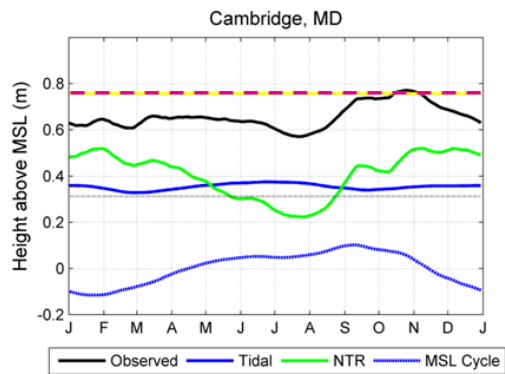
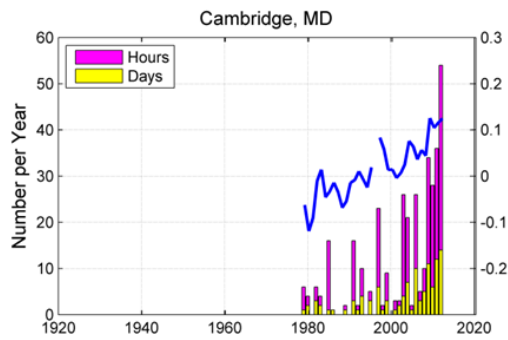
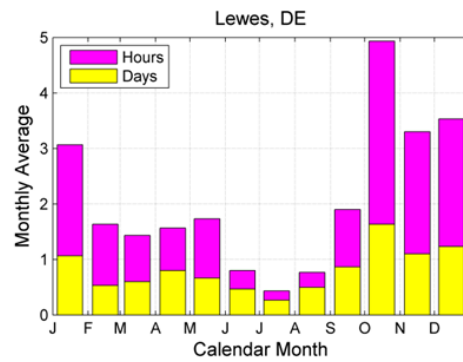
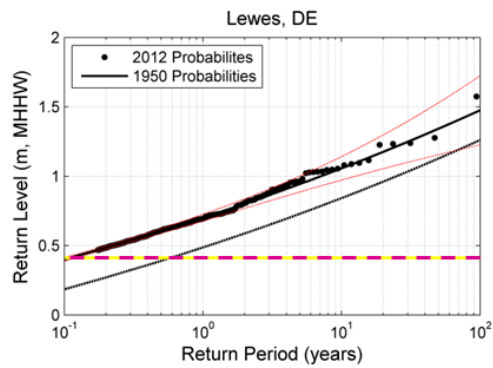
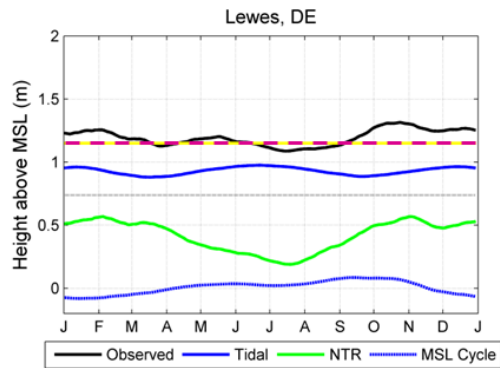
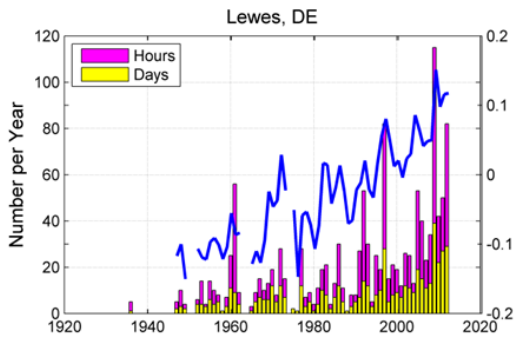


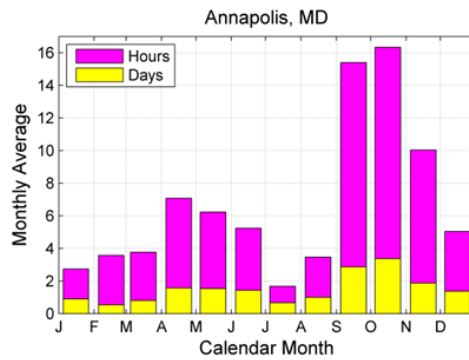
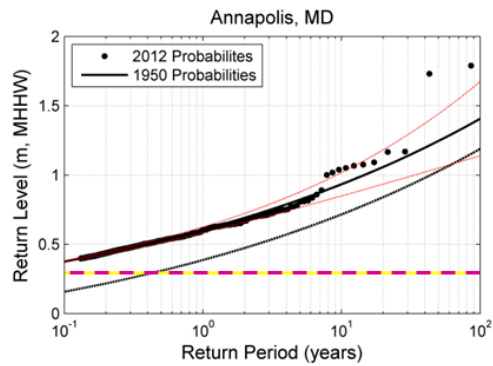
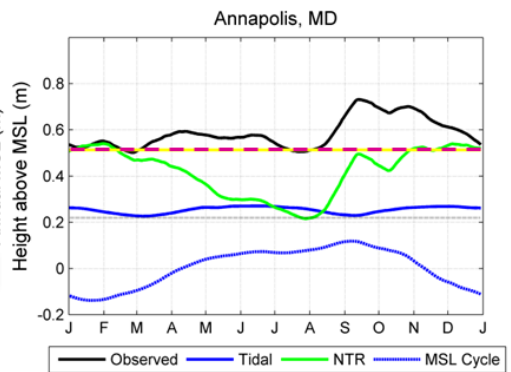
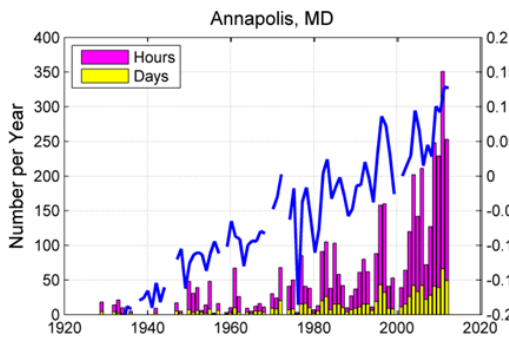
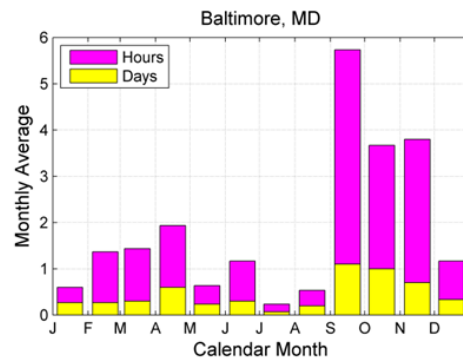
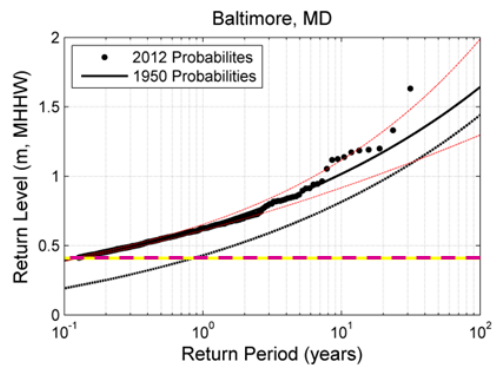
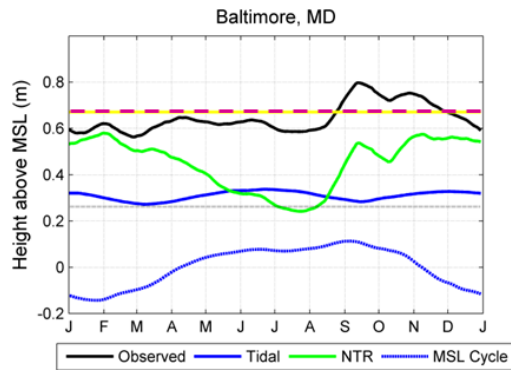
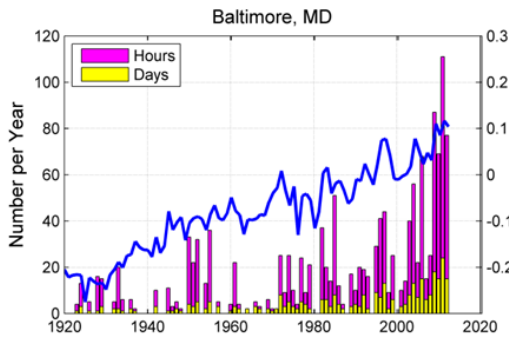


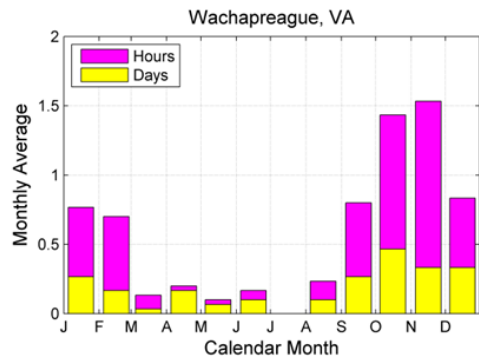
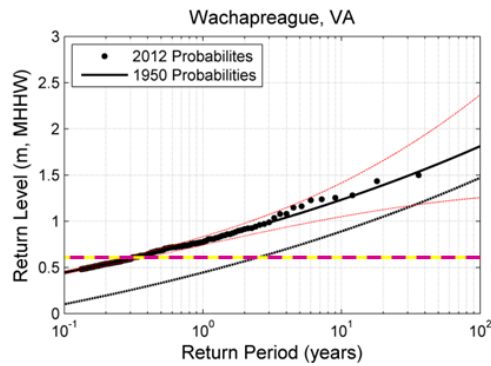
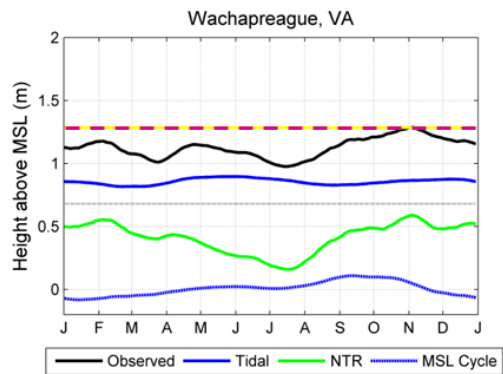
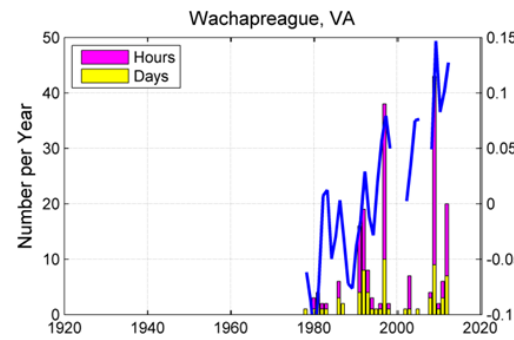
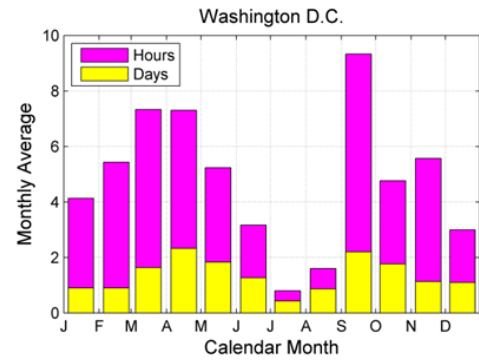
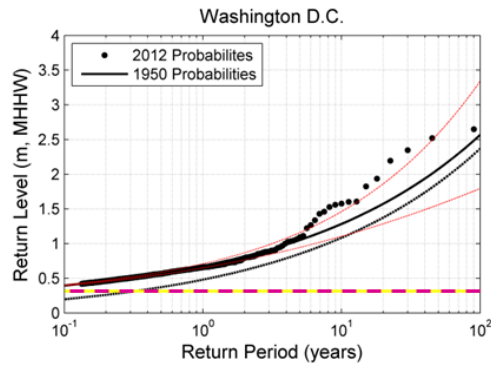
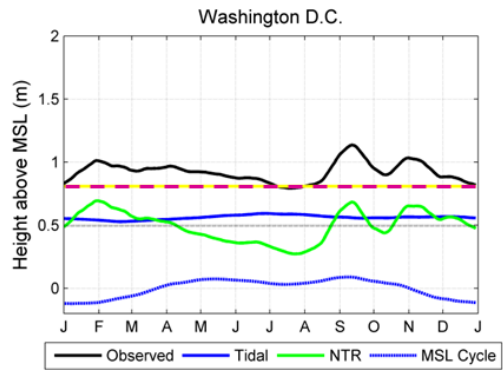
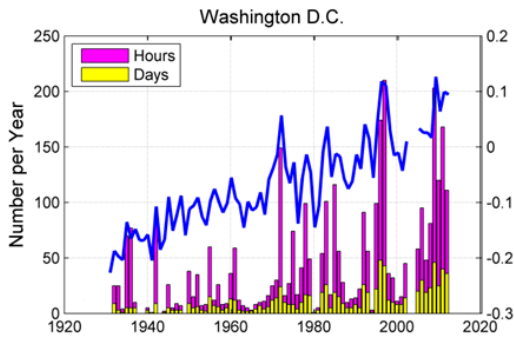


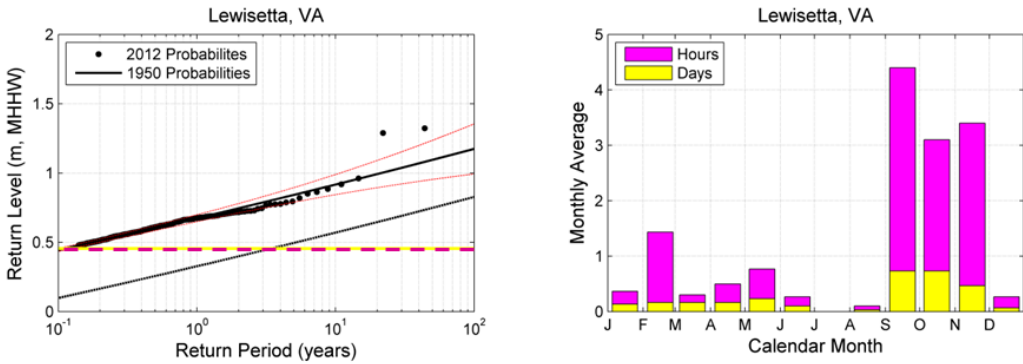
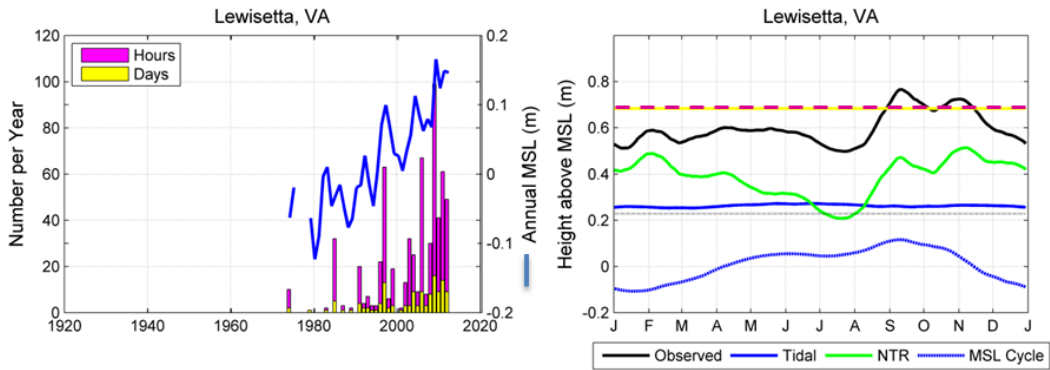
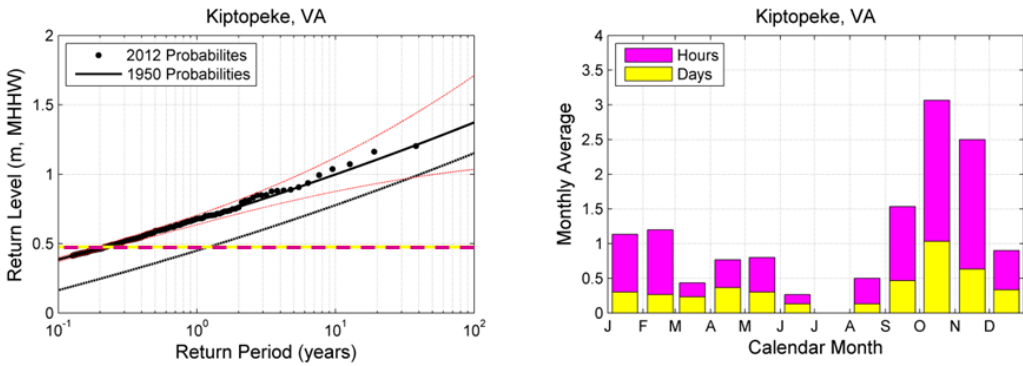
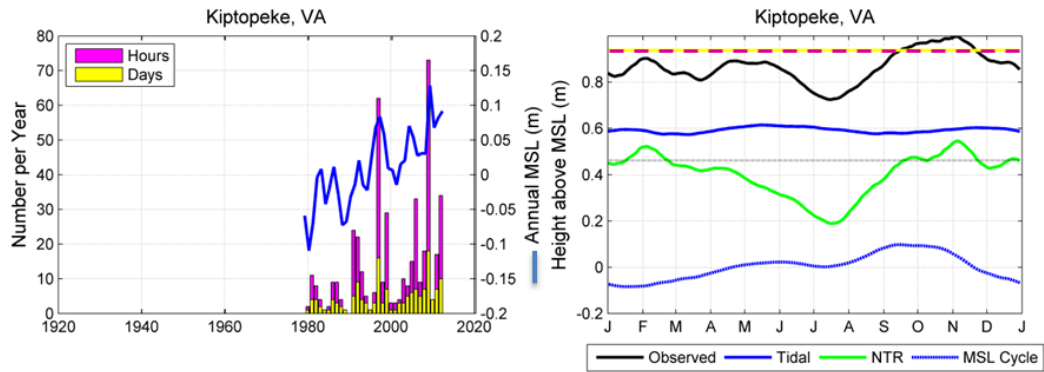


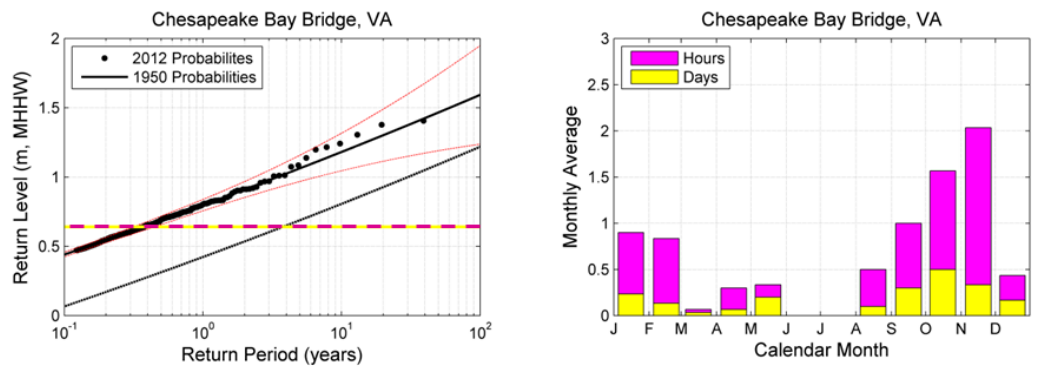
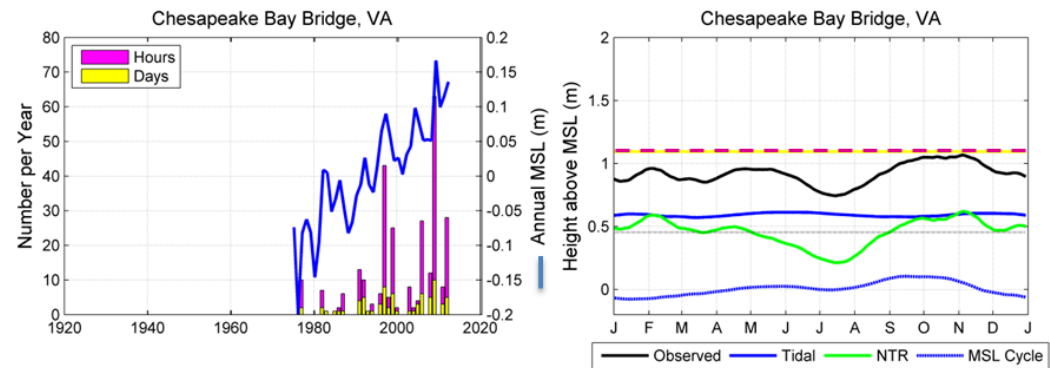
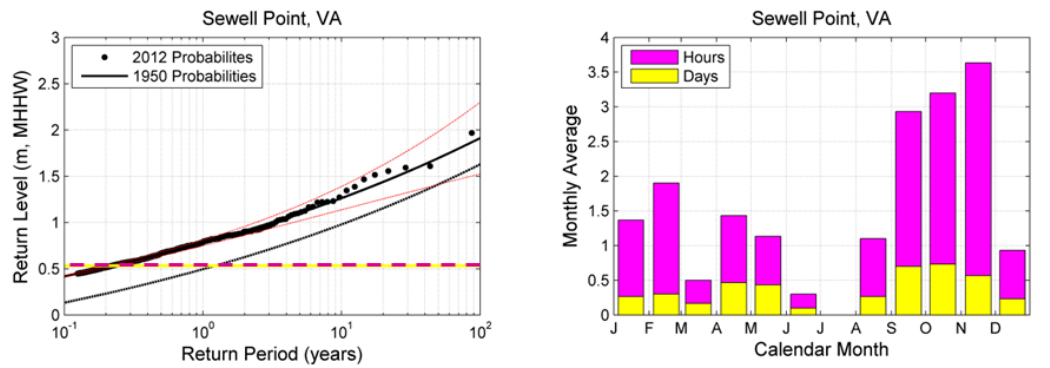
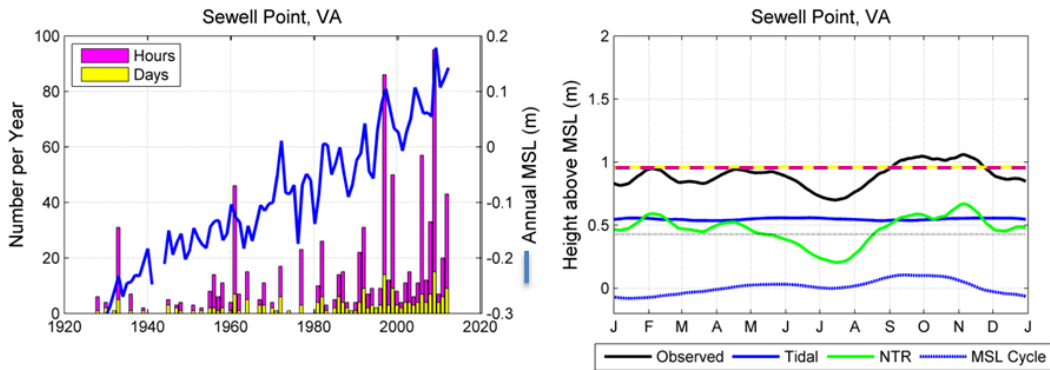


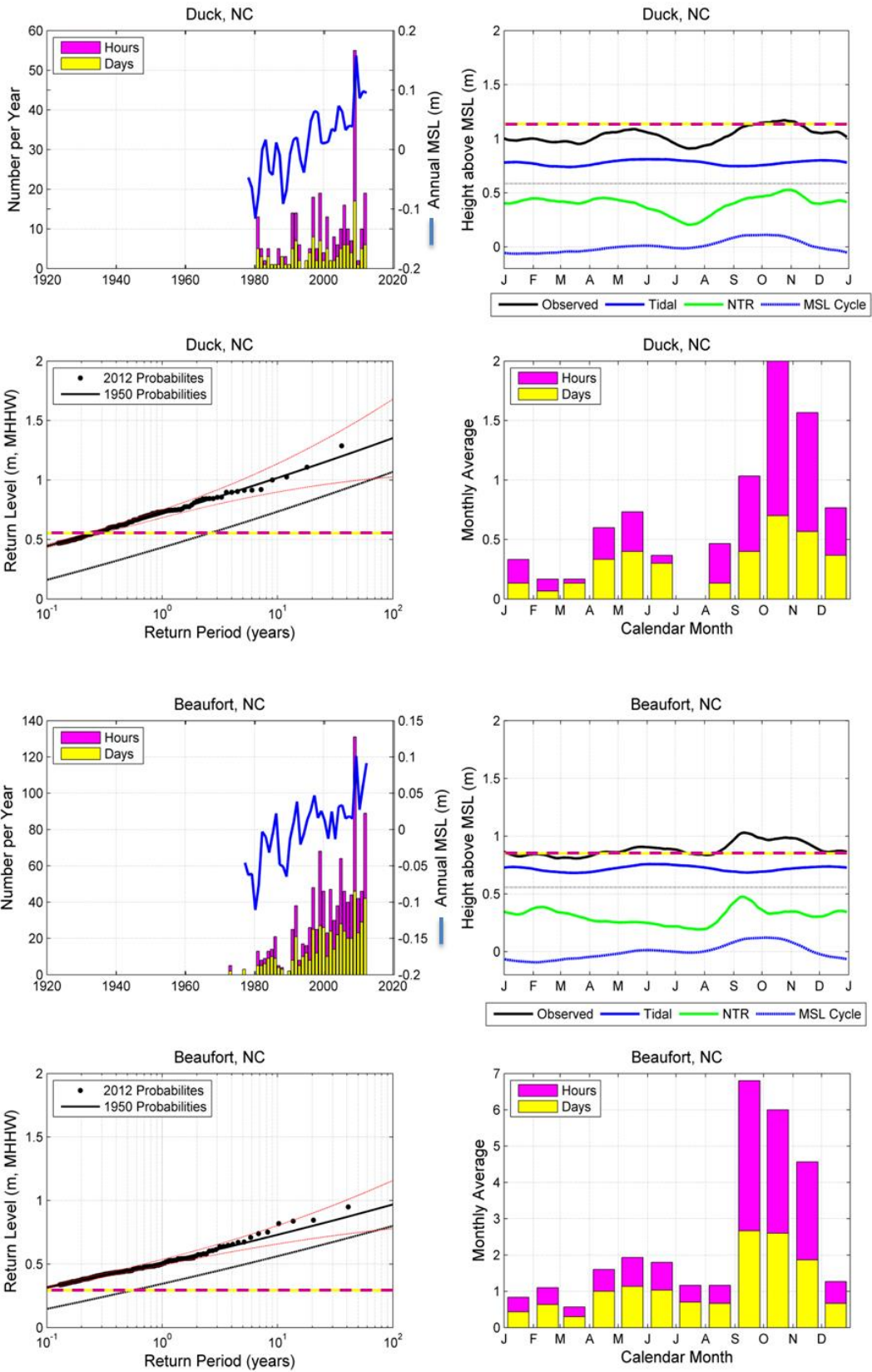


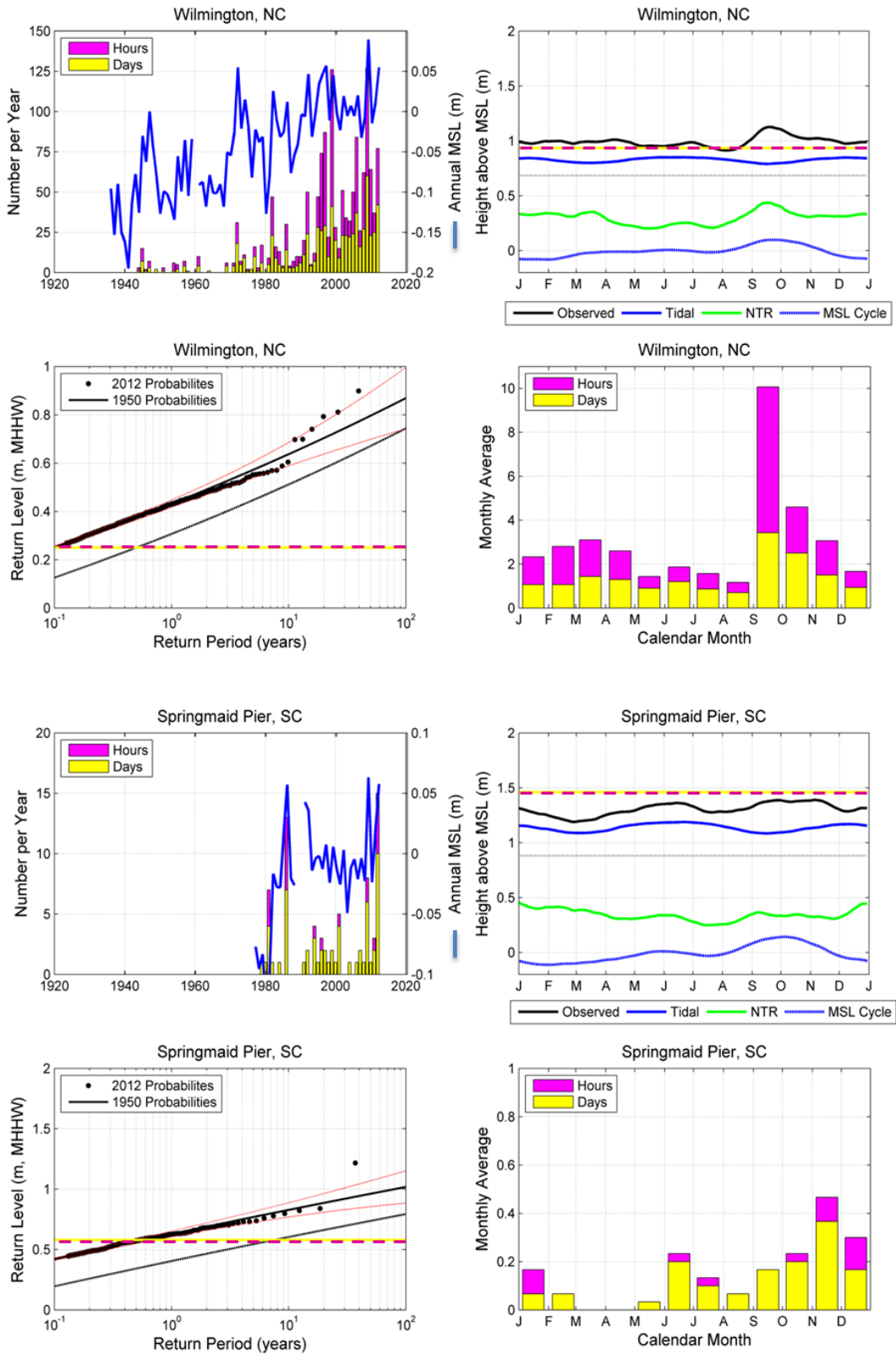


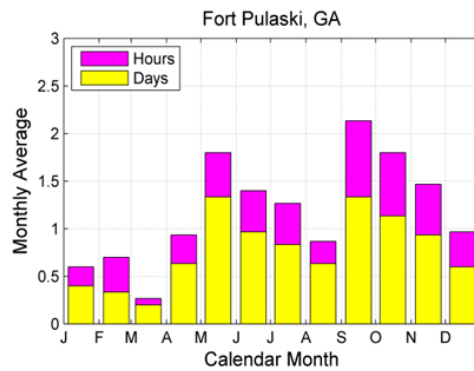
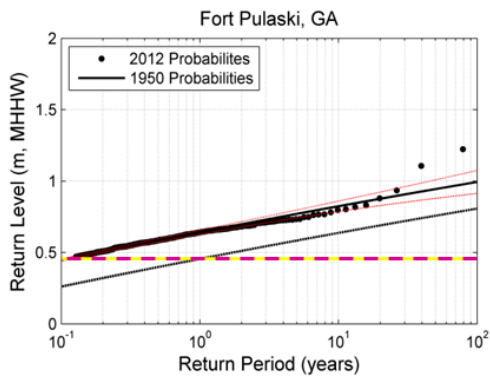
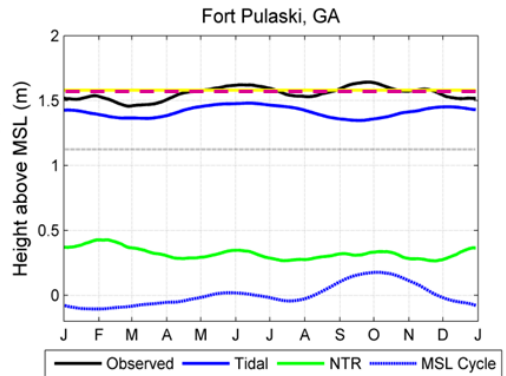
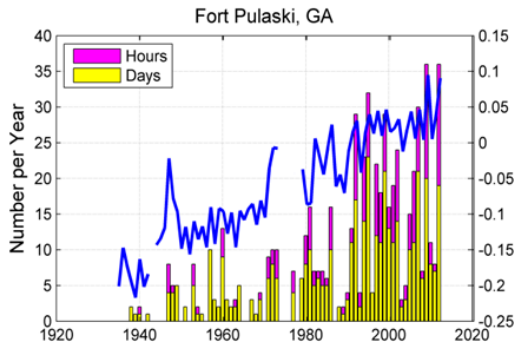
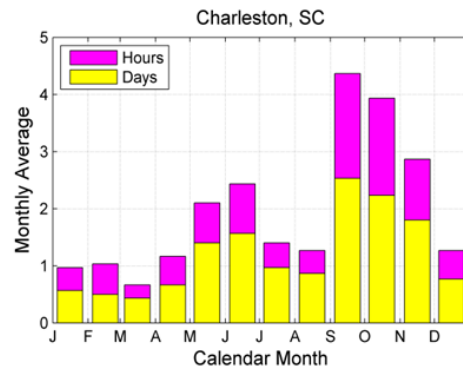
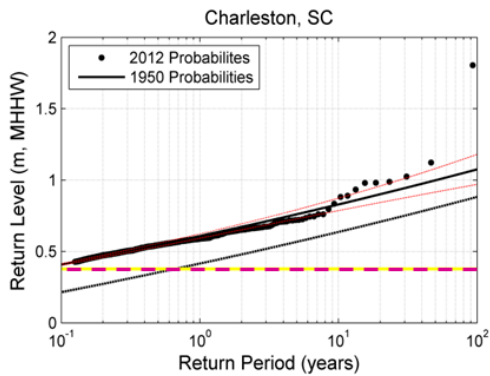
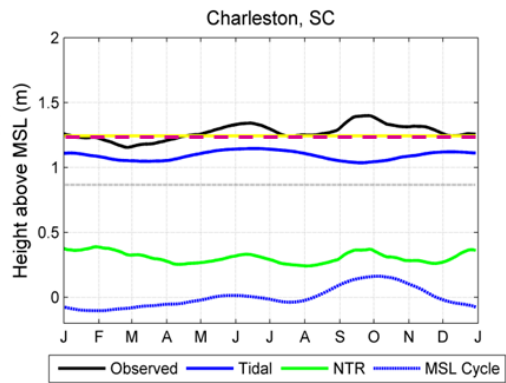
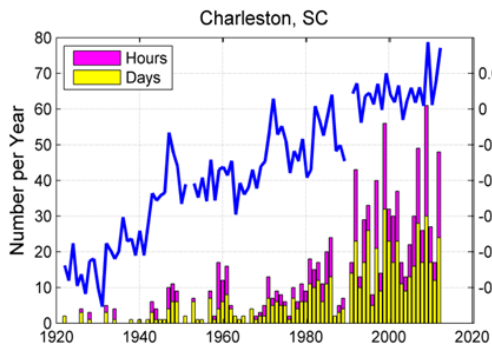


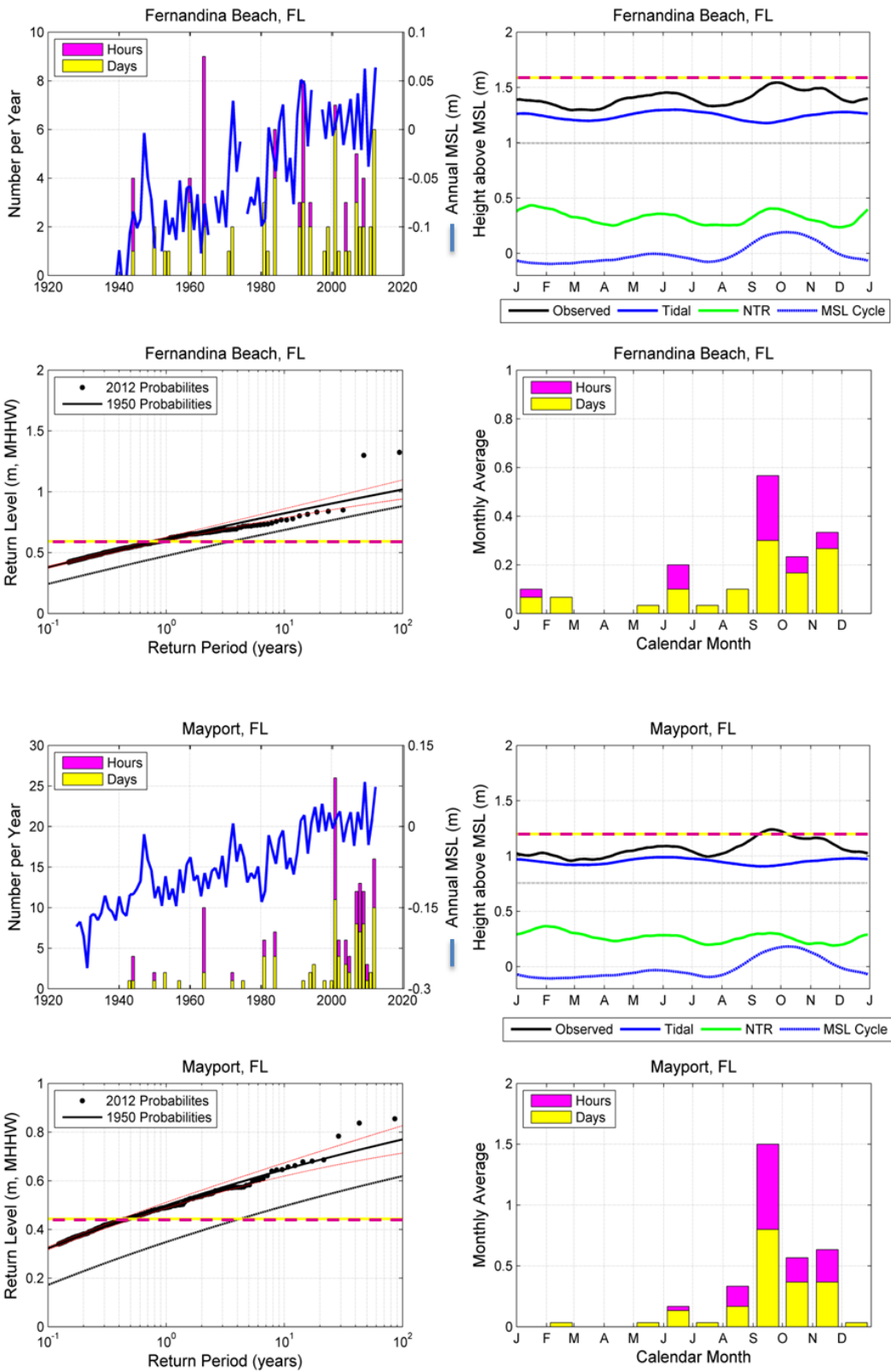


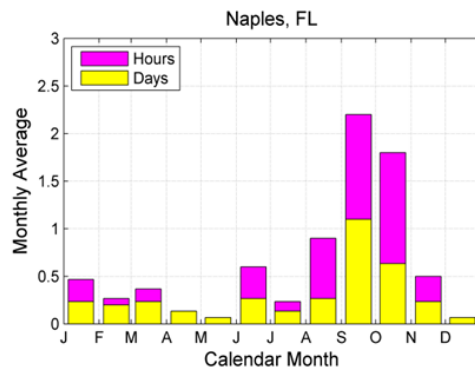
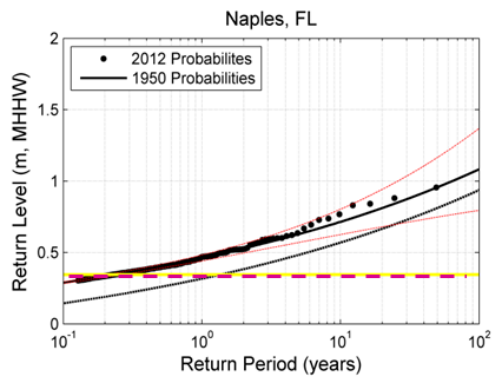
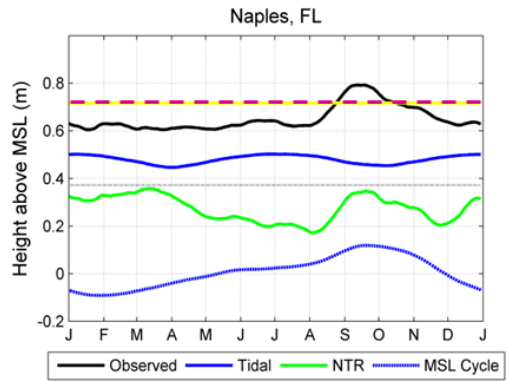
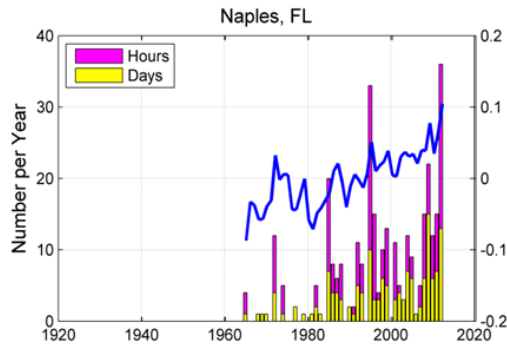
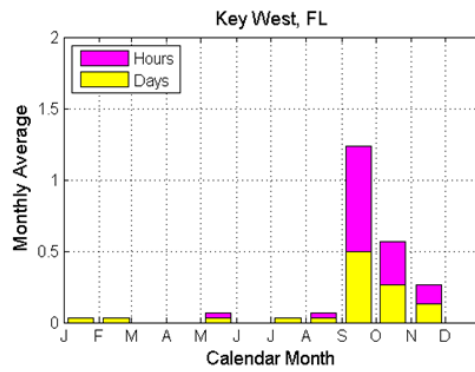
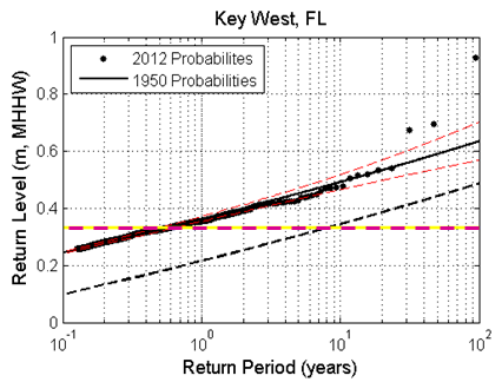
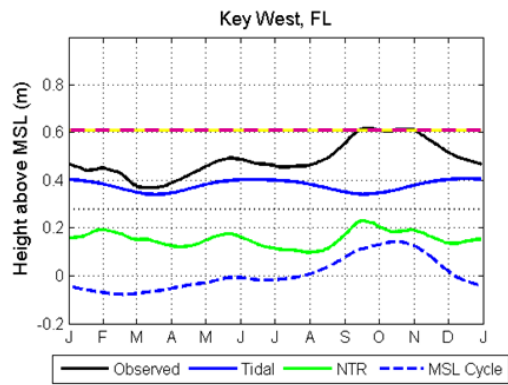
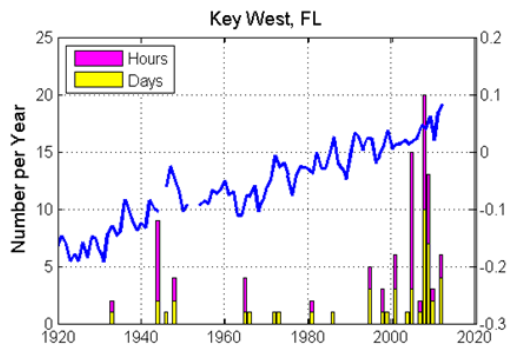


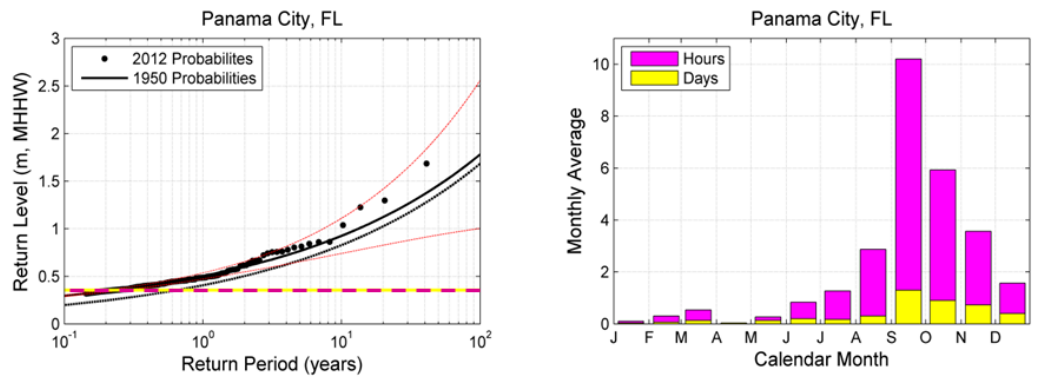
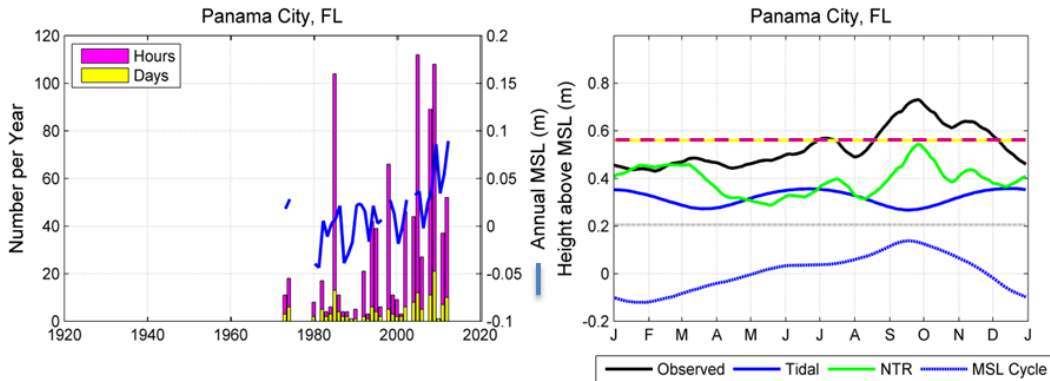
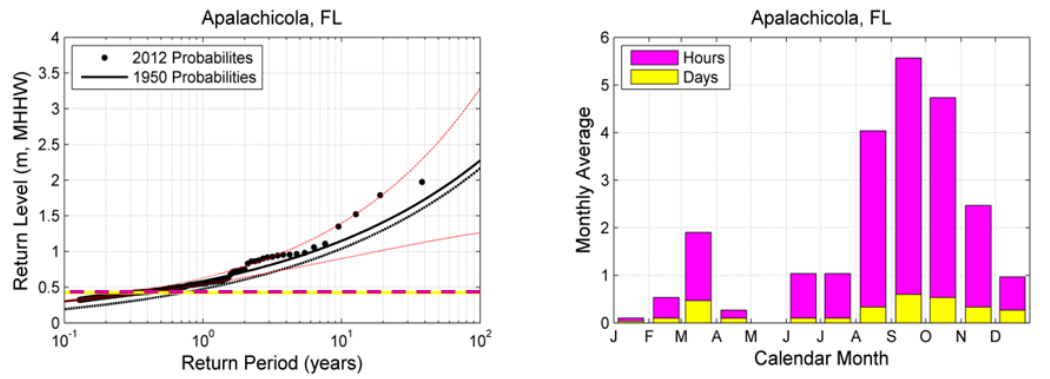
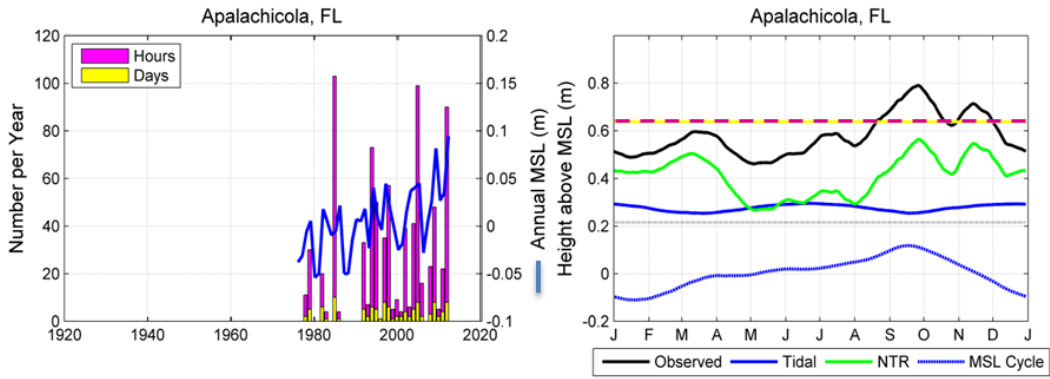


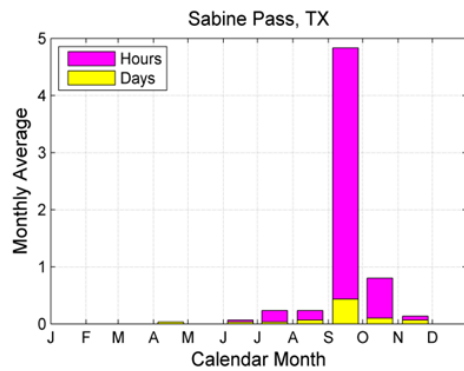
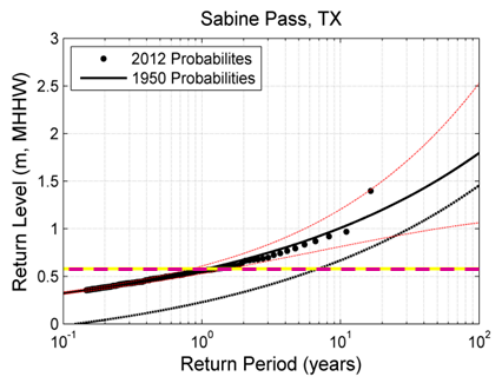
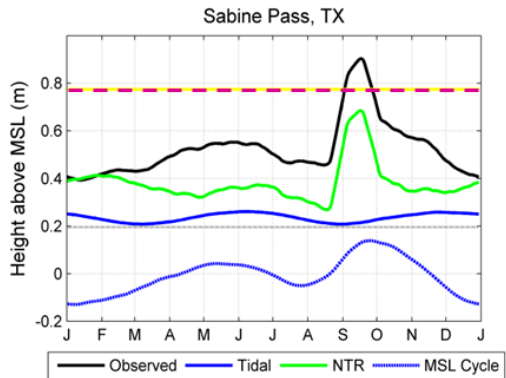
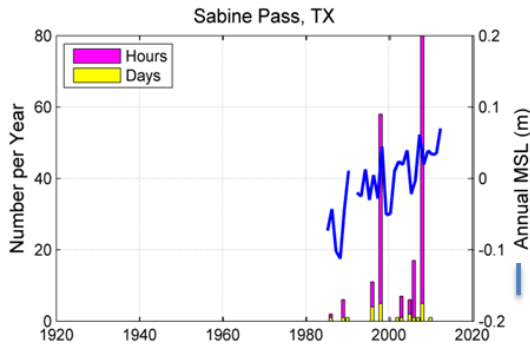
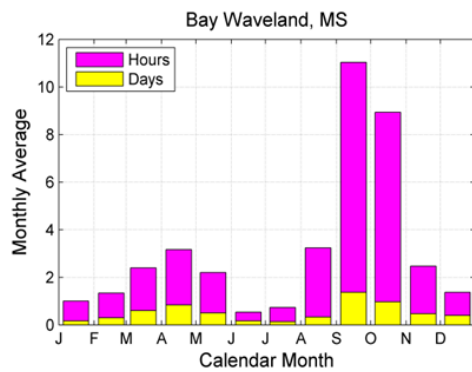
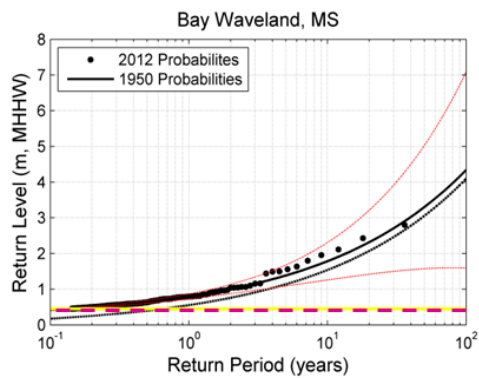
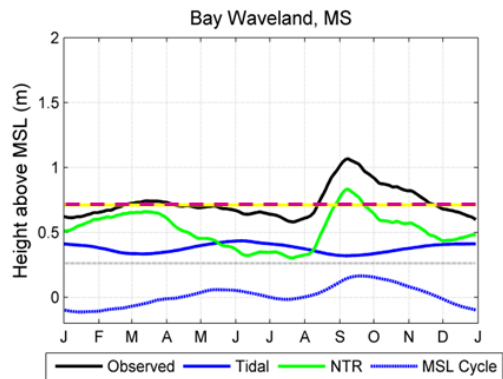
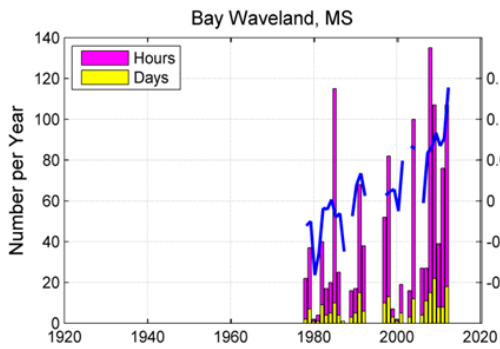


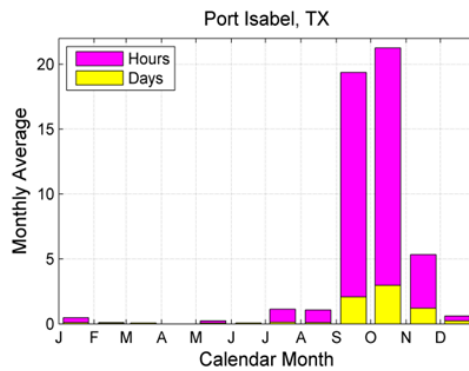
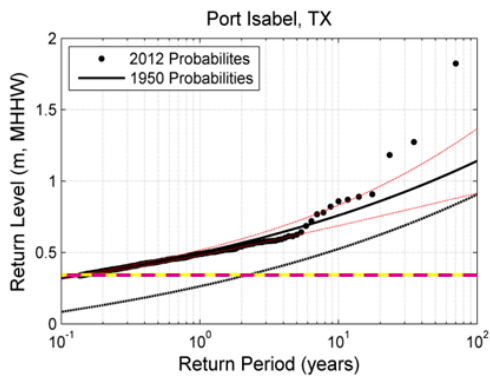
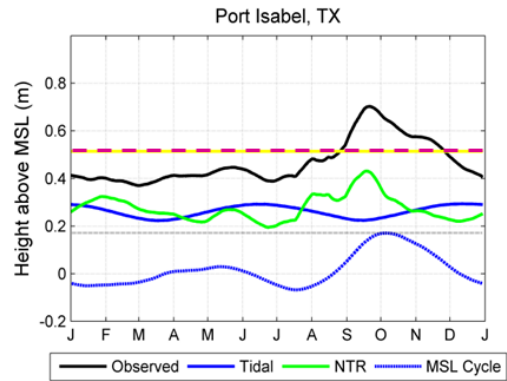
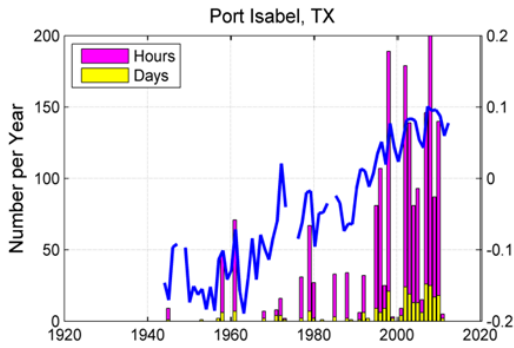
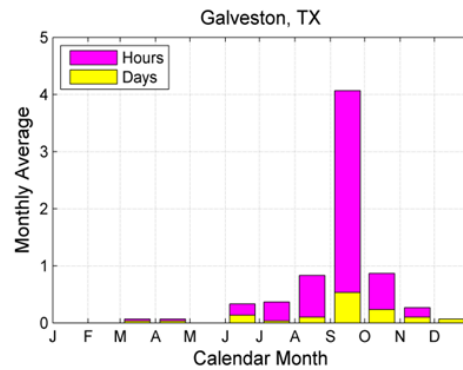
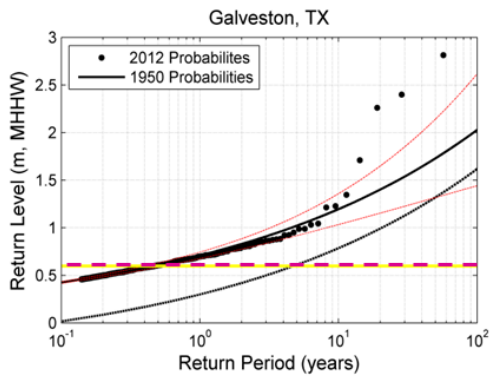
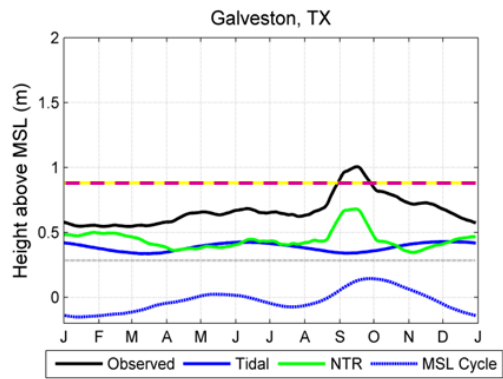
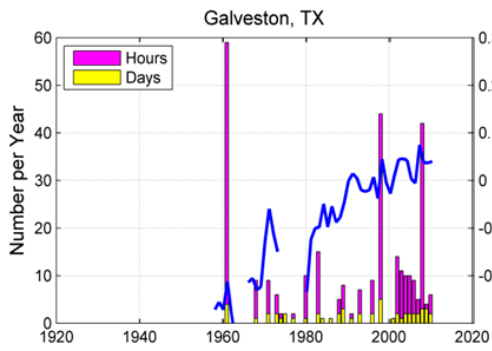


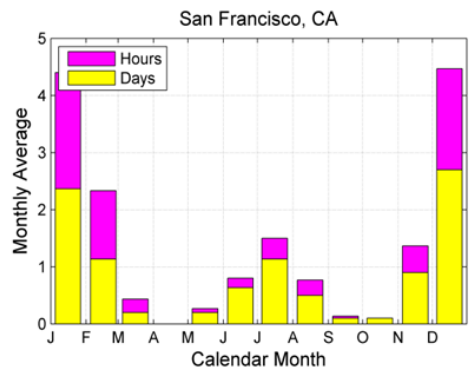
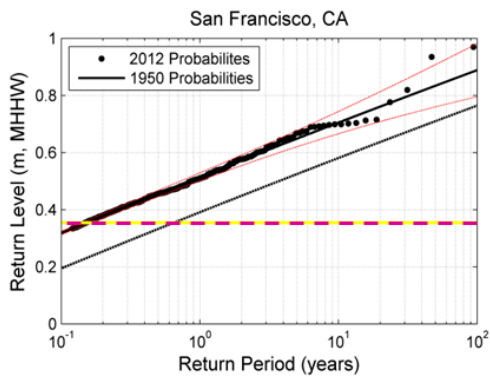
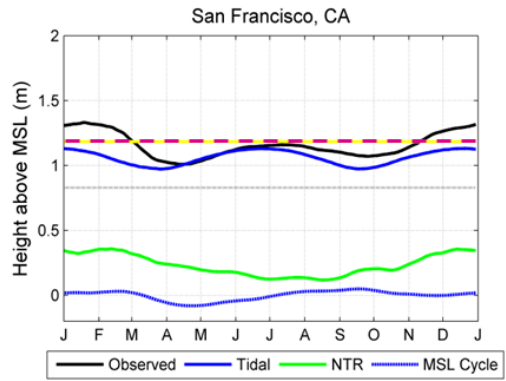
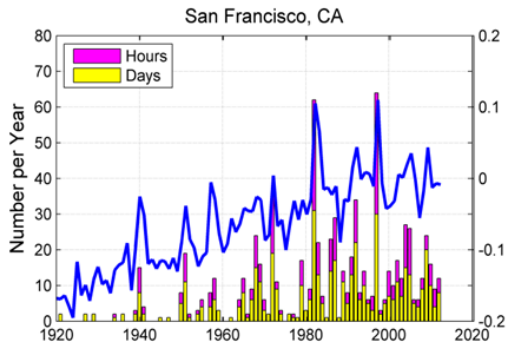
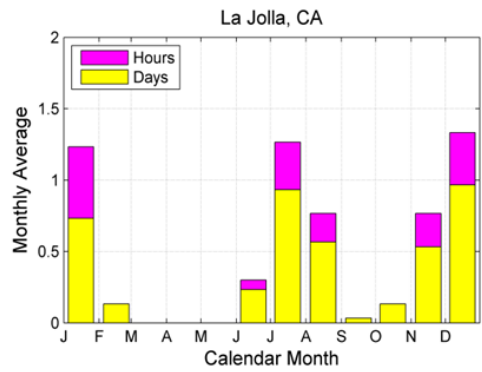
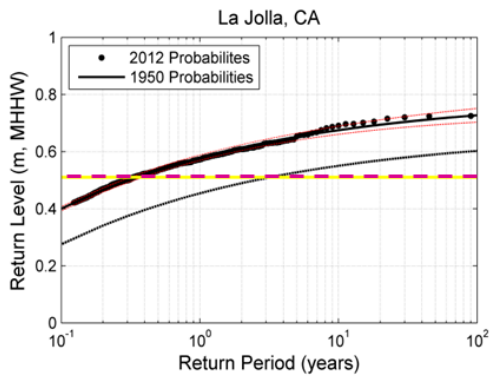
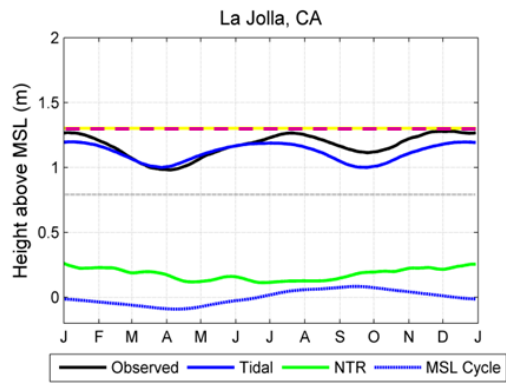
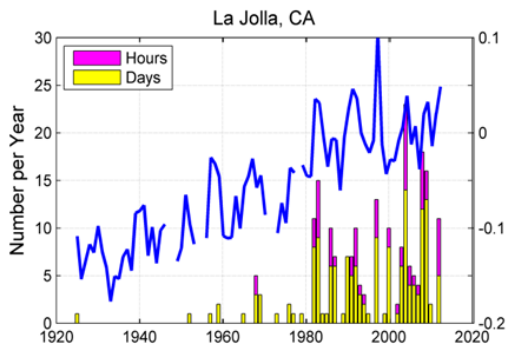


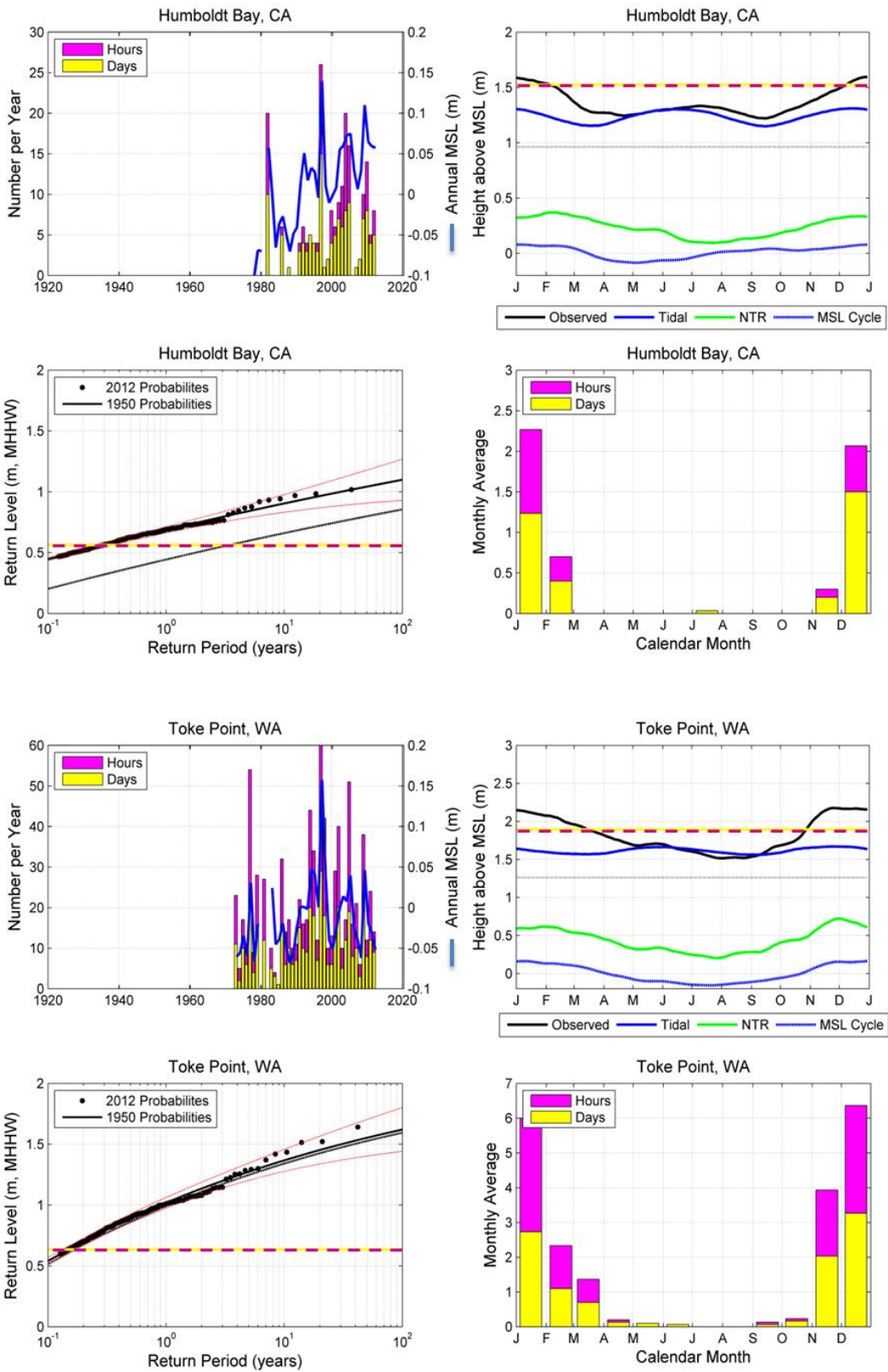


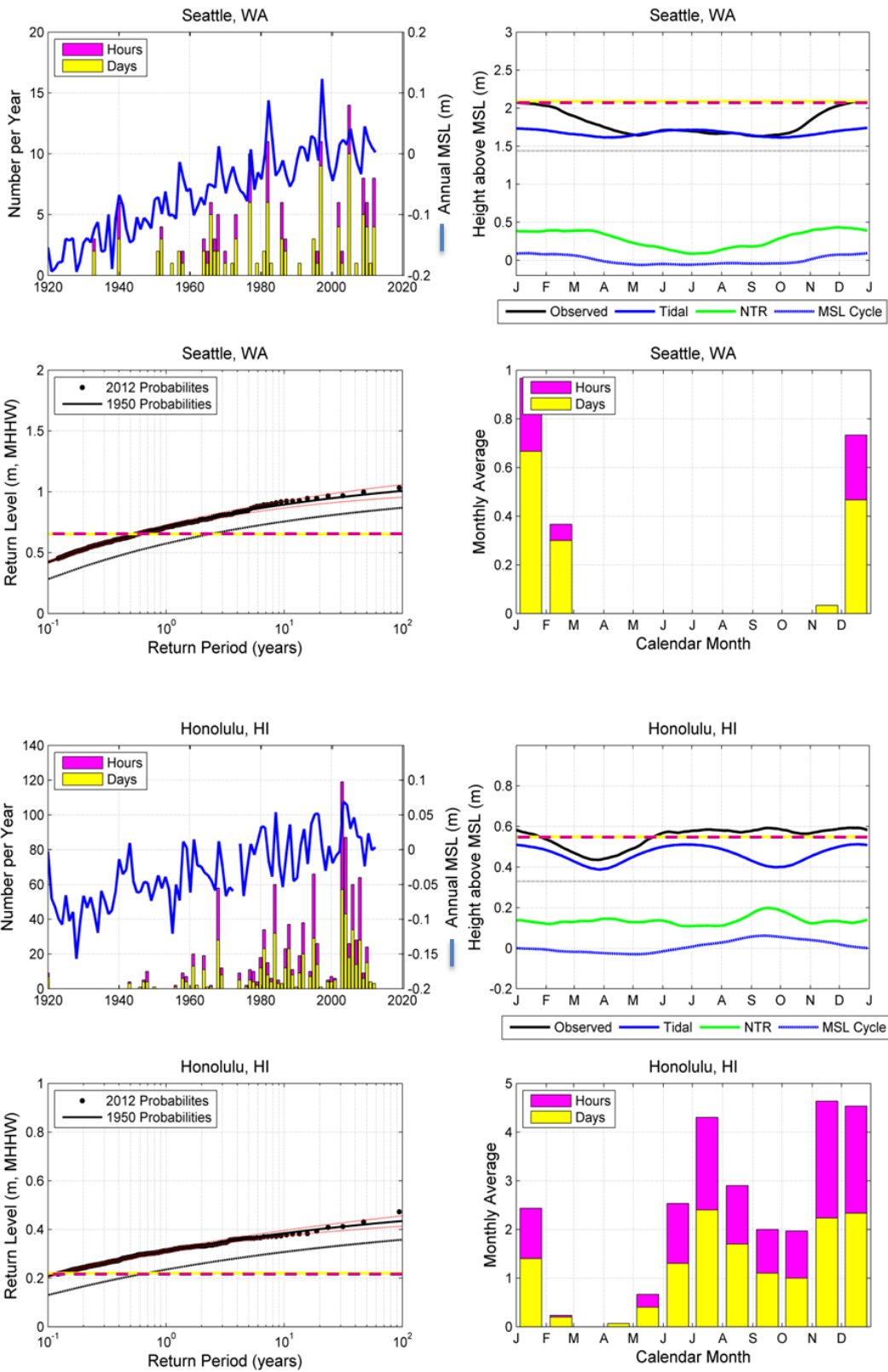












ACRONYMS

AMM	Annual Maximum Method
CO-OPS	Center for Operational Oceanographic Products and Services
ENSO	El Niño Southern Oscillation
GEV	Generalized Extreme Value
GPD	Generalized Pareto Distribution
MHHW	Mean Higher High Water
MSL	Mean Sea Level
NAO	North Atlantic Oscillation
NOAA	National Oceanic and Atmospheric Administration
NTDE	National Tidal Datum Epoch
NTR	Nontidal Residual
NWLON	National Water Level Observation Network
NWS	National Weather Service
ONI	Oceanic Niño Index
PacIOOS	Pacific Integrated Ocean Observing System
PDO	Pacific Decadal Oscillation
POT	Peak Over Threshold
SLR	Sea Level Rise
WFO	Weather Forecasting Offices